ESTIMATION OF
EXTREME WIND WAVE HEIGHTS

by

L.J. Lopatoukhin, V.A. Rozhkov, V.E. Ryabinin, V.R. Swail,
A.V. Boukhanovsky and A. B. Degtyarev

WMO/TD-No. 1041

2000

JCOMM Technical Report No. 9

ESTIMATION OF
EXTREME WIND WAVE HEIGHTS

by

L.J. Lopatoukhin, V.A. Rozhkov, V.E. Ryabinin, V.R. Swail, A.V. Boukhanovsky and A. B. Degtyarev

N O T E

CONTENTS

---oooOooo---

FOREWORD

Wind waves strongly affect all kinds of maritime activities, and their worst effects usually come from the highest waves. The Eleventh Session of the WMO Commission for Marine Meteorology noted the need for maritime service providers to have the capability of predicting in real-time and estimating parameters of the highest wind waves. In response to this requirement a technical paper [Boukhanovsky A.V. et al, 1998] was published by the WMO. It deals with the evaluation of the highest wave h_{max} for short periods of time (approximately 1-3 hours long when the wave field can be considered as a quasi-stationary process), and for a single storm, which can be from one to several days long. The basic purpose of methods considered in that paper is the actual prediction of the highest wave range in a storm.

The current publication continues the analysis of methods available for the evaluation of the h_{max} for longer time periods. It extends the time scale of applications for a series of storms and also considers wave heights of long return period. Such estimates are of crucial value for offshore design and real-time support of corresponding operations. Of course, this is not the only publication, which has been written on this subject. There are many good papers and books. A recent publication on methods available for analysis of wave climate and long return period waves can be found, for example, in the WMO Guide to Wave Analysis and Forecasting (1998), see chapter 9 and Annex III edited by D. Carter and V. Swail. That chapter contains references to many other useful publications.

In the review we did not address such highly important areas of activities as wind/wave observations, data assimilation, numerical modelling, or accurate reconstruction of the wind field for individual cases of the most severe storms. Significant progress has been recently reported in all of these areas. The purpose of this review is to informally complement the WMO guide and other existing publications with an analysis of the methods available for statistical data processing aimed at the estimation of extreme wave parameters. Also, an attempt is made to highlight some results of studies available in the literature of Eastern Europe, which apparently have not received sufficient consideration by the global reader. The scope of the methods described in the review reflects to some extent the preferences and experience of the authors, which have been developed in the course of the thorny process of servicing the offshore industry.

---oooOooo---

mostly focuses on methods available for evaluation of different quantiles of wave height distribution. Each of the considered methods has its advantages and shortcomings and must be used accordingly. In order to compare the methods, it important to examine not only point estimates of the extreme wave heights but also corresponding probabilistic ranges.

9. In order to efficiently use the described methods in practice, it is very important to define the measure of acceptable risk. This involves a very delicate balance of factors where the consequences of the damage, the cost of construction, and the cost of mitigating consequences of a possible accident are major considerations.

---oooOooo---

SUMMARY

1. Despite some significant recent achievements in developing methods and obtaining suitable data for the estimation of extreme wave parameters, the problem of their determination in terms of statistical analysis techniques is still far from having a completely satisfactory theoretical and practical solution. Existing reference books on waves focus mostly on information related to regular features of the wave field, not the extremes.

2. User requirements in terms of data nomenclature, accuracy and reliability are steadily becoming more stringent. The increase in sophistication of marine platforms and the expansion of offshore activities to new regions mean that increasingly expensive property is at risk of being damaged by high waves. Modern offshore operators require not only estimates of extreme wave heights. They need also complementary estimates of parameters associated with extreme waves, starting from the period and direction of the waves and ending with their spectra, associated currents, and estimates of forces acting on the structure. What they are looking for is, rather often, not simple estimates, but informative and authoritative support in their decision-making. That is why the subject of this study reflects only one stage in the development of full-range services for offshore operators and coastal management.

3. Significant recent changes in the area of extreme wave height analysis are related to the availability of new data types and models. At present, we have access to 10-20-year long data series of instrumental wave observations at automatic moored buoys and fixed platforms. Almost all of them are located in coastal areas. The contribution of satellite observations is becoming increasingly valuable in this area of research. Remotely sensed data still require some verification and bias correction. The efficient use of wave observations from polar-orbiting satellites requires data assimilation that produces a continuous field of wave spectrum parameters.

4. Numerical simulation of the wave spectrum by the most sophisticated models, driven by multi-year times series of meteorological fields, now represents the main source of data for wave climate studies, including studies of extreme waves. While most of the wave models are well tuned for forecasting and hindcasting of routine situations, both the models and their meteorological forcing, the analysis of near surface wind, may need additional verification and adjustment for studying extreme waves. There are some very successful examples of producing wind fields in individual severe storms using a combination of objective and subjective methods.

5. The results of the recent meteorological re-analysis project provide, for the first time in the history of marine meteorology, a forcing field that is continuous in time and space and is sufficiently long. Using this data, it is possible to numerically simulate a 40-year long wave series, and detect with considerable accuracy all significant storms affecting any area of interest. Trends of global wave statistics can be determined as well.

6. Wind waves are a complicated poli-modulated, poli-cyclic random process. They are poli-cyclic because of the simultaneous existence in the wave field of wind seas and swell, sometimes including more than one swell system. Poli-modulation is associated with the synoptic, seasonal, and inter-annual variability of wave parameters. Both features must be taken into account in studying extreme waves. The highest possible waves in many locations are often associated with the contribution of swell to the combined wave field. Their occurrence is most likely to occur during a certain season of a year. One should also consider the possible effect of trends associated with climate variations or long-term variability.

7. Two methods of estimating extreme wave heights, namely AMS and BOLIVAR, can take into account multiple variability scales in the extreme waves. The AMS method has the most solid theoretical foundation. The BOLIVAR method represents a further development that includes consideration of the second, third and, potentially other maxima in a year. If one is interested in further breakdown of extreme wave height estimates with respect to wave directions and seasonal variability, this requires adjustment of the corresponding absolute and conditional distributions.

8. Estimates of the highest waves, which are obtained using long time series at individual locations, are random values. This review

INTRODUCTION

Wind waves belong to a high-frequency type of geophysical oscillations, and their characteristic periods are of the order of seconds. Long–term variations of wind wave field statistical parameters are produced by modulation of their generation conditions. The strongest manifestations are on the synoptic temporal scale, but significant scales of such variability also include annual, inter-annual and longer variations.

If wind wave generating conditions are constant, wind waves can be considered a quasi-stationary, small-scale geophysical process. For the deep sea case, the wave heights h obeys the Rayleigh distribution

$$F(h) = 1 - exp\left[-\frac{\pi}{4}\left(\frac{h}{\overline{h}} \right)^2 \right]$$ (I.1)

with $\overline{h}$ denoting mean wave height.

Forristall [Forristall, 1978] proposed another distribution, which is in frequent use now:

$$F(h) = 1 - exp\left[-2.26\left(\frac{h}{h_s} \right)^{2.126} \right]$$ (I.2)

Here $h_s = 1.6\,\overline{h}$ is the so-called "significant" wave height. For a record consisting of n waves, it is equal to the average height of the one-third highest waves. After normalizing with respect to the zero-order moment of the spectrum m_0 the above distributions (1.1) and (1.2) read as follows:

$$F(h) = 1 - exp\left[-\frac{1}{8}\left(\frac{h}{\sqrt{m_0}} \right)^2 \right] \quad,$$

$$F(h) = 1 - exp\left[-\frac{1}{8.42}\left(\frac{h}{\sqrt{m_0}} \right)^{2.126} \right]$$

Comparison of these distributions shows that they are close for small probabilities. At the same time, the relation (1.2) predicts somewhat smaller values of h_{max} for higher waves.

For example, the Forristall relation results in an estimate of the highest wave in a thousand waves, which is equal to 0.907 of the estimate obtained with the Raleigh distribution. Wave heights in a sequence are statistically connected, and their correlation function is as follows:

$$K_h(\tau) = D\,exp(-\alpha\,|\,\tau\,|\,)$$ (I.3),

where D denotes the process variance, α is the decrement, and τ is the time lag.

The most fundamental starting point for derivation of equations governing the wave spectrum evolution is the equation for the conservation of the wave action density N (see e.g., [Komen et al., 1994; Lavrenov, 1998]):

$$\frac{\partial N}{\partial t} + \frac{\partial N}{\partial \varphi}\dot{\varphi} + \frac{\partial N}{\partial \theta}\dot{\theta} + \frac{\partial N}{\partial k}\dot{k} + \frac{\partial N}{\partial \beta}\dot{\beta} + \frac{\partial N}{\partial \omega}\dot{\omega} = G_s$$
(I.4)

N is a function of latitude φ, longitude θ, wave number k, angle β between the direction of wave propagation and the parallel, angular frequency ω, and time t. In the deep sea case the source function G_S is represented as the sum of three terms:

$$G_S = G_{in} + G_{nl} + G_{ds}$$

G_{in} parameterizes spectral wave energy generation by the wind, G_{ds} is the wave energy dissipation, and G_{nl} represents the effect of weak nonlinear interactions on the wind wave spectrum change.

Present spectral wind wave models based on equation (1.4) are rather well developed. They incorporate a representation of all significant mechanisms affecting the wave spectrum evolution and are quite sophisticated numerically. Being forced by wind data (or atmospheric pressure), and data on boundary layer stability, the models compute the two dimensional (with respect of frequency and direction) spectrum $S\,(\omega,\,\beta\,)$ at nodes $\vec{r}_i$ of the numerical grid at times t_j.

For the statistical analysis of long term series, we will use in this study the results of hydrodynamic model simulations. The basic variable will be mean wave height $\overline{h} = \sqrt{2\pi m_0}$, where m_0 is the zero-order moment of the two-dimensional spectrum, i.e.

$$m_0 = \iint S(\omega,\beta\,)d\omega d\beta$$

at fixed locations r_i. The simulations were conducted at the Arctic and Antarctic Research Institute under the supervision of Dr. Igor V. Lavrenov. Another source of input data will be

long-term synoptic wind wave observations $\bar{h}_t$ at automated buoys in several areas of the World Oceans [Buckley, 1988; Boukhanovsky et al., 2000] and estimates $h = \sqrt{h_{ws}^2 + h_{sw}^2}$ from visual ship observations. Here h_{ws} and h_{sw} are wind sea and swell heights, respectively.

Time series of wind wave heights in mid-latitudes and subtropical areas of the World Oceans make alternating sequences of storms and weather windows. We define a storm of duration $\Im$ and intensity h^+ as a situation when the random function $h(t)$ exceeds a predefined value Z. The period Θ during which the wave height is less than this threshold will be called a weather window of intensity h^-.
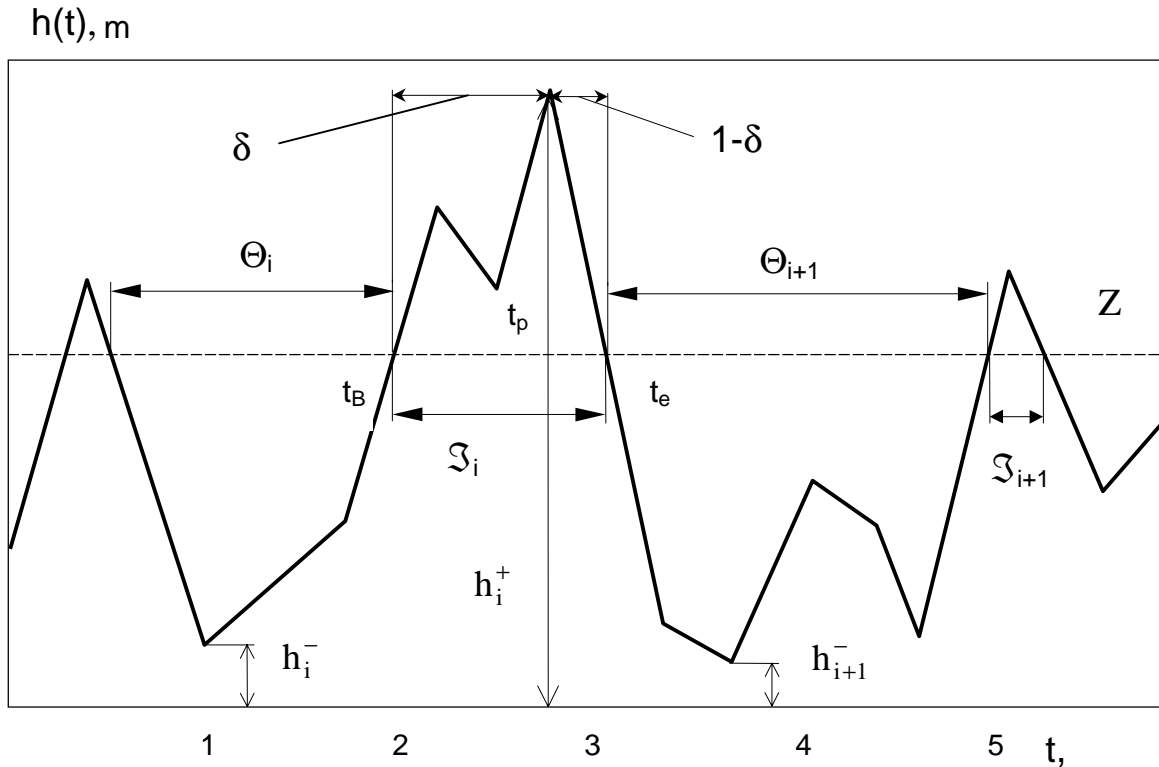

Figure. I.1. Parameters describing storms and weather windows

The parameter δ shows the asymmetry of the storm: $\delta=(t_p-t_b)/\Im$; t_b, t_p, t_e are times of storm start, maximum development, and end, respectively. Fig. 1 clarifies these definitions.

Wave observations or model simulation results can be represented in a more general way by the log-normal approximation of wave height distribution. The corresponding distribution density function reads as follows:

$$f(h) = \frac{s}{h\sqrt{2\pi}} exp\left[-\frac{s^2}{2}(ln\, h - ln\, h_{0.5})^2 \right] \qquad (I.5)$$

where $h_{0.5}$ is the median, and s^{-1} is the r.m.s. deviation of the wave height logarithms. Fig. I.2 gives an example of wave height distribution plotted against probability (I.5) of non-exceedance.

If a wave height series $h(t)$ at times of synoptic observations (i.e. with recording interval of 3 or 6 hours) is being considered as a sample of a stationary random function, then its auto-correlation function for the synoptic variability range can
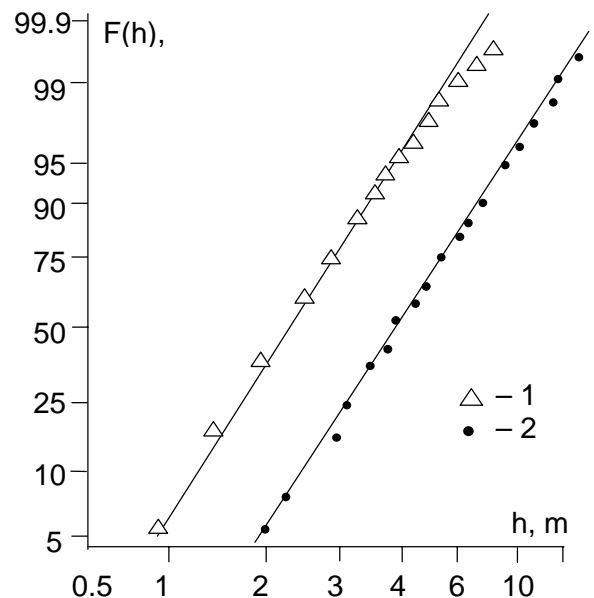

Figure I.2. Combined (wind sea and swell) wave height distribution for February (1) and August (2). Log-normal probability plot. Ocean Weather Station "Lima": data of 1976-1980.

also be written as (I.3), but with other parameters. For example, from two to four consecutive individual waves within the quasi-stationary period are expected to correlate (the whole episode lasting 10-20 seconds). Wave observations at synoptic times are correlated, on average, for 1.5-3 days.

Wind waves also undergo an annual cycle. This results in a corresponding variation of monthly wave characteristics. For example, monthly mean wave heights $\bar{h}_t$ and parameters $h_{0.5}$ and s of distribution (I.5) vary in a cyclical mode from season to season and show stochastic fluctuations from year to year. Fig. I.3 shows the seasonal variation of parameters $h_{0.5}$ and s at Ocean

Weather Station "M" located in the Norwegian Sea. Monthly parameters exhibit explicit seasonal variability, and some stochastic fluctuations are seen as variations of data in the same months of different years. The January median (shown as a horizontal line in boxes in Fig. 1.3.a) of $h_{0.5}$ estimates is approximately 3.2 m. During individual years it can vary from 2.2 to 4.0 m, making the inter-quartile range of (3.5-2.8) = 0.7 m. Such rhythmic variations can be expressed mathematically through a periodically correlated stochastic process (PCSP) with mean $m(t)$ and variance $D(t)$, which are periodic functions of time with period T = 1 year. Its covariance function $K(t_i,t_j) = K(t_i+T,t_j+T)$ depends on both arguments.
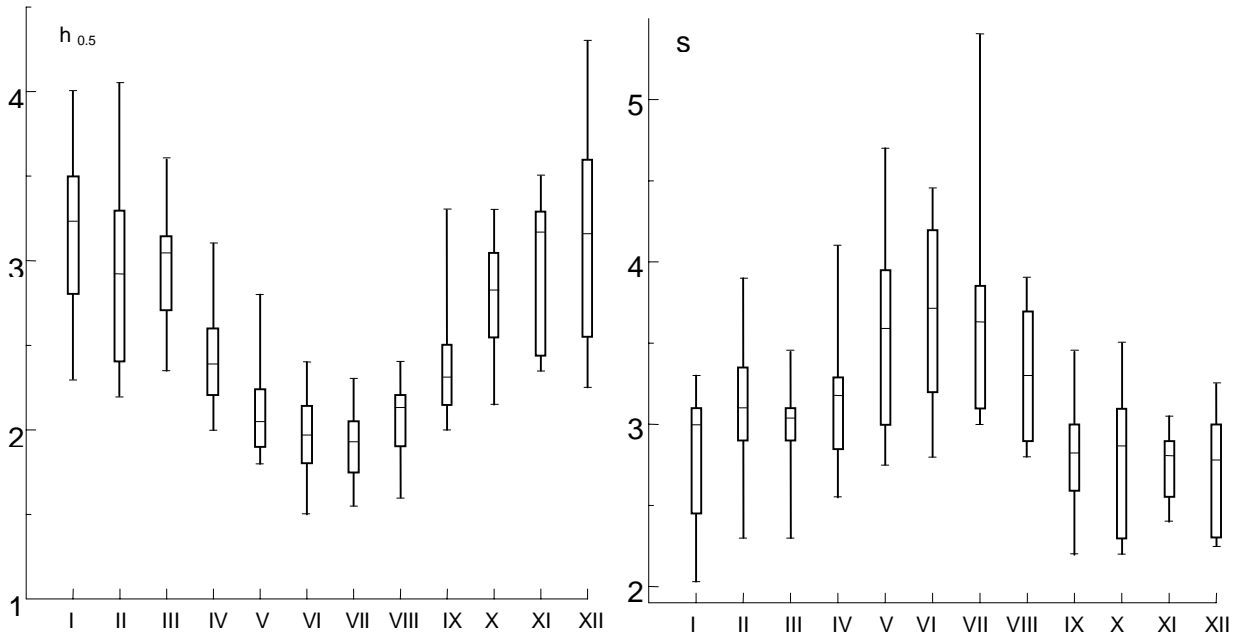

Figura I.3. Estimates of log-normal wave height distribution parameters $h_{0.5}$ and s at Weather Station "M"
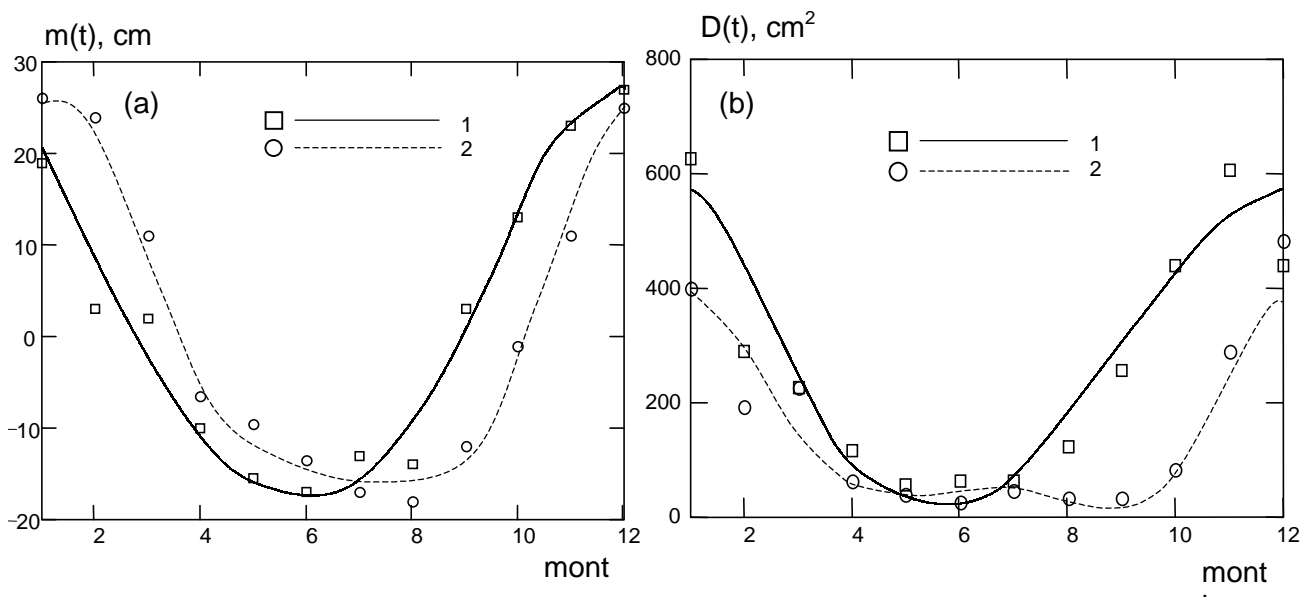

Figura I.4. Mathematicall expectation (a) and variance (b) of monthly mean wave height. All values are centered with respect to the mean annual wave height: (1)- The Baltic Sea, (2) The Black Sea.

PCSP samples, if they are taken at intervals equal to the correlation period T, produce stationary random series. Fig. I.4 shows functions $m(t)$, $D(t)$ obtained in experiments held in the Black Sea and Baltic Sea.

The following stochastic models can be used for the simulation of random series with a priori given properties.

Auto-regression model for the quasi-stationary and synoptic variability ranges

At the quasi-stationary and synoptic intervals of variability the wave process is best described by the stationary auto-regression model AR(p) of order p, namely

$$\xi_t = \sum_{k=1}^{p} \phi_k \xi_{t-k} + \varepsilon_t, \qquad \zeta_t = f(\xi_t) \qquad (I.6)$$

where ϕ_k are coefficients to be computed using the correlation function $K_\xi(\tau)$ as given by relation (I.2), ε_t is white noise with a given distribution function, which has to be compatible with the nonlinear functional transformation $f(\bullet)$ of function ξ_t into, respectively, the Rayleigh (I.1) or log-normal (I.5) distribution of ζ_t.

Stochastic model for sequence of storms and weather windows

A stationary pulse-like random process is a good model for sequence of storms and fair weather intervals. A sample can be generated as follows:

$$\xi(t) = \sum_{k=1}^{n} w_k \left(Z, t - \sum_{j=1}^{k-1} (\Im_j + \Theta_j) \right) \qquad (I.7)$$

where $\Im_j$ and Θ_j are, correspondingly, the duration of the storm and the weather window (with threshold value Z),

$$w(Z,t) = \begin{cases} Z + (h^+ - Z)u(t/\Im) & 0 \le t \le \Im, \\ Z - (h^- - Z)u((t-\Im)/\Theta) & \Im \le t \le \Im + \Theta \\ 0 & (t < 0) \cup (t > \Im + \Theta) \end{cases}$$

h^+, h^- are the highest wave height in storm and the minimum wave height during the weather window. Function $u(t)$ prescribes the shape of the non-dimensional impulse. The triangular shape of this function

$$u(t) = \begin{cases} t/\delta & 0 \le t \le \delta, \\ 1/(1-\delta) - t/(1-\delta) & \delta \le t \le 1 \\ 0 & (t < 0) \cup (t > 1) \end{cases}$$

serves as a good first approximation. Parameter δ, as seen from fig. I.1, defines the asymmetry of function $u(t)$. If $\delta=0.5$, the function is symmetric.

The actual generation of a series of random storms and weather windows is based on the Monte Carlo approach. First, the distribution function $F_\Xi(\cdot)$ and the matrix co-variation function $K_\Xi(\tau)$ are specified which fit the set of four random values $\Xi \sim (h^+, \Im, h^-, \Theta)$ or time series Ξ_t. Secondly, a non-dimensional storm shape function $u(t)$ is chosen. Finally, an ensemble of storms and weather windows is generated numerically.

Stochastic model for extra-annual rhythms

This model is written as follows:

$$\xi(t) = m(t) + \sigma(t)\xi_t \qquad (I.8)$$

Here $m(t)$ and $\sigma(t)$ are periodic functions, and ξ_t is a non-stationary process AP(p) so that

$$\xi_t = \sum_{k=1}^{p} \phi_k(t)\xi_{t-k} + \varepsilon_t \qquad (I.9)$$

Coefficients $\phi_k(t) = \phi_k(t+T)$ are periodic functions of time.

A model that is capable of describing the year-to-year variability of monthly mean wave heights will therefore require twelve values of $m(t)$ and 78 values of $K(t,\tau)$. It is possible to reduce the number of dimensions by considering the following representation of PCSP:

$$\zeta(t) = \sum_{k=-\infty}^{\infty} \eta_k(t) exp(i\omega_k t) \qquad (I.10)$$

Here $\eta_k(t)$ are stationary random processes (components) with mathematical expectation m_k and co-variation function $K_k(\tau)$ that can be obtained by expressing functions $m(t)$ and $K(t,\tau)$ as Fourier expansion series.

Relation (I.10) resembles a Fourier series expansion of $\zeta(t)$. However, both the coefficients and basis functions in it depend on the time variable, and hence (I.10) is not a Fourier expansion. A simpler model for PCSP can therefore be obtained by expanding the function $\xi(t)$ for *each* annual interval, as follows:

$$\zeta(t) = a_0 + \sum_{k=1}^{q} (a_k cos \omega_k t + b_k sin \omega_k t) \qquad (I.11)$$

where a_k and b_k are random values, and q is the order of the model.

For a stationary process it is possible to suppose that values a_k and b_k are independent, while for a non-stationary process they will be dependent. Table I.1 gives average values of means (m_{a_k}, m_{b_k}), variances (D_{a_k}, D_{b_k}), co-variation $K_{a_k b_k}$, and correlation $\rho_{a_k b_k}$ for coefficients of the model of annual rhythms. Hence, instead of model (I.8-I.9) with 90 parameters, a simpler model (I.11) with 20

parameters (see Table I.1) may be used. Monthly mean values of wave heights in the Black Sea were used for the computations. Corresponding values of $m(t)$ and $D(t)$ are shown in Fig. I.4. Coefficient a_0 in the table is equal to the annual average wave height. Coefficients a_1, a_2 correspond to the cosine component of the annual and semi-annual harmonics. Correspondingly, b_1 and b_2 correspond to the sine component. It becomes obvious from the table that a_k and b_k are strongly correlated. For example, the correlation coefficient between a_o and a_1 is 0.66.

All above models make it possible to describe wind waves as a multi-cyclic, multi-modulated random process. The multi-cyclic behavior of waves reflects the co-existence of sea and swell in the combined wave field. Multi-modulation is related to synoptic, seasonal, and extra-annual variability of the averaged wave parameters. Hydrodynamic properties of wind waves can be simulated by models based on equations for wave action density such as (I.4), and models (I.6) – (I.10) are available for the statistical description of the wave field.

At the same time, many practical computations of extreme wave height h_{max}, for example offshore and shelf engineering applications, employ the assumption that wave height series is a sequence of random values. The first approach of this kind is called the method of initial distribution. It is described in the following section.

Table I.1.

Statistical parameters of coefficients a_k, b_k of monthly mean wave height rhythms model (I.11).
The Black Sea

Parameter	m, cm	D, cm^2	$K_{a_k b_k}$ (cm^2) and ρ_{a_k, b_k}				
			a_0	a_1	b_1	a_2	b_2
a_0	80	22	**1**	0.66	0.54	0.22	0.60
a_1	19	42	20	**1**	0.21	0.65	0.47
b_1	12	17	11	6	**1**	-0.26	0.52
a_2	2	39	6	26	-7	**1**	0.15
b_2	4	19	12	13	9	4	**1**

Note: co-variation K_{a_k, b_k} is given below the diagonal and correlation coefficient ρ_{a_k, b_k} is given above the diagonal.

---oooOooo---

CHAPTER 1

Initial Distribution Method (IDM)

This method estimates the extreme wave height h_{max} of a specified return period as the quantile h_p of the wave, height distribution $F(h)$ with probability p. Provided the distribution of individual wave heights during the quasi-stationary interval obeys equation (I.1), then

$$h_p = \bar{h}\sqrt{-\frac{4}{\pi}ln(1-p)} \qquad (1.1)$$

For $p = 0.001$ we obtain $h_p = 2.97\bar{h}$. Thus, the height of wave, which is the highest in a thousand waves, is expected to be almost three times larger than the mean wave height $\bar{h}$. Using approximation (I.5) of long-term wave height distribution, the quantile with probability p can be computed as follows:

$$h_p = h_{0.5}\,exp\left(\frac{U_p}{s}\right) \qquad (1.2)$$

where U_p is the quantile of the standard normal distribution N(0,1). Here quantile h_p should be understood as the wave height which is likely to be observed once (at the standard synoptic observation times) in T years.

In applied studies, the period T is called "return period", and the corresponding probability is defined as

$$p = \frac{\Delta t}{24 \cdot 365 \cdot T}$$

where Δt is the interval (in hours) between subsequent observations (say, 6 hours). Then we get $p = 0.000684/T$. If $\Delta t = 3\ h$, we get $p = 0.000342/T$.

Table 1.1 shows values of h_p corresponding to different choices of Δt and T for $h_{0.5} = 1.0$ and $s = 2.0$ in distribution (I.5). It can be seen that the wave height estimates do depend on the recording interval.

Table 1.1
Estimated 1-year and 100-year return period wave heights at synoptic observation times.
Computations for log-normal distribution with $h_{0.5} = 1.0$ m and $s = 2.0$ and
with three record intervals of 3, 6, and 12 hours

Number of observations per day	Δt, hour	$h_{max} / h_{0.5}$	
		T = 1 year	T = 100 years
8	3	5.5	9.4
4	6	5.0	8.8
2	12	4.5	8.1

There are two traditional data sources for the determination of the wave height distribution $F(h)$. Historically, visual observations onboard ships and at the Ocean Weather Stations were the basis for such calculations.

At present the data are mostly provided by instrumental wave observations from automated buoys and through numerical simulations of waves. Regardless of the source of information, the initial distribution method leads to some ambiguity in the estimates of the h_{max} using quantiles (1.1,1.2).

If relation (1.2) is used in (1.1) as an estimate for $\bar{h}$, then the distribution $F(h)$ of all individual wave heights h during T-year long interval can be represented as the combined distribution

$$F(h) = \int_{0}^{\infty} G(h, \bar{h})f(\bar{h})d\bar{h} \qquad (1.3)$$

with $G(h, \bar{h})$ being wave height distribution (I.1) over the quasi-stationary interval and $f(\bar{h})$ being the long-term (climatic) probability distribution of mean wave height (I.5).

The average number of individual waves N in such a population depends on the mean wave period $\bar{\tau}$. To estimate it, we can assume that the joint distribution of wave heights h and periods τ is governed by multiplication of the individual log-normal distributions

$$f(h, \tau) = f(h)f(\tau\,|\,h) \qquad (1.4)$$

with parameters $h_{0.5}$ and s for the marginal distribution $f(h)$ of wave heights and with parameters $\tau_{0.5}(h)$ and $s_\tau(h)$ for the conditional distribution of wave periods f(τ|h) for a given wave height h. Then the probability that $h_k \leq h < h_{k+1}$ and $\tau_s \leq \tau < \tau_{s+1}$ is equal to

$$p_{ks} = \int\limits_{h_k}^{h_{k+1}} \int\limits_{\tau_s\tau_{s+1}} f(h,\tau)dhd\tau \, ,$$

and the random number of such waves $m_{ks}=p_{ks}N$ is characterized by following the binomial distribution (see Lopatoukhin, Lavrenov et al., 1999]:

$$P_N(m) = C_N^m \, p^m q^{N-m}, \quad q=1-p \qquad (1.5)$$

Here $m = pN$ is the mean number and $\sqrt{Npq}$ is the corresponding r.m.s. deviation.

For small values of probability p, distribution (1.5) tends asymptotically to the Poisson distribution:

$$P(m) = exp[-\lambda]\frac{\lambda^m}{m!} \qquad (1.6)$$

which has mean value λ, and r.m.s. deviation $\sqrt{\lambda}$.

For example, the median $h_{0.5}$ of mean wave height climatic distribution for the southern part of the Baltic Sea is equal to 0.66 (m), and the shape parameter s is equal to 1.81. For the wave periods we have $\tau_{0.5}=3.7(s)$ and $s_\tau=3.4$. Hence the mean number of waves for a year is $N = 8\,400\,000$. The probability p_{ks} that $1 \le h < 2\,(m)$ and $4 \le \tau < 6(s)$ is 0.11. Thus, using (1.5) we have $m = p_{ks}N \approx 924000$ waves per year and $\sigma_m = 910$. For the probability p_{ks} that $3 \le h < 6(m)$ and $6 \le \tau < 8(s)$, which is equal to 0.0000196, relation (1.6) predicts $m = 165$ and $\sigma_m = 13$ (waves).

The initial distribution method results are sensitive to the variation of parameters in extrapolation formulae (1.1) and (1.2). It is particularly sensitive to variations of parameter s for small values of probability p. Quite often the statistical distribution of wave height in an observed sample does not match closely relations (I.1) and (I.5). This results in significant differences in estimates, which are obtained with the help of various methods. For example, if values of h and s computed using the formula for statistical moments are, respectively, $h_{0.5}=0.66$ (m) and $s=1.81$, then the estimate of one-hundred year return wave height in the Baltic Sea is $h_{max} = 7.3$ m. If the median is the same but the

parameter s is determined using the formula for quantile, which gives $s_{(q)}^*=1.95$, then $h_{max}=6.1$ m.

The "true" distribution function F(h) is unknown. We use the observation series to obtain an approximation F*(h), the reliability of which depends on the length of the series and the quality of observations. Usually, the time series are long enough. If, for example, the series is 30-40 years long, and if observations are taken 4-8 times a day, the total number of records is 50–100 thousand. Correspondingly, the method can provide quite a narrow confidence range (provided the approximated distribution is really close to the true one).

For the above example the estimates h0.5=0.66 (m) and s=1.81 were obtained using a simulated data series, which was 35 years long. The time step was 6 hours. The total number of readings was N = 51100. Thus, the standard deviation of the estimate of s is $\tau s=0.014$. For $\sigma_{h0.5}$ the expected deviation is as small as 0.002. Correspondingly, the 90% confidence range for the one hundred year wave height (hp=7.3 m), which is obtained by extrapolation of distribution (I.4) up to probability p=0.684·10–5, is very narrow, namely 7.2-7.4 m.

It is obvious that the initial distribution method cannot, in principle, represent the true variability of maximum wave heights. Even if we consider approximation (I.1), and, particularly, (I.5) ideal, the parameters $\bar{h}, h_{0.5}, s$ that enter these relations still remain random as they are affected by synoptic, seasonal and extra-annual variability. As a result, one point (i.e. single-value) estimates of extreme wave height have considerable inherent uncertainty. Long-period variability also justifies the use of wider confidence limits for interval estimates.

Hence, marked sensitivity of the initial distribution method to input data quality combined with considerable uncertainties of estimates at small probabilities, as well as adoption of some assumptions regarding the possibility of combining approximated distributions (I.1) and (I.5), suggest that there is a need to further develop the method.

---oooOooo---

CHAPTER 2

Method of annual maximum series (AMS)

This method defines h_{max} as the last term of the ranked independent series of wave heights h. Thus it is a random value with the distribution

$$F_m(x) = [F_h(x)]^n \qquad (2.1)$$

which depends on the type and parameters of the original wave height distribution $F_h(x)$ and on the number of data n. For large values of n, the exact distribution (2.1) of independent, similarly distributed random values tends to one of the three following asymptotic distributions:

$$F(x) = exp(-exp(-x)) \qquad (2.2)$$

$$F(x) = \begin{cases} exp(-x^{-\gamma}), & x \geq 0, \gamma > 0 \\ 0, & x < 0 \end{cases} \qquad (2.3)$$

$$F(x) = \begin{cases} exp(-(-x)^\gamma), & x \leq 0, \gamma > 0 \\ 1, & x > 0 \end{cases} \qquad (2.4)$$

It is possible to apply a nonlinear transformation to variable x in distributions (2.2) – (2.4). Then, depending on the value of γ the distributions will converge to a single Generalized Extreme Value (GEV) distribution (see Leadbetter et al., 1986). Such a transformation is convenient if the type of original distribution (2.1) is not known. Then the selection of limiting distribution has to be made using the series data (see Pilon, Harvey, 1993; Hoybye, Laszlo, 1997).

If the original distribution $F_h(x)$ is of exponential type (such as normal, log-normal, and Weibull types), the distribution (2.1) converges to double-exponential distribution (2.2), known as first-limit or Gumbel distribution, which most often reads as follows:

$$F(x) = exp(-exp[-a(x-b)]) \qquad (2.5)$$

Parameters a and b depend on n and $F_h(x)$ as follows

$$F(b) = 1 - 1/n, \qquad a = nf(b) \qquad 2.6$$

where $f(b)$ is distribution density $F_h(x)$ at the point b.

For a quasi-stationary interval, and if the Rayleigh distribution (I.1) is satisfied, the following relation holds [Lopatukhin et al., 1991]:

$$a = \frac{\sqrt{\pi \, ln \, n}}{\bar{h}}, \quad b = 2\bar{h}\frac{\sqrt{ln \, n}}{\pi} \qquad (2.7)$$

If $n = 1000$, the median $\tilde{h}_{0.5}$ of distribution (2.5) is equal to

$$\tilde{h}_{0.5} = 3.05\bar{h} \qquad (2.8)$$

and main quantiles are as follows:

$$\tilde{h}_{0.05} = 2.73\bar{h}, \ \tilde{h}_{0.95} = 3.61\bar{h}, \ \tilde{h}_{0.99} = 3.95\bar{h} \quad (2.9)$$

This shows that the estimate of h_{max}, which can be obtained using the AMS (formula (2.8)), is biased relative to the h_{max} estimate by the Rayleigh distribution ($h_{1/1000} = 2.97\bar{h}$). As a random value, the estimate h_{max} should be located within the limits ($2.73\bar{h}$; $3.61\bar{h}$) in 90% of all cases (for n=1000). Once in a hundred cases the value of h_{max} can exceed $3.95\bar{h}$.

For the log-normal distribution (I.5) with parameters $h_{0.5}$ and s, the parameters in distribution (2.5) read as follows [Hirtzel, 1980, Lopatukhin et al.,1991]:

$$a = \left(\frac{sz}{h_{0.5}}\right)exp\left(-\frac{d}{s}\right), \ b = h_{0.5}\,exp\left(\frac{d}{s}\right),$$
$$d = z - (0.918 + ln\,z)/z, \ z = \sqrt{2\,ln\,n} \qquad (2.10)$$

The corresponding quantiles are

$$\tilde{h}_p = b - \frac{1}{a}ln(-ln\,p) \qquad (2.11)$$

For example:

$$\tilde{h}_{0.5} = b + \frac{0.367}{a}, \ \tilde{h}_{0.05} = b - \frac{1.097}{a}, \ \tilde{h}_{0.95} = b + \frac{2.970}{a} \qquad (2.12)$$

Let us consider a wave height series in the Baltic Sea that contains four observations per day. The distribution parameters are: $h_{0.5}$=0.66(m) and s=1.81. The median $\tilde{h}_{0.5}$ of the annual maximum distribution (2.5) with parameters a=1.76(m) and b=3.29(m) is 4.1(m) The initial distribution method would result in a one-year return period wave height of 3.9(m). Thus the h_{max} estimate obtained from distribution (2.5) with the annual maximum series method is always shifted relative to the estimate (1.2) in the initial distribution method.

The value h_{max} is random, and in a sample with n =365·24/Δt records in 90% of cases it will take a

value between 3.3 - 5.6(m), see (2.12). This means that if observations are taken every 6 hours, and if $h_{0.5}$ and s correspond to the basic climatic distribution, the series of annual maximum wave height h_{max} (recorded once at synoptic observation times) will vary within these limits.

$$P\left\{h_{max}^{(T)} \le h\right\} = P^T\left\{h_{max} \le h\right\} = exp\left[-exp\left[-a\left(h - b - a^{-1}\ln T\right)\right]\right] \qquad (2.13)$$

Distribution (2.13) is of the same type as (2.5) provided

$$a_T = a, \quad b_T = b + a^{-1}\ln T \qquad (2.14)$$

Using (2.13) for the above case one can get the median for a hundred year return wave $\tilde{h}_{0.5}^{(100)} = 6.8$ m. If the initial distribution method was used, the estimate would be 7.3 m.

For the AMS method, the extrapolation to long return periods can be justified only for periods (number of years) T^*, which do not exceed 3-4 lengths of the original data series used for evaluation of the distribution parameters. The estimates of wave heights with return periods of T years, for $T > T^*$, can be understood as bounds of corresponding probability interval for distribution (2.13). For example, the 10^4 year return wave height will be equal to the upper 1% percentile of the probability range, which is computed using an ensemble of one hundred series, each of them being one hundred years long [Lopatoukhin, Lavrenov et al., 1999].

Expressions (2.1), (2.7), (2.10), (2.13) are derived assuming independence of random values in the series. However, wave heights do correlate, both within the quasi-stationary interval, and for series made of synoptic time observations. Hence estimates of h_{max} in the Annual Maximum Series method should be corrected accordingly. The first way of correcting them would be to turn to the equivalent number of "conventionally independent" observations:

$$\hat{n} = \frac{\ln \rho}{\alpha} \qquad (2.15)$$

ρ being the threshold correlation coefficient. If the correlation is less than this threshold value, the correlation [see expression (I.3)] can be considered negligible. Parameter α is the decrement in the correlation function (I.3).

This approach can be used for first guess estimates only because parameter α is mostly chosen arbitrarily. Besides, the use of (2.15) is not fully theoretically justified. The estimation of parameters a and b in expression (2.5) from a sample of annual maximum wave heights h_{max} is used as a rule.

Evaluation of wave heights $h_{max}^{(T)}$ at T year return period, is made using extrapolation of the distribution (2.5). The following formula [Leadbetter et al., 1986] is used:

Fig. 2.1 shows a q-q (quantile – quantile) bi-plot of the empirical distribution function $F^*(x)$, which was computed using 35 annual wave height maxima generated by a model [Boukhanovsky A.V., Lopatoukhin L.J., Rozhkov V.A. 1998]. Empirical values (calculated from a sample) are shown along the x-axis, and theoretical values are shown along the y-axis. Such bi-plots will be used often in this paper. The statistical background for such presentations can be found elsewhere [Denby et al., 1983]. A thin cloud of points along the diagonal suggests that double exponential distribution (2.5) is a good approximation.

Estimates of parameters a* and b* can be made using methods of moments, quantile, maximum likelihood [Boukhanovsky, Davidan et al., 1996]. Also it is possible to use the method of L-moments, which was developed in [Hosking et al., 1985; Hosking, 1988; 1989; 1990]. Each of these methods uses different inputs for computation of a* and b*. Correspondingly, statistical properties of values a^*, b^*, (i.e. means and variances) will also be different. For example, if we use the maximum likelihood method for values $A=b$, $B=a^{-1}$ that would transform (2.5) into

$$F(h) = exp\left[-exp\left[-\frac{h - A}{B}\right]\right], \qquad (2.16)$$

then we will get the following statistical characteristics of parameters:

$$\sigma_{A^*} = \sqrt{1 + \frac{6}{\pi^2}(1 - \gamma)^2} \frac{B^*}{\sqrt{n}},$$

$$\sigma_{B^*} = \frac{\sqrt{6}}{\pi\sqrt{n}}B^*,$$

$$\rho_{A^*B^*} = 1 \Big/ \sqrt{1 + \frac{\pi^2}{6(1 - \gamma)^2}}$$

while the β% uncertainty limit for quantile h_p^* will look as follows:

$$\left|h_p - h_p^*\right| \le U_\beta \sqrt{D_h} \qquad (2.17)$$

Here $\sigma_{A^*}, \sigma_{B^*}, \rho_{A^*B^*}$ are r.m.s. deviations and coefficient of correlation of estimates A^*, B^*, $\gamma = 0.577126$, $g = \ln(-\ln(p))$, U_β is β% quantile of the normal distribution,

$$D_h = \sigma_{A^*}^2 + \sigma_{B^*}^2 g^2 - 2\rho_{A^*B^*}\sigma_{A^*}\sigma_{B^*}g$$

Thus, an Annual Maximum Method estimate h_{max} = 4.8 (m) of 35 year return wave height in the Baltic Sea is covered by the 95% - confidence limits interval from 4.4 to 5.2 (m). A hundred year return wave height, according to (2.13) is $h_{max}^{(100)}$ =5.1 (m),

and it has a 95% - confidence limit range of 4.6-5.6 (m). The AMS methods uses data series made of all annual wave height maxima.

Such series cannot be too long because we very rarely have observations lasting more than 30 – 40 years. This is why the confidence limits range for AMS h_{max} estimates is sufficiently broad.
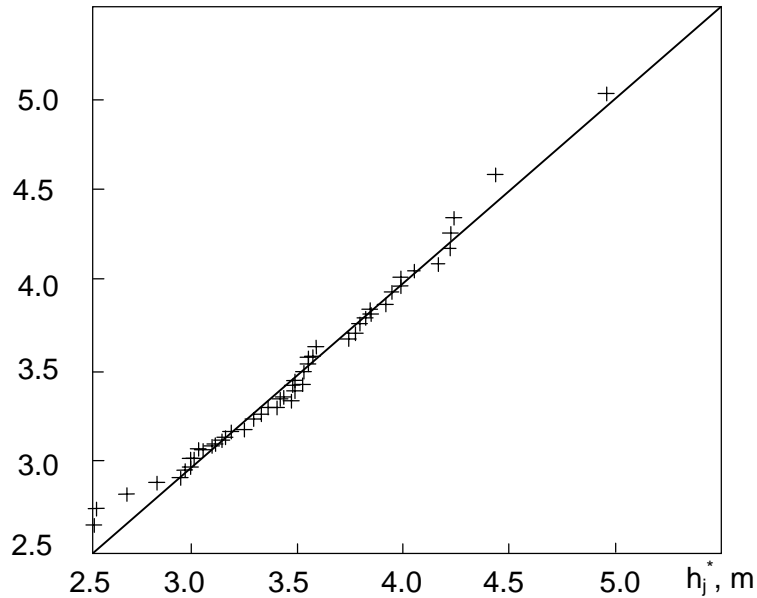

Figure 2.1. Biplot of 35 annual maxima of wave height h_j^* and corresponding quantiles h_j of distribution (2.5). The Baltic Sea

---oooOooo---

CHAPTER 3

Joint distribution of wave directions and heights

If a wave field is comprised of several wave patterns, then each of the patterns /wind sea or swell(s)/ can be described by a corresponding wave height h, period τ, for example $\overline{h}, \overline{\tau}$ and direction of propagation β.

The joint distribution density $f(h, \beta)$ is used most frequently for the probabilistic description of the wave field. An example of corresponding recurrence $f(h,\beta)dhd\beta$ (%) for the Baltic Sea (autumn) is given in Table 3.1 and is shown in Fig. 3.1.

The analysis of such joint distributions is specific because (h,β) represents a system of random values where h is a scalar value and β is an angular value. The coefficient of colligation C_f will be used to check the hypothesis that random values h and β are independent, as follows:
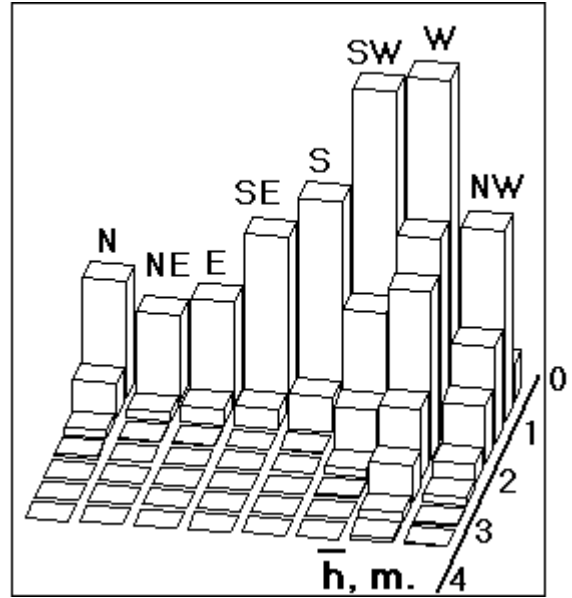

Figure 3.1. Probability of wave heights by direction
The Baltic Sea

Table 3.1.
Joint probability (%) of mean wave heights and directions.
The Baltic Sea. Autumn. Total number of observations N=12770.

h, m	N	NE	E	SE	S	SW	W	NW	f(h) dh
0.0-0.5	1	1	2	3	4	4	3	1	19
0.5-1.0	4	3	3	5	7	10	11	6	49
1.0-1.5	1	<1	1	1	1	4	6	3	18
1.5-2.0	<1	<1	<1	–	<1	1	5	2	9
2.0-2.5	<1	–	–	–	–	<1	2	1	3
2.5-3.0	–	–	–	–	–	<1	1	<1	1
>3.0	–	–	–	–	–	–	<1	<1	<1
f(β)dβ	6	4	6	9	12	20	29	14	100

$$C_f = \frac{f(h,\beta)}{f(h)f(\beta)} \qquad (3.1)$$

Also we will use regression lines:

$$m_{h/b} = \int_0^\infty h f(h/\beta)dh \qquad (3.2)$$

$$m_{\beta/h} = \int_0^{2\pi} \beta f(\beta/h)d\beta \qquad (3.3)$$

and scedastic (conditional variance) curves:

$$D_{h/\beta} = \int_0^\infty (h - m_{h/\beta})^2 f(h/\beta)dh \quad , \qquad (3.4)$$

$$D_{\beta/h} = \int_0^{2\pi} (\beta - m_{\beta/h})^2 f(\beta/h)d\beta \qquad (3.5)$$

According to [Mardia, 1972] the regression is estimated as the mean direction

$$\overline{\beta} = arctan\left[\overline{S}\Big/\overline{C}\right] \qquad (3.6)$$

while expression

$$D_\beta = 1 - R \qquad (3.7)$$

with

$$\overline{C} = \frac{1}{n}\sum_{i=1}^n \cos\beta_i, \quad \overline{S} = \frac{1}{n}\sum_{i=1}^n \sin\beta_i, \quad R = \sqrt{\overline{C}^2 + \overline{S}^2}$$

gives an estimate for conditional variance (3.5). The value

$$\sigma = \sqrt{-2ln(1 - D_\beta)} \qquad (3.8)$$

that follows from an analogy with a wrapped normal distribution can be used as a measure of spreading of angular value β. It is similar to the r.m.s. deviation. Tables 3.2 and 3.3 are based on the data from Table 3.1, and present conditional means /see (3.2),(3.3)/ and variances /see (3.4),(3.5)/ for height of waves from different directions.

Table 3.2.
Conditional means (3.2), variance (3.4), and r.m.s. deviation of wave height h for given direction β

β	N	NE	E	SE	S	SW	W	NW
$m_{h|\beta}$, m	0.8	0.7	0.6	0.6	0.6	0.8	1.3	1.1
$D_{h|\beta}$, m²	0.1	0.1	0.1	0.1	0.1	0.2	0.5	0.4
$\sigma_{h|\beta}$, m	0.4	0.3	0.3	0.3	0.3	0.5	0.7	0.6

Table 3.3.
Conditional means (3.3), variance (3.5), and r.m.s. deviation of wave direction β for given wave height h

h, m	0.25	0.75	1.25	1.75	2.25	2.75	3.25	3.75
$m_{\beta|h}$, ⁰	189	239	264	273	276	275	275	275
$D_{\beta|h}$, rad².	0.60	0.68	0.38	0.13	0.09	0.05	0.03	0.03
$\sigma_{\beta|h}$, ⁰	78	86	56	30	25	18	14	13

The computations show that values of c_f differ from 1, lines of regression (3.2) and (3.3) are not parallel to co-ordinates, conditional variance $D_{\beta|h}$ differs from the absolute variance $D_\beta = 0.59$ rad², $\sigma_\beta = 76°$. This suggests that the two-dimensional distribution density f(h,β) has to be approximated by expression

$$f(h,\beta) = f(h)f(\beta|h) \qquad (3.9)$$

Among existing approximations of f(β|h) the most useful is the Mises distribution. Its mean μ and scale k parameters depend on wave height h:

$$f(\beta|h) = \frac{1}{2\pi I_o(k(h))}exp[k(h)cos[\beta - \mu(h)]],$$

where $\qquad |\mu(h)| < \infty, \quad k(h) > 0.$ $\qquad$ (3.10)

Here

$$I_0(k) = \sum_{r=0}^{\infty}\frac{1}{(r!)^2}\left[\frac{k}{2}\right]^{2r} \qquad (3.11)$$

is the modified first type zero-order cylindrical function. Variation of parameters μ and k makes it possible to reconstruct all angular distributions, from uniform to a narrow one.

Comparisons of f(h,β) and approximation (3.10) for parameters μ and k taken from Table 3.4 showed satisfactory agreement.

We can use the distribution F(h|β) for any given β to estimate h_{max} with the help of both methods of initial distribution and the annual maximum series. The absolute wave height distribution is a mixed distribution of waves coming from different sectors of wave directions β_i:

$$f(h) = \sum_i \gamma_i f(h/\beta_i). \qquad (3.12)$$

Here γ_i are weight coefficients, which meet the compliance condition that $\sum_i \gamma_i = 1$. Computation of extreme values for individual directions is then made by simple adjustment of omni-directional wave height distribution *f(h)* with distribution of wave height for given directions *f(h|β_i)*. Wave height *h(T)*, expected to occur once in *T* years for direction β will be equal to a certain quantile of the omni-directional distribution *f(h)*.

Table 3.5 provides estimates of a hundred year mean wave height, both directional and omni-directional, based on data from Table 3.1.

Table 3.4.
Parameters μ and k of conditional distribution of wave heights (3.10). Data from Table 3.1

h, m	0–0.5	0.5–1.0	1.0–1.5	1.5–2.0	2.0–2.5	2.5–3.0	3.0–4.0
μ, ⁰	189	239	264	273	276	275	275
k	0.8	0.7	1.8	4.2	6.5	7.2	7.8

Table 3.5
Directional and omni-directional estimates of one hundred year wave height.
AMS method. The Baltic Sea

β	N	NE	E	SE	S	SW	W	NW	omni-directional
h(100), m	2.7	2.4	2.3	2.4	2.7	4.0	5.1	4.4	5.1

It is seen that the highest waves in the Baltic Sea mostly propagate from the west. If traditional computations of absolute and conditional distributions are used, a discrepancy often occurs that the omni-directional wave height estimate exceeds the maximum (over all directions) estimate computed taking into account directional distribution [Proceedings, 1986]. Estimates of long return period wave heights, if they are based on relation (3.12), eliminate this typical discrepancy.

---oooOooo---

CHAPTER 4

MENU (MEan Number of Up-crossings) Method

The highest wave h_{max} is observed when a storm is passing the point of observations. To estimate it we have to consider waves as a random process. Let us denote the wave height series as $\xi(t)$. A storm takes place when $\xi(t)$, $t \in [t_b, t_e]$ exceeds Z, and h_{max} is the maximum value of $\xi(t) \geq Z$ within interval (t_b, t_e), see Fig.I.1.

The function $\xi(t)$ can cross level Z having positive $\xi'(t) > 0$ or negative $\xi'(t) < 0$ derivative. At the beginning (index b) and ending (index e) times we have $\xi'(t_b) > 0$, $\xi'(t_e) < 0$. At a point of maximum and minimum function $\xi(t)$ has zero derivative $\xi'(t) = 0$, and it reaches its maximum at time t if in the vicinity of this value of t the second derivative is negative, $\xi''(t) < 0$. Thus it is possible to employ the theory of impulses (see [Tikhonov, et all, 1987]) to derive the distribution of extreme values of random process $\xi(t)$. To do so, we need to know the joint distribution density $f(\xi, \xi', \xi'')$[Rice, 1944].

For a stationary Gaussian process $\xi(t)$ with mathematical expectation $m_\xi = 0$ and co-variance function $K_\xi(\tau) = \sigma_\xi^2 \rho(\tau)$ this distribution reads as follows:

$$f\left(\xi, \xi', \xi''\right) = \frac{1}{(2\pi)^{3/2} \sigma_1 \sqrt{v}} exp\left\{-\frac{1}{2v}\left[\sigma_2^2 \xi^2 + 2\sigma_1 \xi \xi'' + \sigma_\xi^2 (\xi'')^2\right] - \frac{2(\xi')^2}{2\sigma_1^2}\right\} \qquad (4.1)$$

where σ_1^2 and σ_2^2 are variances of $\xi'(t)$ and $\xi''(t)$, and $v = \sigma_\xi^2 \sigma_2^2 - \sigma_1^4 \geq 0$.

It follows from (4.1) that maximum ξ_m distribution density reads [Longuet-Higgins, 1957]

$$f(\xi_m) = \frac{1}{\sigma_\xi \sqrt{2\pi}}\left[\frac{\sqrt{v}}{\sigma_1 \sigma_2} exp\left(-\frac{\sigma_2^2}{2v}\xi_m^2\right) - \frac{\sigma_1^2 \sqrt{2\pi}}{\sigma_\xi^2 \sigma_2}\xi_m exp\left(-\frac{\xi_m^2}{2\sigma_\xi^2}\right)\Phi\left(\frac{\sigma_1^2}{\sigma_\xi \sqrt{v}}\xi_m\right)\right] \qquad (4.2)$$

where $\Phi(x)$ is the probability integral.

A random process $\eta(t)$ obeying the log-normal distribution (I.5) can be examined in terms of functionally transformed Gaussian process variables:

$$\eta(t) = exp[\xi(t)], \qquad \ln \eta(t) = \xi(t) \qquad (4.3)$$

Then the maximum distribution density η_m will be:

$$f(\eta_m) = \frac{1}{\sigma \eta_m \sqrt{2\pi}}\left[v\, exp\left(-\frac{\ln^2 \eta_m}{2\sigma^2 v^2}\right) + \sqrt{2\pi(1-v^2)}\frac{\ln \eta_m}{\sigma} exp\left(-\frac{\ln^2 \eta_m}{2\sigma^2}\right)\Phi\left(\frac{\ln \eta_m}{\sigma v}\sqrt{1-v^2}\right)\right] \qquad (4.4)$$

Where $v^2 = 1 - \frac{1}{\sigma^2}\left[\frac{K_\eta^{(4)}(0)K_\eta(0)}{(K_\eta''(0))^2} - 3\right]^{-1}$,

$$K_\eta(\tau) = \sigma_\eta^2 \rho_\eta(\tau) + m_\eta^2 = exp\left[\sigma^2(1 + \rho_\xi(\tau))\right];$$

$$m_\eta = exp\left(\frac{\sigma^2}{2}\right), \quad \sigma_\eta^2 = exp(\sigma^2)\left[exp(\sigma^2) - 1\right]$$

$K_\eta''(0), K^{(4)}(0)$ are second and fourth derivatives of function $K_\eta(\tau)$ at $\tau = 0$.

The largest maximum amongst all ξ_m (or η_m) is called the absolute maximum and we consider it equal to h_{max}. The distribution of h_{max} tends to the same three types of distribution (see (2.2-2.4)) as does the distribution of the maximum value in a sample of independent random values [Leadbetter et al., 1986].

Another possible approach to determination of h_{max} for random process $\xi(t)$ uses dependence of value h on the time t needed to reach this value for the first time (i.e. the first up-crossing). A formal solution to this problem was derived in 1933 by L.S. Pontriagin for the Markov processes only. Nevertheless, there are some relations between the mean value of t and other characteristics of extreme values such as the average number of up-crossings of value h by function $\xi(t)$. Athanassoulis et al., [1995a, 1995b] used these relations to estimate h_{max} on the basis of time series of wave

heights taken at standard observation times. The series was represented as periodically correlated stochastic process (PCSP):

$$X(t) = \overline{X}_{tr}(t) + m(t) + s(t)W(t) \qquad (4.5)$$

where the first expansion coefficient represents the linear trend, m is seasonal variation of the parameter *X* mean value, *s* is the seasonal variation of standard deviation, and *W* is a stationary random process (in a general case it is a non-Gaussian process).

This method is called MENU (MEan Number of Up-crossings). It relates extreme value of any wind wave parameter possible once in *T* years to a certain value x*. At this value the mathematical expectation *M(x*; t, t+T)*, i.e. the mean number of up-crossings of value x* by random process *X(t,γ)* during time interval [*t; t+T]*, will be equal to one. Here *γ* is a sample number such as, say, 1960-1999. For brevity we shall omit parameter *γ* in further formulae. The process *X(t)* can represent any random parameter related to waves such as height, period, any other distribution parameter, etc. Nevertheless, the most useful application of this method is associated with processing of wave heights or any function related to wave heights (e.g. wave height logarithms).

The function *M(x*; t₁, t₂)* can be represented as follows:

$$M\left(x^*; t_1, t_2\right) = \int_{t_1}^{t_2} \int_0^\infty x' f_{\tau,\tau}\left(x^*, x'\right) dx' d\tau \quad (4.6)$$

and therefore its computation requires knowledge of $f_{t_1,t_2}(x, y)$, i.e. the joint distribution density of the process X(t₁) and its derivative Y(t₂), which, in accordance with (4.5), could be expressed through distribution density f $_{W,W'}$.

The approximation of f $_{W,W'}$ (x,y) in [Athanassoulis et al., 1994] was based on the Plackett distribution [Plackett,1965]

$$f(x, y, \psi) = \frac{\psi(\psi - 1)(x + y - 2xy) + \psi}{\sqrt{(1 + (\psi - 1)(x + y))^2 - 4\psi(\psi - 1)xy}}$$

$$(4.7)$$

where parameter ψ is related to the correlation coefficient ρ$_{xy}$ via the following formula:

$$\rho_{xy} = \frac{\psi^2 - 1 - 2\psi \log \psi}{\psi^2 - 1} \qquad (4.8)$$

Correlation coefficient or parameter ψ could be estimated directly from the data or in accordance with maximum likelihood method.
Hence, the MENU method determines extreme values through solving the equation

$$M\left(x^*; t, t+T\right) = 1 \qquad (4.9)$$

To solve the integral equation (4.9) in a general case, requires integration with respect to time, for rather long ranges, and taking an improper integral with respect to the other variable *X*. In practice, however, a simplified approach is used, which supposes that *W* is a Gaussian random process [Athanassoulis et al., 1995a].

This approach makes it possible to take the integral with respect to variable *X* analytically. The simplification is valid if the original wave height time series, which is used to compute the extreme wave heights, is distributed log-normally with sufficient accuracy. This is particularly important for the "tail" of the distribution.

Then, assuming that *X(t) = ln(h)*, equation (4.9) takes the following form [Athanassoulis et al., 1995a]:

$$\int_t^{t+T(x^*)} Q(\tau) \left(\frac{1}{2C} - \frac{D}{4C} \sqrt{\frac{\pi}{C}} \exp\left(\frac{D^2}{4C}\right) \right) \left[1 - erf\left(\frac{D}{2\sqrt{C}}\right) \right] \exp(-E) d\tau = 1 \qquad (4.10)$$

where

$$C = \frac{\sigma_X^2}{2\left(\sigma_X^2 \sigma_{X'}^2 - \sigma_{XX'}^2\right)}; \qquad E = \frac{\left(x^* - m\right)^2 \sigma_{X'}^2 + 2x^* \sigma_{XX'} m' - 2\sigma_{XX'} mm' + \sigma_X^2 m'^2}{2\left(\sigma_X^2 \sigma_{X'}^2 - \sigma_{XX'}^2\right)};$$

$$D = \frac{\sigma_{XX'} m - \sigma_X^2 m' - x^* \sigma_{XX'}}{\sigma_X^2 \sigma_{X'}^2 - \sigma_{XX'}^2}; \qquad Q = \frac{1}{2\pi \sigma_X \sigma_{X'} \sqrt{1 - \rho_{XX'}^2}}; \rho = \frac{\sigma_{XX'}}{\sigma_X \sigma_{X'}}.$$

In the above relations x* denotes the up-crossing level (the wave height) occurring once in time *T*. Functions σ and *m* are, respectively, the standard deviation and mathematical expectation that can be obtained from (4.5) using an approximation with low order Fourier expansion. The standard error

function is called "erf", as usual. Therefore, if we have any multi-year time series *{X(t), 0≤ t ≤Tend}* where *X* may be *h(t)* or *ln(h(t)+c)*, then the MENU method can lead to the following simplified procedure of estimation of return period *T* associated with the level *x*.* The procedure

involves several steps [Athanassoulis,1995, Stephanakos, 1999]:

1. Reindexing of X(t) series as follows:

$$\left\{X\left(j,t^\alpha\right), j = 1,2,\ldots,J, \quad 0 \le t^\alpha \le T^\alpha\right\}$$

T^α = 365 × 24 (hours) is one year

$t_k^\alpha = \left(k - \frac{1}{2}\right)\Delta t, \quad k = 1,2,\ldots,K = T^\alpha/\Delta t$ where Δt is the sampling interval.

2. Making the time series trend-free

   a) Obtaining the sequence of mean annual values

$$\overline{X}(j) = \frac{1}{K}\sum_{k=1}^{K} X\left(j,t_k^\alpha\right)$$

   b) Fitting the data points to linear function

$$X_{tr}(t) = B_0 + B_1 t/T^\alpha$$

   c) Deleting the trend $Y(t) = X(t) - \overline{X}_{tr}(t)$

3. Derivation of seasonal characteristic

$$m\left(t_k^\alpha\right) = \frac{1}{J}\sum_{j=1}^{J} Y\left(j,t_k^\alpha\right),$$

$$s\left(t_k^\alpha\right) = \sqrt{\frac{1}{J}\sum_{j=1}^{J}\left[Y\left(j,t_k^\alpha\right) - m\left(t_k^\alpha\right)\right]^2}$$

(4.11)

4. Low-order Fourier series representation for m (order $\mu - 1$) and s (order $\sigma - 3$). See Fig.4.1.

5. Time series decomposition in accordance with (4.5)

$$W\left(j,t^\alpha\right) = \frac{Y\left(j,t^\alpha\right) - \mu\left(t^\alpha\right)}{\sigma\left(t^\alpha\right)}$$

(4.12)

6. Obtaining the joint probability density f(X,X')

$$X'(t) = B_1/T^\alpha + \mu'(t) + \sigma'(t)W(t) + \sigma(t)W'(t)$$ (4.13)

Considering the density of (W,W'), there are several ways to model it:

   a) Use bi-variate Plackett model (4.7) - (4.8) with uni-variate marginal densities estimated from the uni-variate samples of *W(t)* and *W'(t)*, respectively.

   b) Use the bi-variate Plackett model with both uni-variate marginals log-normal for the joint density of *(W(t), W(t+Δt))*, and by means of bi-variate linear transformation

      W(t) = W(t); W'(t)=(W(t+Δt)-W(t))/Δt,

      calculate the f^WW'

   c) Assume that the joint density $f_{t,t+\Delta t}^{WW}$ is a bi-variate normal density, and, by means of previous linear transformation, obtain the density $f_{t,t}^{WW'}$

7. Calculating the coefficients in (4.10) with the help of (4.5), (4.13) and low-order Fourier expansions for *m* and *s*.

8. Numerical solution of equation (4.10) for given level *X** that yields the return period *T(X*).*
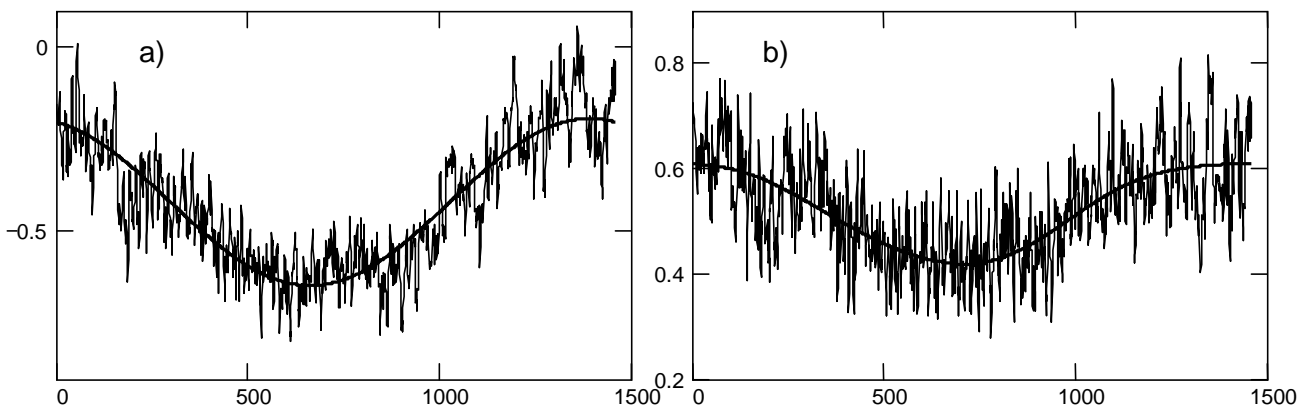

Figure.4.1. Seasonal variability of ln h1/3 time series for the Baltic Sea.
(a) Seasonal mean value *m(tᵅ)* and its 1st order Fourier representation (b) Seasonal standard deviation *s(tᵅ)* and its 3rd order Fourier representation. Axis of abscissa is annual time *tᵅ* (6-hour intervals)

---oooOooo---

CHAPTER 5

Peak Over Threshold Method (POT)

The Initial Distribution or MENU methods require rather long data series for estimation of h_{max}. If the number of years is denoted by n, and number of observations per day is denoted by m then the total length of the series will be N. For example, for $n = 30$, $m = 4$, $N = 30 \cdot 4 \cdot 365 \approx 44000$. The Annual Maximum Method (AMS) excludes from the analysis those storms that are not the strongest in a particular year but could be the strongest in other years. This is one reason why the Peak-Over-Threshold method is used in estimating the highest wind waves [Muir L.R., El-Shaarovi, 1986]. The method is based on studying the sample of h_{max} for the k strongest storms observed during n years. The selection of the k strongest storms requires the biggest effort in POT and is its most subjective procedure. As a rule, the first step is the selection of a large number of storms, for which h_{max} is determined. In the following step only the strongest storms are considered. Usually, 20-30 storms are taken for a 30-40 year long interval.

It is assumed in the POT method that there is no dependence between wave heights in consecutive storms (i.e. wave heights in different storms are not correlated). Then the distribution function for maximum wave heights can be written as follows:

$$F(h) = \sum_{k=0}^{\infty} [G(h)]^k \, p_k \qquad (5.1)$$

where G(h) is the distribution for wave heights exceeding a predefined threshold Z during a year

and p_k is distribution within a year of the number of storms during which maximum wave height exceeded Z. The Poisson distribution (1.6) is always used for p_k for sufficiently large values of Z.

In a particular case, when one can clearly see that storminess during the period of observations underwent considerable year-to-year variability, the geometrical distribution is a good approximation for p_k:

$$p_k = (1-\lambda)\lambda^k, \quad \lambda = 1 - p_0 \qquad (5.2)$$

where p_0 is the probability of occurrence of years when waves are below threshold Z.

If the case $(h \geq Z)$ is not rare (i.e. for small values of Z), one can use for p_k the truncated normal distribution:

$$p_k = \frac{1}{c\sqrt{2\pi}\sigma} exp\left[-\frac{(k-\lambda)^2}{2\sigma^2}\right],$$

$$c = \frac{1}{2}\left[erf\left(\frac{\lambda\sqrt{2}}{2\sigma}\right)+1\right] \qquad (5.3)$$

with parameters λ, σ, c.

Table 5.1 gives, as an example, statistical characteristics of number of strong storms in various seas. They were derived with values of Z that were equal to two-three times the annual mean wave height.

Table 5.1.

Probability of occurrence p_k (%), mean values of $\overline{k}$ and r.m.s deviation σ_k of the number of strong storms k in a year

Sea, number of years	pk, %						$\overline{k}$	σ_k
	k=0	k=1	k=2	k=3	k=4	k=5		
Baltic Sea, 35 years	37	34	17	6	5	1	1.09	1.16
Barents Sea, 41 years	37	27	24	10	2	–	1.15	1.12
Black Sea, 35 years	23	26	31	9	6	5	1.66	1.42
Caspian sea, 39 years	46	21	28	5	–	–	0.92	1.00

The table reveals marked inter-annual variability of strong storm numbers. For example, in 46% of years there were no strong storms in the Caspian Sea. The two last columns in the table contain values of $\overline{k}$ and σ_k that are close to each other. This means that the Poisson distribution is a good approximation for this case.

Summing up the infinite series (5.1) for the distribution of storm numbers (1.6), (5.2), and (5.3) will lead, respectively, to

$$F(h) = exp(-\lambda(1-G(h))) \qquad (5.4)$$

$$F(h) = \frac{1-\lambda}{1-\lambda G(h)} \qquad (5.5)$$

$$F(h) \approx \frac{1}{2c} exp(-\lambda(1 - G(h))) \cdot \left[1 - erf\left[\frac{\sqrt{2}}{2}\left(\sigma[1 - G(h)] + \frac{\lambda}{\sigma} \right) \right] \right] \quad (5.6)$$

For *G(h)* double exponential see (2.2) or Weibull, see (2.3), distributions are used the most often, as follows:

$$G(h) = exp\left[-exp\left(\frac{h - A}{B} \right) \right] \quad (5.7)$$

$$G(h) = 1 - exp\left[-\left[\frac{h - C}{A} \right]^B \right] \quad (5.8)$$

where *A, B* and *C* are parameters.

Substituting (5.7) or (5.8) into (5.4)–(5.6) one can obtain at least six types of combined distributions. The Poisson – Gumbel distribution shown in (5.9) below is the most widely used.

$$F(h) = exp\left\{ -\lambda\left\{ 1 - exp\left(-exp\left[\frac{h - A}{B} \right] \right) \right\} \right\} \quad (5.9)$$

It follows from (5.3)–(5.5) that transformation of *G(h)* into *F(h)* is relatively straightforward. At the same time, the actual form of p_k and parameters *(λ,σ)* affect the value of quantile h_p. There is some freedom in the interpretation of distribution *G(h)* as probability *P{h≥Z}*.

One can include in the analysis all wave height observations exceeding *Z* during a single storm (i.e. when there are several cases where $h \geq Z$ during a single storm) or, to represent the storm in the sample by its single maximum wave height *h(t)*.

The difference between corresponding empirical distributions *(h > Z)* and *(h+ > Z)* is shown in Fig. 5.1 (q-q bi-plots of (5.7)).
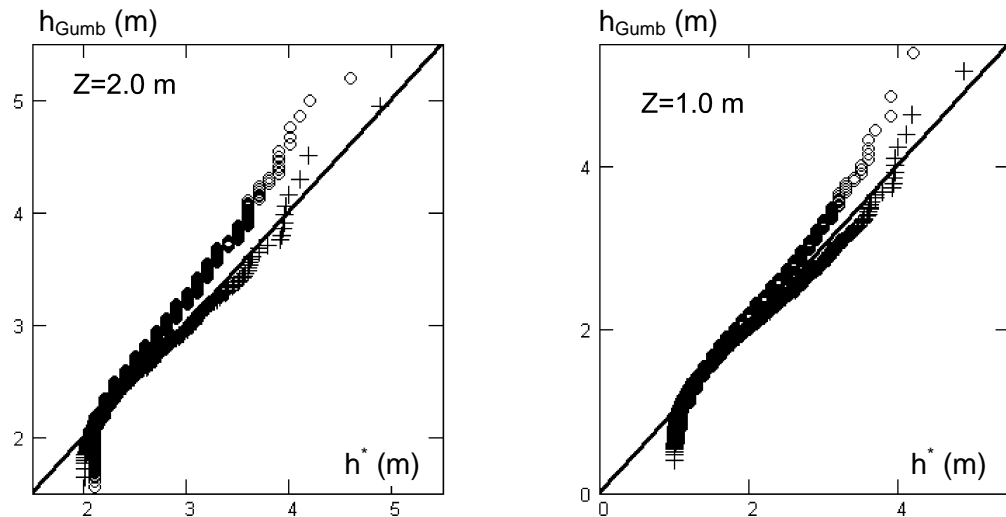

Figure 5.1 Biplots of Gumbel distribution and observed distributions *G(h)* in storms with maximum wave heights exceeding *Z = 2.0 m* and *Z = 1.0 m*. The Baltic Sea.
Straight line shows the theoretical expression. Sign *o* shows all values exceeding a predefined threshold.
Sign + shows the single highest waves in a storm (i.e. one wave for a storm).

It can be seen that even for sufficiently small values of *Z (Z = 1(m))* both distributions are approximated fairly well by the Gumbel distribution (except for the utmost "left tail" of data). In the case when Function *G(h)* is determined using wave heights at all synoptic observation times (i.e. more than once in a storm), the "left tail" is given more weight and, hence estimates of long return period waves are lower in comparison with *G(h)* computed using the wave heights h+, which were counted only once and therefore coincided with maxima in the storms.

In computations of wave heights, the sample should include only the highest waves in all selected storms. The wave height h_{max} with return period of *T* years is taken to be equal to the quantile h_p, *p=(1−1/T)%* of distribution *F(h)*.

According to (5.9) this distribution depends on the mean number λ of storms in a year, which, in turn, depends on the threshold value *Z*. Thus, h_p (including h_{max} as its particular case) is a function of *Z*. It follows from (5.9) that:

$$h_{max}(Z) = (A - B)ln\left(ln\left(1 + \frac{1}{\lambda T}\left[exp\left(-exp\left(-\frac{Z - A}{B} \right) - 1 - \frac{1}{N} \right) \right]^{-1} \right) \right) \quad (5.10)$$

where *N* is number of storms in *T* years.

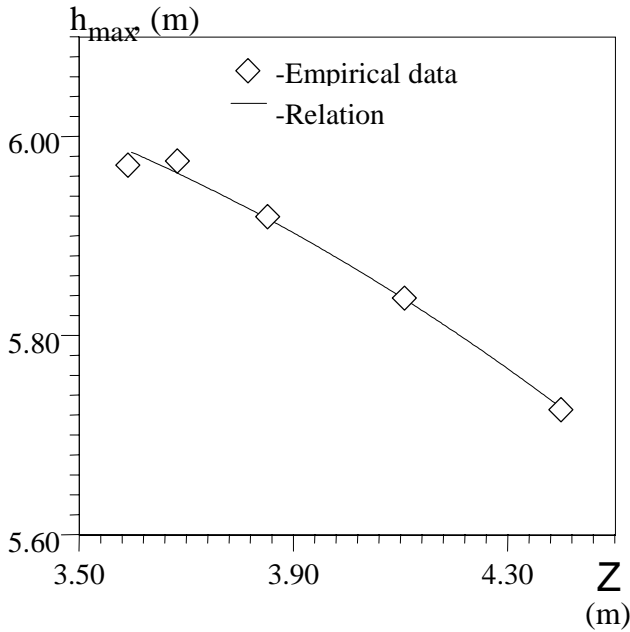The results of computations using relation (5.10) are shown in Fig. 5.2.

Figure 5.2. h_{max} (at 100 year return period) versus Z for the Gumbel distribution

It follows from (5.10) and Fig. 5.2 that quantile h_p in the POT method decreases as Z increases.

Further, it follows from Table 5.1 that function p_k in relation (5.1) can be computed using the Poisson distribution (1.6). Then it is possible to derive the following relation between T and $F(h)$:

$$T = \frac{1}{\lambda F(h)} \tag{5.11}$$

The uncertainty range for estimate h_p computed using relation (5.10) can be derived via (5.11) and (5.9). It is related to the random nature of estimates A* and B* in (5.7) and (5.9) and, as well, to the same random nature of estimates λ* in (1.6). This means that the POT method gives the "true" value of h_{max} that is located in a two - dimensional

area of uncertainty range. The first co-ordinate of this area characterises the possible range of estimates h_p* in terms of wave height (due to uncertainty in *A** and *B**) while the other is related to uncertainty in *p** (due to variations of λ* resulting from using data for a limited number of storms). These areas are shown in Fig. 5.3.

Thus, the POT method estimates depend on the choice of approximations for corresponding distributions. Of course, estimates obtained using other methods do also. However, unlike other methods, in the POT approach the uncertainty is connected both with the wave height h_p^* and return period. For example, the 25 year wave height estimate in Fig.5.3 is found to be in the range of $7.2 - 8.4$ (m), and return period is in the range of 20-45 years.
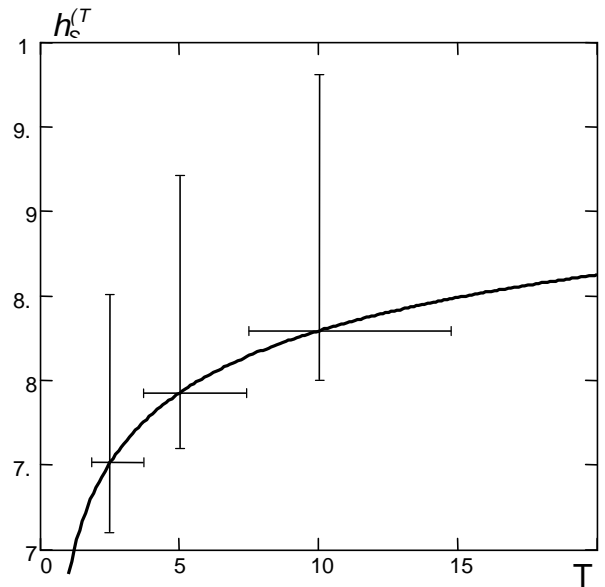

Figure 5.3. Joint uncertainty ranges of POT significant wave height estimates at return periods of 25, 50, and 100 years.

---oooOooo---

CHAPTER 6

Storms and weather windows

The synoptic variability of wind waves is traced back to the frequency of passage of atmospheric disturbances, their strength, the duration of their action on the water surface and the geographic properties of the area. The variability manifests itself as a sequence of alternating storms and weather windows, which can be represented formally (see Fig. I.1) as a sequence of positive (a storm) and negative (a weather window) fluctuations of the random process $\xi(t)$ relative to some fixed value Z.

Let $h(t)$ denote wave heights measured at synoptic observation times. $\Im$ and Θ denote the duration of a period when wave height deviations from Z were positive and negative, respectively.

Then the maximum wave height during the storm is

$$h^+ = \max_{0 \leq t \leq \Im}\{\xi(t)\} \qquad (6.1)$$

The minimal wave height during the weather window is

$$h^- = \min_{0 < t < \Theta}\{\xi(t)\} \qquad (6,2)$$

A system of the four interconnected random variables $\Xi = (h+, h-, \Im, \Theta)$ can be used to parameterize the pulse-like stochastic process shown in fig. I.1.

Table 6.1 gives a description of the data series that were used to study the synoptic variability of wind wave heights [Rozhkov et al., 1999; Boukhanovsky, Lavrenov et al., 1999].

Table 6.1.
Data used in computation of storms and weather windows

Sea	φ, λ	Depth, (m)	Record Length, years	Annual means $h_{0.5}$, (cm)	s	Winter $h_{0.5}$ (cm), s	Spring $h_{0.5}$ (cm), s	Summer $h_{0.5}$ (cm), s	Autumn $h_{0.5}$ (cm), s
Baltic	55°20' 20°30'	30	1957-1991	66	1.8	77 1.7	60 2.0	55 2.3	75 1.8
Black	43°10' 34°00'	2200	1954-1988	73	2.5	92 2.1	73 2.9	60 3.8	72 2.8
Mediterranean	35°10' 35°05'	1070	1980-1994	60	2.6	75 2.2	65 2.8	51 4.3	54 3.2
Barents	71°05' 35°09'	180	1980-1989	119	2.0	143 2.2	115 2.1	97 2.2	129 2.1

For $h(t)$ a multi-year long (10-35 years) time series of mean wave height was taken as simulated by a wave model. The model was driven at regular synoptic times by gridded atmospheric pressure fields. The computations represented a variety of physiographic conditions in internal and marginal seas.

Table 6.2 provides mean *(m)* and root mean square deviation *(σ)* values of four-variable random functions Ξ that were computed using samples from a sequence of storms (from 150 to 1000 storms).

The threshold value Z was taken, correspondingly, equals to quantiles $h_{0.5}$, $h_{0.25}$, $h_{0.75}$, $h_{0.9}$. The breakdown of values is done by seasons, so that synoptic variations of the wind wave fields are described taking into account the annual cycle.

It can be seen from the table 6.2 that for $Z=h_{0.5}$ the average storm duration $\Im$ is two days, while the average duration of weather window Θ is 2–3 days. For larger values of Z, such as $h_{0.75}$, $\Im$ is reduced to one day, and Θ increases.

Random functions $\Im$ and Θ represent duration of over-shots and under-shots. Therefore their distributions should asymptotically tend to the exponential law [Leadbetter, 1986]:

$$F(x) = 1 - exp\left(-\frac{x}{\bar{x}}\right) \qquad (6.3)$$

Figs. 6.1 and 6.2 depict quantiles of distributions $F^*(\Im)$ and $F^*(\Theta)$ as the *q-q* bi-plots. It can be seen that the hypothesis that $F^*(x)$ belongs to a class of exponential distributions is confirmed. Hence *m* and σ should be nearly equal (as seen from Table 6.2). Table. 6.3 gives correlation coefficients between different random functions in system Ξ.

Table 6.2

Estimates of means (m) and r.m.s. (σ of the highest mean waves h+ in storms, lowest mean waves h– in weather windows, duration of storms ℑ and duration of weather windows Θ for thresholds Z that correspond to different quantiles of wave height climatic distributions (left column)

| %	Z, (cm)	h+, (cm)		h–, (cm)		ℑ, (hours)		Θ, (hours)		N
		m	σ	m	σ	m	σ	m	σ	
WINTER (XII,I,II)										
Baltic sea										
25%	53	124	75	37	12	72	79	31	32	653
50%	77	145	73	43	17	55	56	59	60	615
75%	114	185	66	54	30	39	37	111	125	434
Black sea										
50%	92	175	76	61	17	46	38	58	57	656
75%	126	200	72	67	25	34	28	92	95	517
SPRING (III,IV,V)										
Baltic sea										
25%	43	92	52	32	9	70	76	28	26	793
50%	60	105	49	40	15	40	41	57	60	792
75%	83	131	51	40	21	34	33	130	148	482
Black sea										
50%	73	110	49	55	11	37	40	61	62	794
75%	91	141	54	56	18	33	34	159	188	409
SUMMER (VI,VII,VIII)										
Baltic sea										
25%	42	80	34	32	10	61	59	30	30	852
50%	55	84	32	36	12	43	42	42	43	915
75%	74	104	32	38	18	31	27	115	126	518
Black sea										
50%	60	80	17	49	11	39	39	61	71	806
75%	72	88	17	52	15	28	26	120	158	558
AUTUMN (IX,X,XI)										
Baltic sea										
25%	51	117	71	37	11	75	88	33	30	704
50%	75	139	68	44	17	56	61	64	70	623
75%	109	173	63	54	27	43	39	106	131	480
Black sea										
50%	72	110	45	55	13	38	36	59	62	751
75%	91	141	47	56	18	34	28	132	146	393
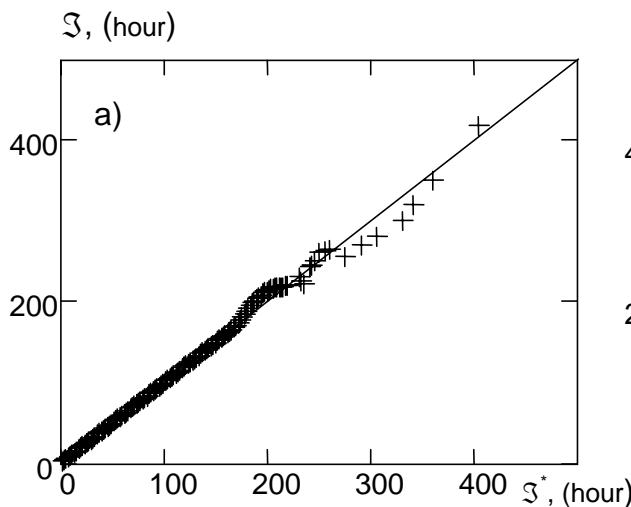
Figure 6.1. Empirical distribution of storm duration F(ℑ) /quantile bi-plot of exponential distribution (6.3)/. The Baltic Sea.
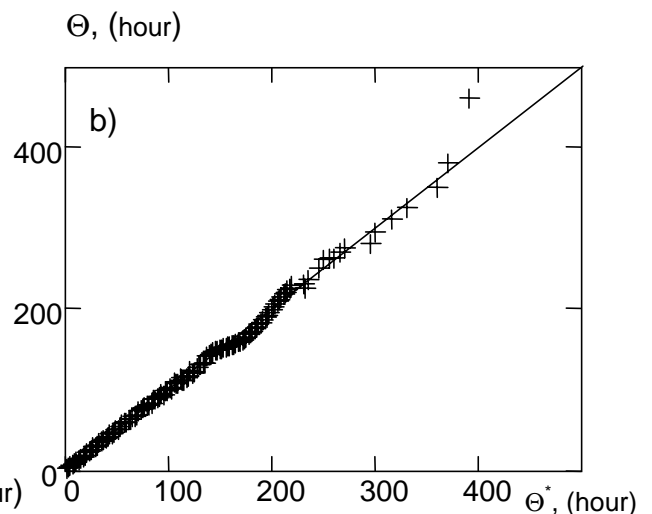
Figure 6.2. Empirical distribution of weather window duration F(Θ) /quantile bi-plot of exponential distribution (6.3)/. The Baltic Sea.

Table 6.3
Correlation coefficients ρ between impulse parameters

Values	(h+,h−)	(h+,Θ)	(h−,ℑ)	(ℑ,Θ)	(h+,ℑ)	(h−,Θ)
ρ	-0.1÷0.15	-0.15÷0.05	-0.1÷0.1	-0.1÷0.1	0.5÷0.8	-0.55÷-0.7

Hence, in the first approximation it is possible to consider parameters *(h+, h−), (h+,Θ), (h−,ℑ), (ℑ,Θ)* independent while parameters *(h−, Θ), (h+,ℑ)* are dependent because their correlation coefficient is in the range of 0.5–0.8.

Hence, the four-dimensional distribution *F(h+, h−, ℑ , Θ)* can be expressed as a product of two two-dimensional distributions *F(h+, ℑ)* and *F(h−,Θ)*, each of them being equal to

$$F(x, y) = F(x)F(y|x) \qquad (6.4)$$

i.e. to multiplication of the marginal distribution *F(x)* and conditional distribution *F(y|x)* where *x = {ℑ,Θ}* and *y = {h+, h−}*.

It follows from definitions (6.1) and (6.2), that the values *h+* and *h−* are extreme values in a sample, so the asymptotic distributions of *F(h+)* and *F(h−)* are close to relations (2.2) - (2.4).

For example, the distribution of *h+* should asymptotically tend towards

$$F\left(h^+ \mid \Im\right) = \begin{cases} \exp\left[-\exp\left(-\dfrac{h^+ - A(\Im)}{B(\Im)}\right)\right], & h^+ \geq Z \\ 0, & h^+ < Z \end{cases} \qquad (6.5)$$

where *A(ℑ)* and *B(ℑ)* are parameters depending on the conditional moments *m(ℑ), σ(ℑ)* via the following relations

$$B(\Im) = \frac{\sqrt{6}}{\pi}\sigma(\Im),$$
$$A(\Im) = m(\Im) - 0.5772B(\Im) \qquad (6.6)$$

Empirical conditional distributions *F(h+|ℑ)* are compared with approximation (6.5) in Fig. 6.3. It can be seen that approximation (6.5) is acceptable. Parameters *A* and *B* for various seas are presented in Table 6.4.

In [Angelides et al., 1981; Boukhanovsky, Lopatoukhin, Ryabinin, 1998] distributions of *h+* are approximated using a family of 3-parameter Weibull distributions

$$F(y/x) = 1 - exp\left[-\left(\frac{y - Z}{A(x) - Z}\right)^{B(x)}\right] \qquad (6.7)$$

where the third parameter *Z* determines the threshold, and two first parameters *A* and *B* are estimated using data in the sample. In those papers a constant value *Z=1.0 m* was adopted for all seasons. Distribution (6.5) with parameters *A* and *B* from Table 6.4, which are dependant on season, function ℑ, and on variable *Z*, is more accurate than the previous approximation (6.7).

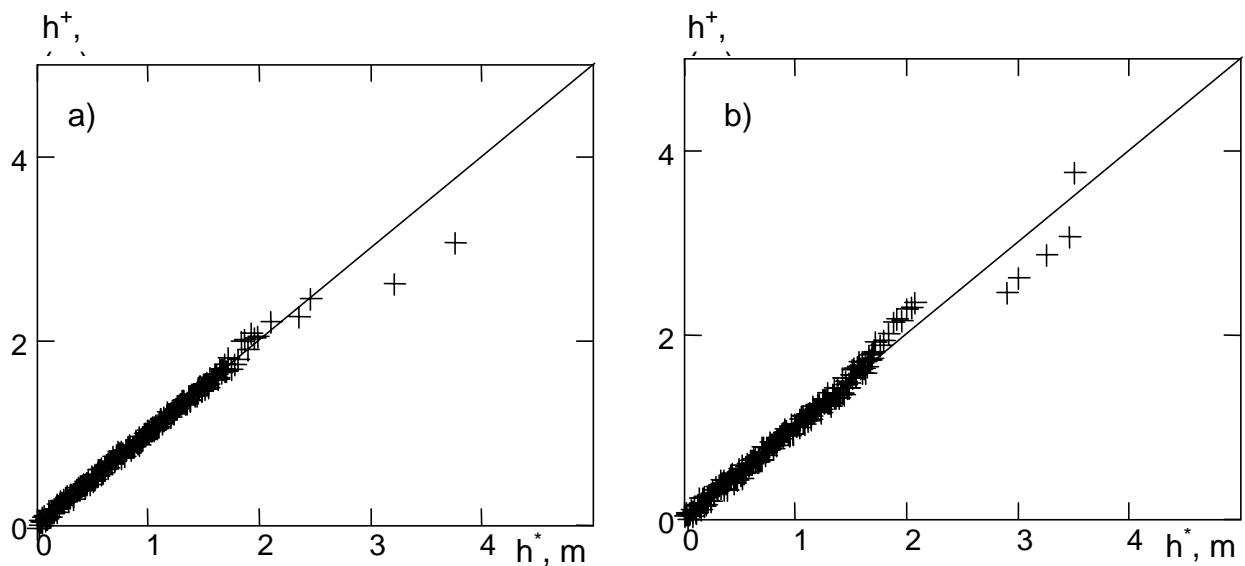**Figure 6.3**. Empirical conditional distribution *h+* (m) of highest waves in storms of different duration ℑ/quantile bi-plot of distribution (6.5)/, a: ℑ ≤ 50 hours, b: 50 < ℑ ≤ 100 hours. Baltic Sea.

Table 6.4.
Parameters A and B of distribution (6.5) for cold and warm seasons and various seas

$\Im$, (hours)	Winter		Summer		Winter		Summer	
	A, (m)	*B*, (m)	*A*, (m)	*B*, (m)	*A*, (m)	*B*, (m)	*A*, (m)	*B*, (m)
The Black Sea					**The Mediterranean Sea**			
0-25	0.19	0.24	0.06	0.05	0.12	0.17	0.04	0.05
25-50	0.51	0.61	0.11	0.12	0.43	0.48	0.09	0.12
50-75	0.60	0.53	0.10	0.12	0.56	0.66	0.13	0.12
>75	0.71	0.60	0.08	0.19	0.50	0.37	0.09	0.08
The Baltic Sea					The Barents Sea			
0-25	0.18	0.19	0.07	0.10	0.22	0.15	0.14	0.12
25-50	0.42	0.48	0.18	0.23	0.45	0.57	0.33	0.39
50-75	0.54	0.57	0.16	0.29	0.52	0.51	0.53	0.34
>75	0.71	0.67	0.16	0.19	0.52	0.37	0.28	0.37

The Monte-Carlo approach and use of expressions (6.3)-(6.5) make it possible to reproduce the whole variety of values of function Ξ:

$$\Im_k = F_{\Im}^{-1}\left(\gamma_1^{(k)}\right), \quad \Theta_k = F_{\Theta}^{-1}\left(\gamma_2^{(k)}\right)$$
$$h_k^+ = F_{h^+/\Im}^{-1}\left(\gamma_3^{(k)}/\Im_k\right), \quad h_k^- = F_{h^-/\Theta}^{-1}\left(\gamma_4^{(k)}/\Theta_k\right) \quad (6.8)$$

Here $\left\{\gamma_i^{(k)}\right\}$ denotes a system of four pseudo-random numbers.

Using a sample of Ξ as a set of impulse parameters in expression (I.7) one can get a stochastic model for a sequence of storms and weather windows. Fig. 6.4 compares correlation functions $K^*(\tau)$ computed by empirical data and impulse model (I.7) with the parameters estimated by (6.8). The similarity between correlation functions of the simulated process and empirical data depends, in a general case, on the shape of the impulse, the correlation between parameters

$\Xi = (h+, h-, \Im, \Theta)t$, and on the probability distributions Ξt, Ξs for various thresholds.

The correlograms in fig. 6.4 are computed using the impulse process model (I.7) accounting for the correlation (6.8) between parameters Ξ but not the correlation between Ξt and Ξs of the sequence of impulses. The figures show good agreement between variances of the simulated and observed process and times of the first zero level crossing.

Let us consider the dependence between two consecutive impulses using a storm classification based on instrumental wave observations in the Black Sea. The data came from a directional wave-rider installed at depth of about 85 m off the town of Gelendzhik. The measurements were recorded every three hours, and every hour during storms. The duration of each record is 20 minutes. The total duration of the series is approximately three years, and it contains more than 6000 wave height records ranging from 0 up to 8.5 m.
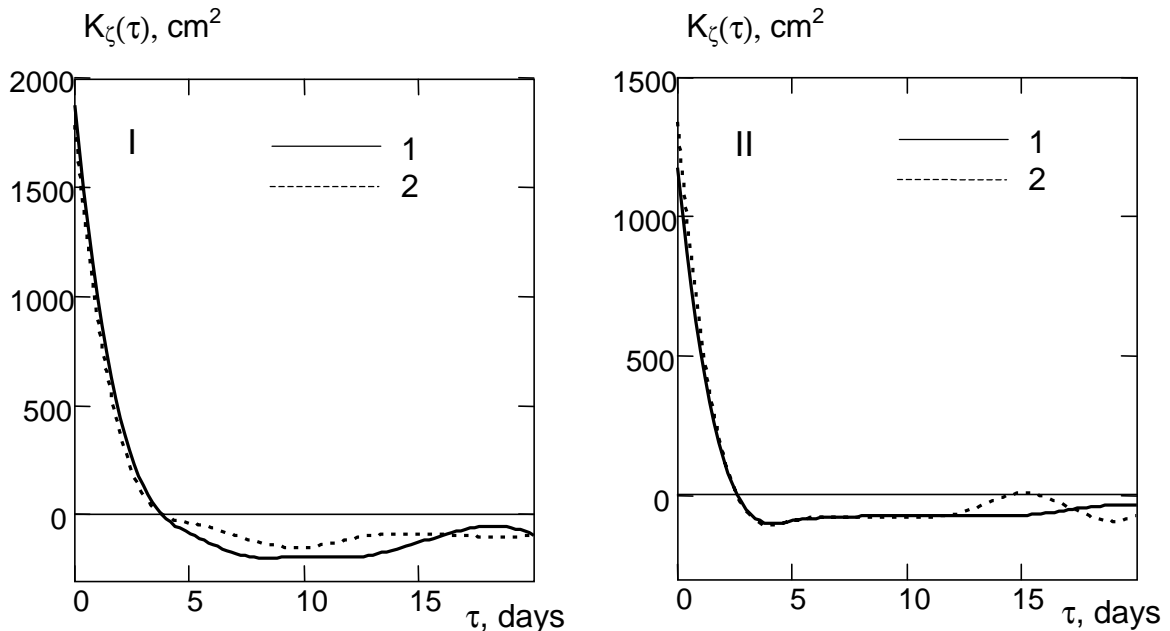

Figure 6.4. Estimates of wave height correlation function on synoptic time scales for Baltic (I) and Black (II) Seas. 1: impulse model , 2: empirical data

The data analysis shows that storm shapes are quite diverse and there are many ways to classify them. The classification results will depend significantly on the selection of Z. For smaller values of Z, shapes are increasingly variable, while for larger values of Z they become more uniform.

In [Boukhanovsky, Lavrenov, et al., 1999] five storm classes were specified (see Table 6.5). The dominating categories correspond to fully developed seas (I), and to wind waves not fully developed due to limitations of fetch or wind duration (II). The categories III and IV correspond to combined waves.

Storms of category V, which are defined as series of storms with wave heights exceeding a threshold Z, usually have the longest duration. Doubling of Z leads to almost complete disappearance of storm category V so that only four first categories remain.

B.V. Divinsky used methods of discriminant analysis and came up with a more detailed classification of storms than is given in Table 6.5. He proposed eight types of storms for wave heights exceeding mean seasonal wave height $h=Z$ and four types for wave heights exceeding $h=2Z$ and $h=3Z$. These are given in Table 6.6. Further, B.V. Divinsky considered the correspondence between each storm type and dominating meteorological conditions. It is worth mentioning that, in spite of differences in the classification methods, the whole set of storm shapes for wave heights exceeding $h=2Z$ fell almost similarly into four groups. Some differences in percentage in Tables 6.5 and 6.6 are due to varying criteria for attributing a storm to a certain category.

Weather windows can also be classified similarly. Table 6.7 shows a corresponding classification proposed by B.V. Divinsky.
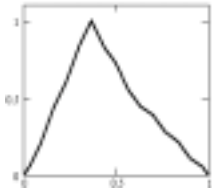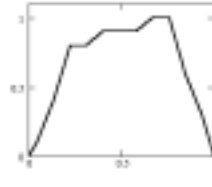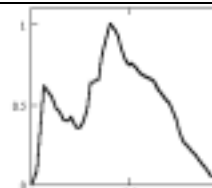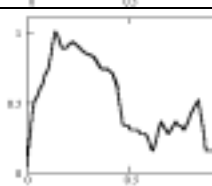
Table 6.5
A classification of storm shapes
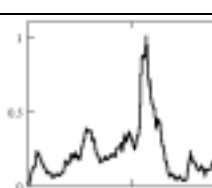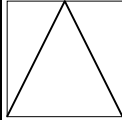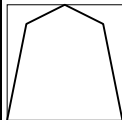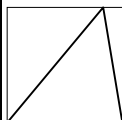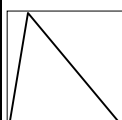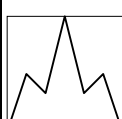
Category	Non-dimensional shape — abscissa is $(t-t_b)/\Im$, ordinate is h/h^+	Threshold Z=1.0 $\overline{\overline{h}}(t)$ where $\overline{\overline{h}}(t)$ is seasonal mean wave height				Threshold Z=2.0 $\overline{\overline{h}}(t)$ where $\overline{\overline{h}}(t)$ is seasonal mean wave height			
		P, %	N	Wave height h (cm)	Duration S (hour)	P, %	N	Wave height h (cm)	Duration S (hour)
I		50%	110	$h_{95\%}=207$ $m_h=61$ $\sigma_h=57$ $h_{5\%}=21$	$S_{95\%}=45.5$ $m_S=11.0$ $\sigma_S=14.2$ $S_{5\%}=1.0$	49%	78	$h_{95\%}=241$ $m_h=105$ $\sigma_h=59$ $h_{5\%}=44$	$S_{95\%}=25.8$ $m_S=6.9$ $\sigma_S=8.0$ $S_{5\%}=0.7$
II		15%	33	$h_{95\%}=203$ $m_h=84$ $\sigma_h=54$ $h_{5\%}=22$	$S_{95\%}=71.7$ $m_S=28.7$ $\sigma_S=22.4$ $S_{5\%}=5.0$	24%	38	$h_{95\%}=267$ $m_h=121$ $\sigma_h=63$ $h_{5\%}=43$	$S_{95\%}=38.3$ $m_S=14.8$ $\sigma_S=10.3$ $S_{5\%}=1.8$
III		6%	13	$h_{95\%}=273$ $m_h=138$ $\sigma_h=75$ $h_{5\%}=33$	$S_{95\%}=95.5$ $m_S=44.9$ $\sigma_S=25.4$ $S_{5\%}=8.5$	13%	20	$h_{95\%}=207$ $m_h=137$ $\sigma_h=61$ $h_{5\%}=66$	$S_{95\%}=36.0$ $m_S=19.6$ $\sigma_S=11.0$ $S_{5\%}=5.0$
IV		19%	41	$h_{95\%}=273$ $m_h=108$ $_h=63$ $h_{5\%}=44$	$S_{95\%}=82.5$ $m_S=40.9$ $_S=23.3$ $S_{5\%}=12.2$	13%	20	$h_{95\%}=277$ $m_h=134$ $_h=60$ $h_{5\%}=42$	$S_{95\%}=110.5$ $m_S=34.0$ $_S=25.1$ $S_{5\%}=3.5$
V		10%	22	$h_{95\%}=197$ $m_h=104$ $_h=64$ $h_{5\%}=31$	$S_{95\%}=135.8$ $m_S=70.0$ $_S=41.5$ $S_{5\%}=9.5$	1%	2	$h_{95\%}=181$ $m_h=181$ $_h=1$ $h_{5\%}=180$	$S_{95\%}=184.5$ $m_S=118.8$ $_S=65.7$ $S_{5\%}=53.1$

Table 6.6
A classification of storm shapes based on discriminant analysis

Type	Shape	Description	Threshold					
			1h	**2h**	**3h**	*1h*	*2h*	*3h*
			Number of storms			%		
I		Monotonic increase and decrease of wind	39	21	14	20.3	23.1	41.2
II		Stable wind at phase of maximal storm development	40	39	4	20.8	42.9	11.8
III		Duration of increase is considerably longer than one of decrease. This type is specific for "slow" storms	33	16	7	17.1	17.6	20.6
IV		Expressed asymmetry of the shape with domination of the decrease phase. This type is specific for "quick" storms	37	15	9	19.3	16.4	26.4
V		The discriminant analysis gives a separate type for this storm shape. It bears some similarity to type IV. This shape is typical for fast and deep cyclones	12	*	*	6.3	*	*
VI		Intermittent increase and decrease of waves caused by instabilities of the atmospheric flow. They are typical for a shallow or a slow moving cyclone	8	*	*	4.2	*	*
VII		Passage of a deep cyclone with distinct separation of fronts. Depending on the cyclone track wind wave field either develops having swell as its background or generates swell as a residual signal	19	*	*	9.9	*	*
VIII		A "chain" of storms, which cannot be separated due to small threshold value of Z	4	*	*	2.1	*	*

A matrix of probabilities that a certain storm category in Table 6.5 (for *h=Z*) will transform into another category is shown in Table 6.8 It follows from the table that there is some weak correlation between categories of consecutive storms.

The annual cycle of storms manifests itself in variations of monthly mean wave height $\bar{h}(t)$ between seasons. Also, synoptic variability is higher in winter than in summer.

Such cyclical variations can be expressed as

$$\xi(t) = m(t) + \sigma(t)[\xi_t + \eta(t)] \qquad (6.9)$$

where *m(t)* is the multi-year norm (i.e. annually averaged value) of mean wave height. It is equal to the mathematical expectation of the periodically correlated random process. *σ(t)* is r.m.s. deviation of monthly mean wave heights from m(t). The process ξ(t) can be modelled by (I.8)-(I.9) or (I.10)-(I.11). Lastly, *η(t)* is an impulse-like random process, which can be represented by (I.7) with parameters (6.8).

Table 6.7
A classification of weather windows
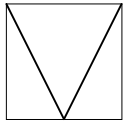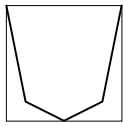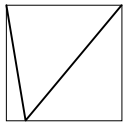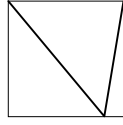
Type	Shape	Description	Threshold					
			1h	*2h*	*3h*	*1h*	*2h*	*3h*
			Number of weather windows			%		
I		Smooth decrease and then increase of storm activity	31	22	16	14.9	22.2	47.1
II		Wind waves in the "window" are much weaker than the selected threshold value *h*	67	17	14	32.2	17.2	41.2
III		Gradual increase of storm activity or result of passage of a chain of storms with different tracks	39	14	*	18.8	14.1	*
IV		Strong residual wave field that is decaying after storm passage	49	16	*	23.6	16.2	*
V		Wave heights close to the threshold value *h*	22	30	4	10.5	30.3	11.7

Table 6.8.
Probability matrix of transformation of one storm category into another

Storm category	I	II	III	IV	V
I	0.5	0.1	0.1	0.2	0.1
II	0.3	0.1	0.2	0.2	0.2
III	0.6	0.2	0.1	0.1	---
IV	0.3	0.2	0.2	0.3	---
V	0.2	0.3	0.2	0.4	---

---oooOooo---

CHAPTER 7

Method of quantile function (BOLIVAR)

The basis of the POT method is independence of wave heights in different storms. In the previous chapters we showed, however, that a storm sequence may be regarded as a Markov' s chain. In order to exclude the limitations of the POT method and to take into account the asymptotic characteristics of AMS, let us consider n samples, consisting of heights h_{ij}^+ of the largest waves in the k strongest storms in year number $i,(i=1,..,n; j=1,..,k)$.

In accordance with definition (6.1), each of these samples is comprised of wave heights observed during different storms (no more than one height is taken from each storm). Let us sort each of the samples in decreasing order. This will give us the following ranked series:

$$\left(h_{11}^+ \ge h_{12}^+ \ge \ldots \ge h_{1k}^+\right) \ 1^{st} \ year$$
$$\left(h_{21}^+ \ge h_{22}^+ \ge \ldots \ge h_{2k}^+\right) \ 2^{nd} \ year$$
$$\ldots\ldots\ldots\ldots\ldots\ldots \quad (7.1)$$
$$\left(h_{n1}^+ \ge h_{n2}^+ \ge \ldots \ge h_{nk}^+\right) \ n^{th} \ year$$

The number k of elements in each sample may vary but $k \ge 1$. For $k = 1$ (i.e. one storm in a year) this constitutes a sample of the highest waves.

$$\left(h_{11}^+, \ldots, h_{n1}^+\right) \quad (7.2)$$

for all n years considered. Their distribution was discussed in Chapter 2 of this review.

The maximum wave height h_{max} which is possible once in n years, is the extreme (i.e. last term) element of the samples, both (7.2) and (7.1).

The order statistics h_{ij}^+ are estimates of quantiles x_p. Their probabilistic properties are represented by the joint probability distribution function

$$G(x_1, \ldots, x_k) = P\left\{h_{i1}^+ < x_1, \ldots, h_{ik}^+ < x_k\right\} \quad (7.3)$$

This is called the quantile function. A method of estimation of highest waves, which is based on equations (7.1)-(7.3), is called BOLIVAR [Boukhanovsky, Lopatoukhin, Rozhkov, 1997; Boukhanovsky, Lopatoukhin, Rozhkov, 1998 (a,b); Rozhkov et al., 1999; Boukhanovsky, Lavrenov, Lopatoukhin, Rozhkov, 1999]. Its name is derived from characters of the author names.

Heights h^+ of the highest waves in a sequence of storms in a single year can be considered correlated. Fig. 7.1 shows point diagrams of the highest waves h_{i1}^+ and h_{i2}^+ in the two strongest storms during an individual year in the Black, Baltic, and Barents Seas.

It can be seen from Fig. 7.1 that there is a relationship between h_{i1}^+ and h_{i2}^+. This is related to the fact that h^+ in the second strongest, the third and other corresponding storms in a single year must be lower than the maximum one by definition, which generates a correlated sequence of maximum wave heights in storms.
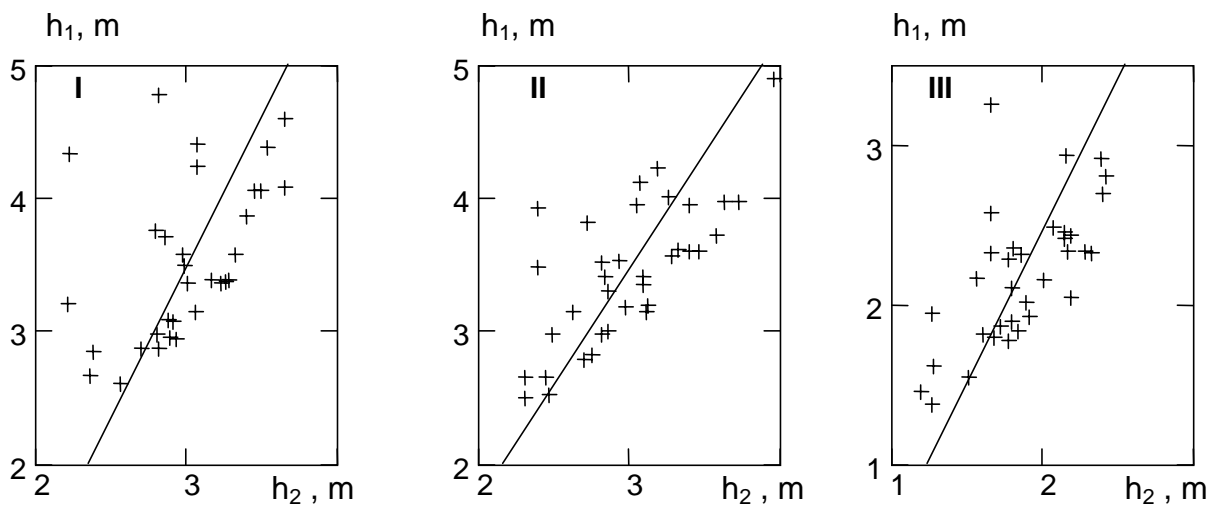

Figure. 7.1: Point diagram of first and second annual maxima (+) of mean wave heights in the Black (I), Baltic (II) and Barents (III) Seas. The solid line represents linear regression.

It is known from statistics that ranking of a sample with the distribution density *f(x)*, even if initially not correlated, leads to correlation between its statistic of ith and jth order [David, 1969]:

$$cov\left(x_i^*, x_j^*\right) \approx \frac{i}{n}\left(1 - \frac{j}{n}\right)\frac{1}{nf\left(x_{i/n}\right)f\left(x_{i/n}\right)}$$

In particular, for *n* ≈ *30–40* the correlation between the first two elements in the ranked sample reaches 0.6 – 0.7. Assuming that not only the extreme element of the sample h_{i1}^{+} but also the following element h_{i2}^{+} has the same asymptotic distribution , we get:

$$G\left(x_1, x_2\right) = G\left(x_1\right)G\left(x_2 | x_1\right) \qquad (7.4)$$

where *G(•)* is Gumbel distribution (2.2).

Then the parameters of the conditional distribution *G(x₂|x₁)* should depend on parameters of *G(x₁)*. Fig. 7.2 shows a comparison of empirical distributions of the first (annual highest), second and third highest wave heights with the theoretical distribution (2.2).

Fig. 7.2 confirms the hypothesis that the empirical data is distributed according to (2.2). Fig. 7.3 shows quantile diagrams (the median, upper and lower 10% bounds of the distribution) of the first eight maxima of wave height. It can be seen that distributions of ranked wave heights in a single year are similar. Thus, with some degree of approximation, it is possible to produce certain generalized relations between medians Me(h$_k^+$)/Me(h$_1^+$) and r.m.s deviations $\sigma_{h_k^+}/\sigma_{h_1^+}$ of the first and other maxima. These are represented in fig. 7.4.
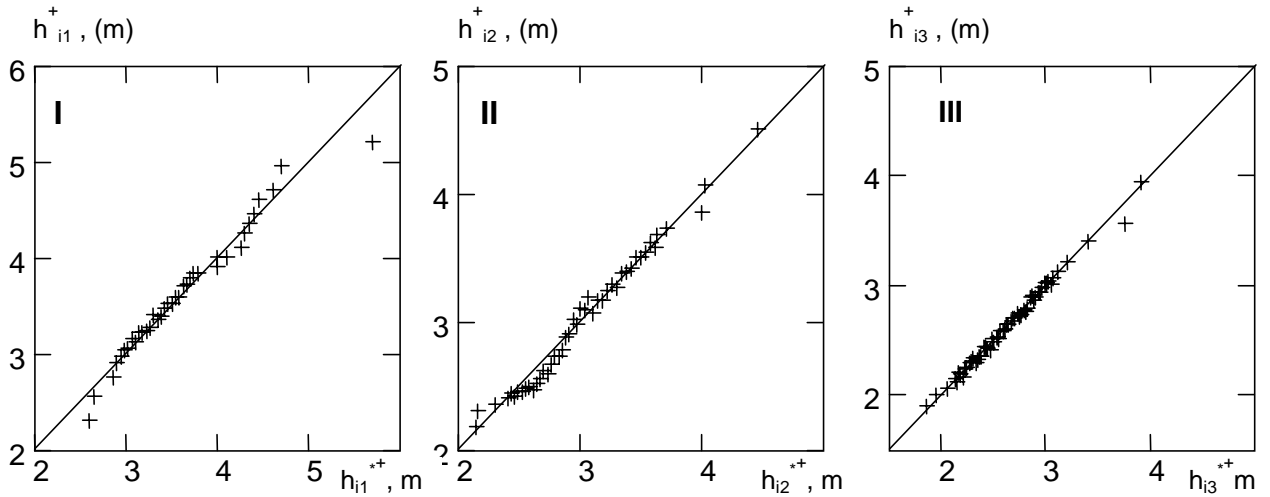

Figure.7.2: Bi-plots of annual maxima distribution.
The Black sea. I, II, III: the first, second, and the third annual maxima, respectively.
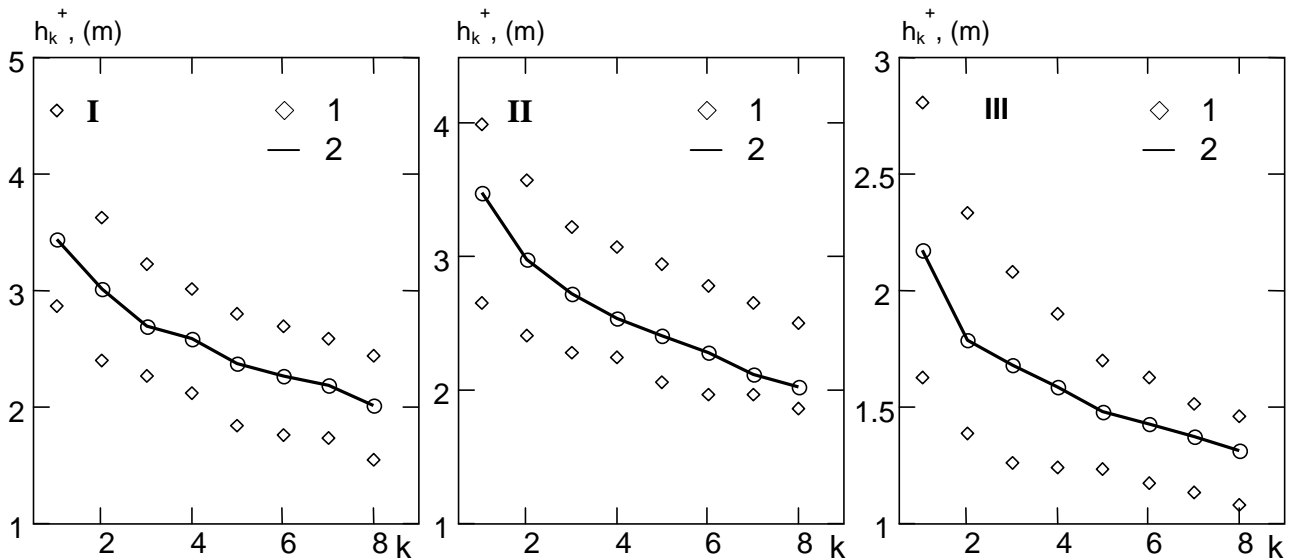
Figure. 7.3: Quantile diagrams for consequential annual maxima *h$_k$* in the Black (I), Baltic (II) and Barents (III) Seas. 1: upper and lower 10% bounds of distribution, 2: median.
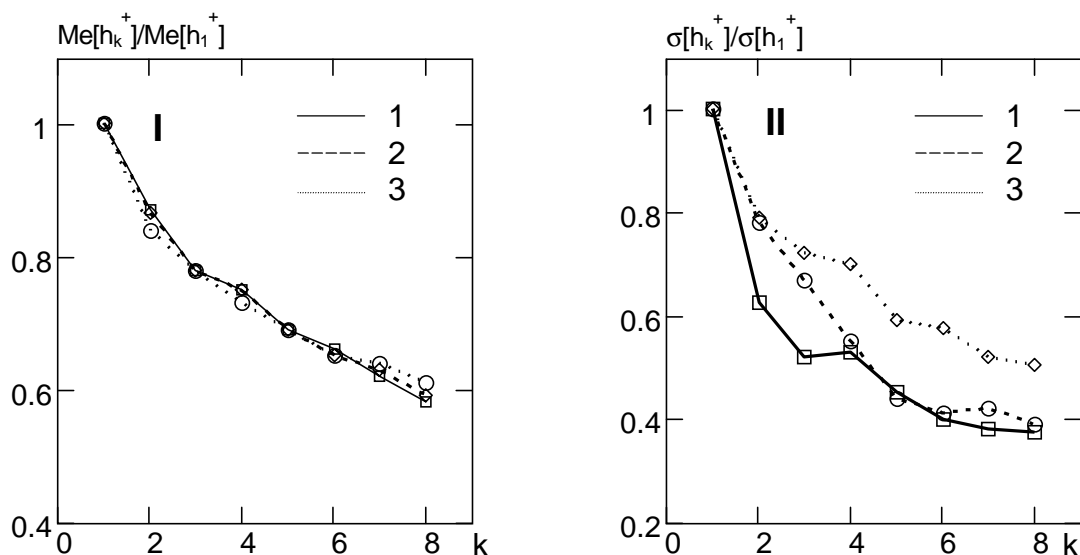
Figure. 7.4. Normalised median (I) and r.m.s deviation (II) of consequential annual maxima h_k.
1: Black Sea, 2: Baltic Sea, 3: Barents Sea.

Stochastic simulation based on the storm and weather window model (6.9) is the main technique for computing the distribution (7.3). It takes into account both intra-annual and year-to-year cycles. Fig. 7.5 shows quantile diagrams (the median, upper and lower 10% distribution bounds) computed using a 35-year (see table 6.1) and a 100-year simulated series, from (6.9). It follows from Fig. 7.5 that the agreement between observed and simulated data is satisfactory, which, in turn, confirms the correct choice of probabilistic model.

Let us consider distributions (7.3) and (5.1). Let p_k denote the probability that during the year number i the number of storms of certain intensity was k. Then the multi-dimensional distribution of probability of maximum wave heights in a sequence of storms that exceed a specified threshold will be

$$F(x_1, \ldots x_m) = \sum_{k=1}^{m} p_k(x_1, \ldots, x_k), \quad m = 1,2,3\ldots$$

Distribution (7.5) generalizes (5.1) because it does not require an assumption that wave heights in the storms are independent. Distribution (7.3) is valid for waves from different storms. According to the way the distribution (7.1) was constructed, it makes it possible to distinguish wave heights that are to be expected once in 100 or 50 years, and also to estimate wave heights h_1^+ and h_2^+, that can take place during a single year during an interval of n years. For example, the height of the first annual maximum in the southern part of the Baltic Sea, at a return period of 100 years, is $h_1^{(100)}$ =5.1 m.

This coincides with the prediction by the AMS method. The second annual maximum, at 100 year return period, is $h_2^{(100)}$ =4.1 m.
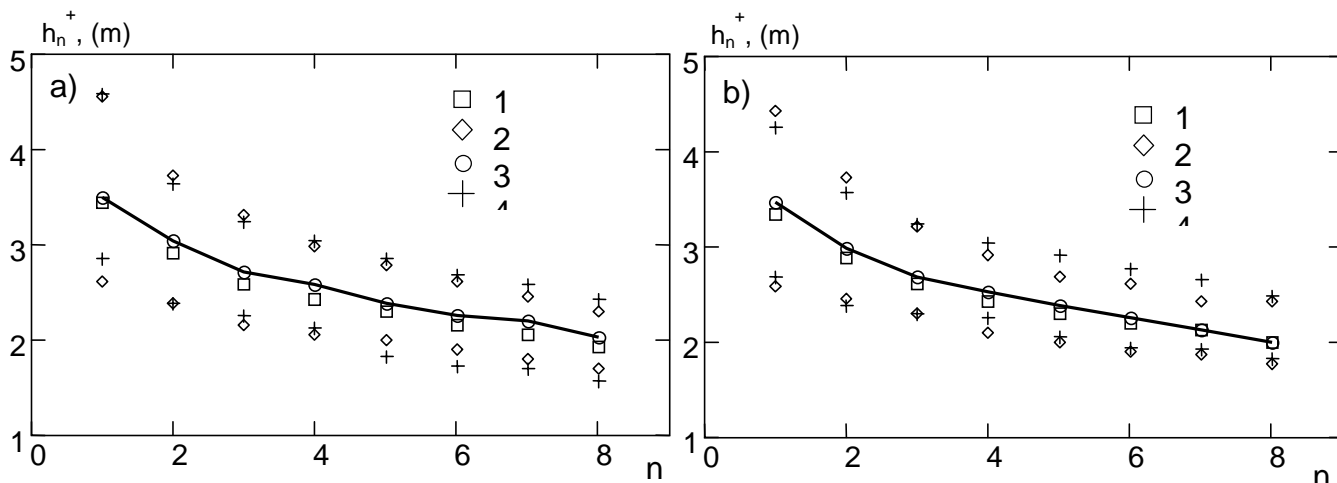
Figure 7.5: Medians (1,3) and deciles (2,4) of wave heights in the eight strongest storms in (a) the Black and (b) the Baltic Seas. (1,2): data from Table 6.1. (3,4): simulations using the probabilistic model (6.9).

This differs from the wave height possible once in 50 years, which is $h_1^{(50)}$ =5.0 m. For a point in the Barents Sea we obtained the following estimates: $h_1^{(100)}$ = 6.4m, $h_2^{(100)}$ = 4.6m, $h_1^{(50)}$ = 6.0m, $h_2^{(50)}$ =4.4 m.

Fig. 7.6 shows distributions of the first, second, and third annual maxima in the southern part of the Baltic Sea on the Gumbel probability plot (see (2.5)). They were computed using (7.3). In addition, the figure contains distributions $G(h)$ of all maxima exceeding Z =3.9 m and Z=3.2 m.

It can be seen from fig. 7.6 that for wave heights exceeding a sufficiently high value (i.e. 3.9 m), the contribution of the second maxima to distribution $G(h)$ is insignificant. Distribution $G(h)$ corresponds closely to that of all first annual maxima (up to the accuracy of assigning a certain probability $p_n=1/\lambda T$ to its quantiles).

At the same time, the question of whether the distribution can be reliably estimated using data on its several upper quantiles remains open. It can be seen that for a somewhat lower threshold level $Z=3.2\ m$, data (6) denoted by circles represent a mixture of first, second, and third annual maxima. This gives more weight to the "left" tail of the distribution and, in turn, leads to lower estimates for long return period wave heights.
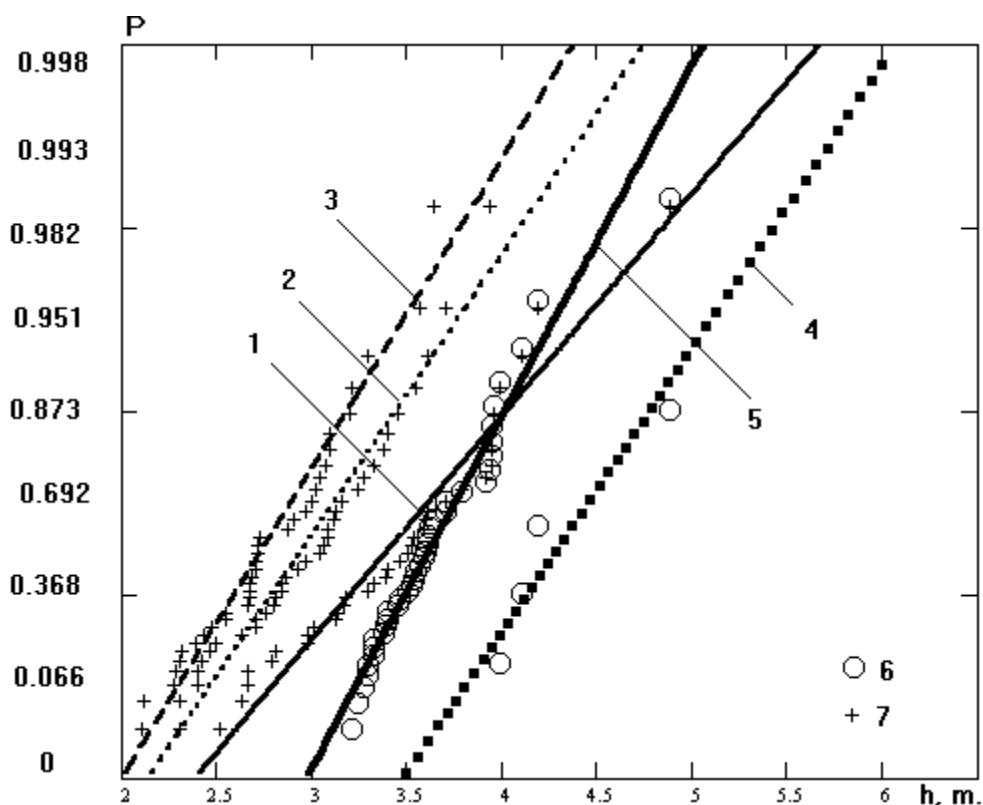
Figure 7.6: Distribution of annual wave height maxima.
1,2,3: The first, second, and third maxima simulated using (7.3). 4: Distribution of all maxima exceeding Z=3.9(m). 5: Distribution of all maxima exceeding Z=3.2 (m). 6: A mixture of all strong storms.
7: Samples made of observed first, second, and third maxima.

---oooOooo---

CHAPTER 8

Annual cycle of extreme wave heights

Monthly mean wave heights $\overline{\overline{h}}$ form a data set, which provides the most convenient information for studying intra–annual variations of extreme wave heights. Twelve values of monthly mean wave heights, which are observed during a year numbered i, form a sample h_{ij}. Examination of these samples for n years, i.e. h_{ij}, i = 1,...,n, shows that the annual extreme value of wave height $\max\limits_{j}(h_{ij})$, $\min\limits_{j}(h_{ij})$ can be observed during various months. Table 8.1 shows how often an annual maximum $\overline{\overline{h}}_{\max}$ was observed during a certain month.

Table 8.1

Frequency of occurrence (%) of annual maximum $\overline{\overline{h}}_{\max}$ in different months

Sea	Months							
	IX	X	XI	XII	I	II	III	IV
Baltic	3	6	34	27	17	3	10	0
Black	0	0	3	26	26	37	8	0
Mediterranean	0	0	0	7	33	34	13	13
Barents	0	10	20	20	10	30	10	0

Thus, the period, during which $\overline{\overline{h}}_{\max}$ can occur, is almost half a year long, from autumn to the next spring. For example, during 35 years of observations the annual maximum in the SE part of the Baltic Sea took place in September in 3% of cases, and in October in 6% of cases.

The distribution function of monthly mean extremes $\overline{\overline{h}}_{\max}$ can be represented as a mixture:

$$F_{max}(x) = \sum_{k} p_n F_k(x) \qquad (8.1)$$

where p_n is frequency of occurrence (similar to that given in Table 8.1) and $F_k(x)$ is the distribution of monthly mean for the nth month over several years.

Monthly mean wave heights are obtained through averaging values observed at synoptic times. Therefore, we can assume that $F_n(x)$ follows the normal distribution. Table 8.2 gives maximum $\overline{\overline{h}}_{\max}$ and minimum $\overline{\overline{h}}_{\min}$ estimates of yearly extremes, yearly means m, r.m.s. deviations σ, estimates of skewness (A) and kurtosis (E) for different seas.

Table 8.2.

Characteristics of monthly mean wave height extremes

Sea	T	Max					Min				
		m	σ	A	E	$\overline{\overline{h}}_{\max}$	m	σ	A	E	$\overline{\overline{h}}_{\min}$
	(years)	(m)	(m)			(m)	(m)	(m)			(m)
Baltic	35	1.20	0.20	0.75	0.86	1.81	0.51	0.04	-0.68	-0.45	0.41
Black	35	1.21	0.16	0.54	-0.05	1.59	0.57	0.04	-1.00	0.06	0.46
Mediterranean	15	0.99	0.16	1.42	2.20	1.45	0.48	0.03	0.70	0.48	0.42
Barents	10	1.82	0.15	0.58	-1.13	2.08	0.95	0.08	-0.73	0.36	0.77

Coefficients of skewness and kurtosis for the normal distribution are equal to zero. For $T = 35$ (years) the 95% confidence limits will be $|A^*| < 0.8$ and $|E^*| < 1.4$, and for $T = 10$ (years) $|A^*| < 1.2$, $|E^*| < 1.8$. Only the estimates A^* for $\overline{\overline{h}}_{\min}$ in the Black Sea and (A^*, E^*) for $\overline{\overline{h}}_{\max}$ in the Mediterranean Sea do not satisfy this condition.

Quantiles x_p of the normal distribution are as follows: $x_{0.9} = 1.28$, $x_{0.95} = 1.64$, $x_{0.975}=1.96$, and $x_{0.99}=2.33$.

Hence, we can assume for $\overline{\overline{h}}_{max}$ possible once in 100 years (at probability 0.99 when annual maximums were used):

$$\overline{\overline{h}}_{max} = m^* + 2.33\sigma^*$$

where m^* and σ^* are corresponding estimates.

The mathematical expectation of ith order statistics $x_{(i)}$ for normally distributed samples is [David, 1969]:

$$m_{x_{(i)}} \approx \Phi^{-1}\left(\frac{i-0.375}{n+0.25}\right) \qquad (8.2)$$

and the variance is

$$D_{x_{(i)}} \approx \frac{\left(\frac{i}{n+1}\right)\left(1-\frac{i}{n+1}\right)}{(n+2)\varphi^2_{i/(n+1)}} \qquad (8.3)$$

where $\Phi(\bullet)$ and $\varphi(\bullet)$ are the function and density of the normal distribution.

In Table 8.3 values of $\overline{\overline{h}}_{max}$ for the T year interval from Table 8.2 are compared with the corresponding quantile of the distribution and the 95% confidence range bounds of estimate x_p^*. The latter was computed using relations (8.2), (8.3).

Also, the table gives quantiles of the 95% probability interval for the double exponential distribution (2.5) which can be interpreted as an asymptotic approximation of the last term in the ranked sample of monthly extremes.

If the initial distribution is normal, then the distribution of extreme values will obey (2.5) with parameters *a* and *b* determined as follows [Hirtzel, 1984; Lopatoukhim et al., 1991]:

$$a = \sqrt{2\ln N}$$
$$b = a - \frac{\ln\ln N + \ln 4\pi}{2\sqrt{2\ln N}} \qquad (8.4)$$

Table 8.3.

Estimates of $\overline{\overline{h}}_{max}$ by initial data and models (8.2)-(8.4)

Sea	T	$\overline{\overline{h}}_{max}$	Model (8.2)-(8.3) T-year estimate			Model (2.5), (8.4) T-year estimate		
	(years)	(m)	$M[\overline{\overline{h}}_{max}]$	$h_{0.025}$	$h_{0.975}$	$M[\overline{\overline{h}}_{max}]$	$h_{0.025}$	$h_{0.975}$
Baltic	35	1.81	1.62	1.42	1.82	1.63	1.49	1.87
Black	35	1.59	1.54	1.34	1.75	1.56	1.44	1.74
Mediterranean	15	1.45	1.27	0.87	1.66	1.28	1.15	1.49
Barents	10	2.08	1.98	1.14	2.81	2.08	1.94	2.31

It can be seen from Table 8.3 that, for *T>15* years, the estimates of the order statistics $x_{1-1/T}$ of annual extreme values follow normal distribution fairly well and are close to the median of distribution (2.5). Confidence ranges of h_{max} are close to the probability intervals of the double exponential distribution (2.5).

If *T≤15* years, models (8.2)-(8.3) and (2.5), (8.4) lead to different estimates. It is obvious that it is difficult to justify the use of asymptotic theory for samples of short length.

If distribution (8.1) differs considerably from the normal one, estimates of probabilistic characteristics can be obtained using the Monte-Carlo approach. The median of the simulated series of $\overline{\overline{h}}_{max}$ in the Mediterranean Sea was estimated to be 1.39 m. The 95% probability range was 1.26 – 1.55 m.

In a case when the frequency of occurrence p_i in (8.1) is unknown, it can be computed using stochastic models (I.8)-(I.9) or (I.10)-(I.11).

Table 8.4.

Estimates p_i (%) based on observations and simulation. The Black Sea

Month	XI	XII	I	II	III
p_i, Table 8.1	3	26	26	37	8
p_i^*, model (I.8)-(I.9)	1	29	26	35	9
95% confidence limits	±1	±4	±4	±4	±2

Table 8.4 shows comparisons of values p_i from Table 8.1 with values p_i^* obtained using the model of periodically correlated random process [see (I.8)-(I.9)] for given values of mathematical expectation $m(t)$ and covariance function $K(t,\tau)$.

It follows from Table 8.4 that the estimates p_i and p_i^* are very close and their difference does not exceed the confidence range:

$$I_{0.95_k} = 4\sqrt{\frac{p_k^*\left(1-p_k^*\right)}{T}}$$

where T is the sample length (years), see Table 8.1.

There are different approaches towards description of wind wave seasonal variability. In the reports [Bacon et al., 1989; Stanton, 1984] seasonal changes of extreme waves in the Atlantic Ocean are studied. It is suggested that distribution (2.5) with periodic parameters $a(t)$ and $b(t)$ could be used to reproduce seasonal variations of minimum and maximum wave heights. Then the distribution of annual maxima is represented as the product

$$F(h) = \prod_{t=1}^{12} exp\left[-exp\left[-a(t)(h-b(t))\right]\right] \quad (8.5)$$

Formula (8.5) interprets the annual extreme wave height as maximum maximorum, i.e. as the maximal value of all maximal wave heights in individual months. Unlike (8.5), model (8.1) makes it possible to determine the probability p_n that the annual maximum will take place during a certain month. Values p_n can be estimated using observations in various seas and it also is possible to simulate them using the model of intra-annual cycles (I.8)-(I.11).

Annual variations of wind waves justify the need to consider them as a periodically correlated non-stationary random process obeying the log-normal distribution (I.5) with periodic parameters $h_{0.5}(t)$ and $s(t)$. An illustration of usefulness of this approach is given in Fig I.3 showing annual variations of the $h^*_{0.5}$ and s^*. These were computed using wave height measurements at synoptic times. In some papers [see (Athanossoulis G.A., Stephankos Ch.N., 1995; Rossouw J. et al., 1995; Stephanakos, 1999)] similar graphs for mean wave heights and their variances are provided.

Fig. (I.3) suggests that the function of wave height distribution at synoptic times $F_h(x,t)$ must take intra-annual cycles into account. This can be written as follows:

$$F_h(x,t,\theta) = \int\limits_{\langle h_{0.5},s\rangle} F_h(x,y,\sigma)f_{h_{0.5},s}(y,\sigma,\theta(t))dyd\sigma \quad (8.6)$$

where $F_h(x,y,\sigma)$ is the climatic log-normal distribution $(h_{0.5}=y, s=1/\sigma)$. Variables $h_{0.5}$ and s in (8.6) form a system of random numbers with a two-dimensional distribution density $f_{h_{0.5},s}(\bullet)$. This distribution depends on a set $\theta(t)$ of parameters $\left(a_{h_{0.5}},a_s\right)$ and $\left(b_{h_{0.5}},b_s\right)$ for location values and scales. According to [Smirnov et al., 1969] the median $h_{0.5}$ is asymptotically normally distributed (see, e.g., ["Veter i volny" (Wind and waves), 1974]). Parameter s may be estimated by quantiles $h_{0.25}$ and $h_{0.75}$ as follows

$$s = \frac{1.35}{ln\left(h_{0.25}/h_{0.75}\right)}$$

Fig 8.1 shows bi-plots of normal distribution for values $h^*_{0.5}$ and σ. It can be seen that the distribution of $h_{0.5}$ and of standard of wave height logarithm σ is approximated by the normal distribution.
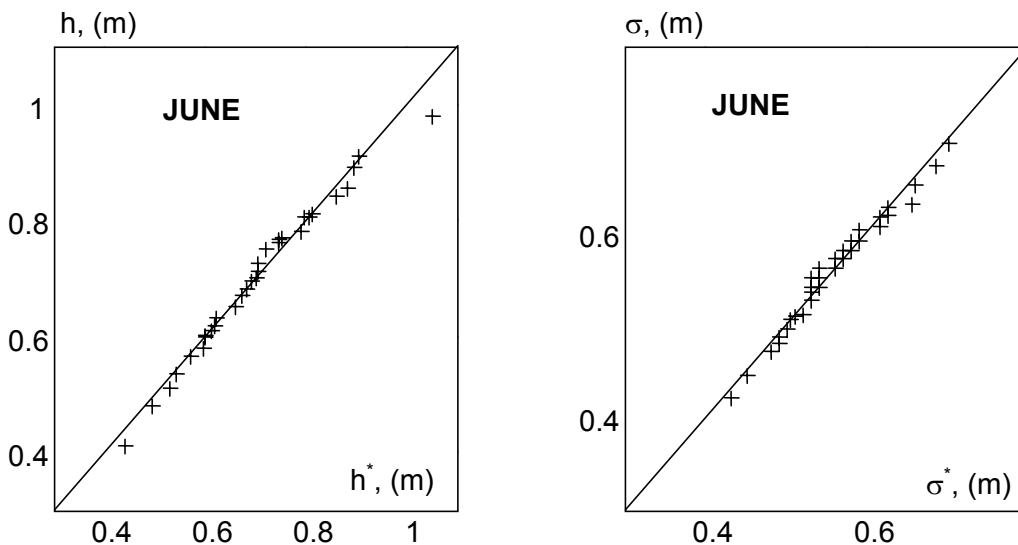

Figure 8.1: Normal distribution bi-plots of median $h_{0.5}$ and standard deviation σ of wave height logarithms. The Baltic Sea

Table 8.5 shows estimates of random values $h_{0.5}$, s, distribution quantiles for different seas and seasons. In the rows containing sea names, the time series length T (in years) is also given, as well as parameters $h_{0.5}$ and s, which are calculated for the whole time series, i.e. without the seasonal cycle. The table also shows quantiles of the highest mean wave height in a season. These correspond to the first term in ranked samples h_{ij} consisting of 360 values (90 days 4 times each) per year.

Table 8.5.

Estimates of quantiles h_p, mathematical expectation M (m), standard deviation σ (m),

of median $h_{0.5}$ (m), parameter s, and maximal wave height $\overline{h}_{max}$ for different seas and seasons.

Variable X denotes $\{h_{0.5}, s, \overline{h}_{max}\}$. Data correspond to mean wave heights at synoptic times

X	Winter			Spring			Summer			Autumn		
	$h_{0.5}$ (m)	s	$\overline{h}_{max}$ (m)	$h_{0.5}$ (m)	s	$\overline{h}_{max}$ (m)	$h_{0.5}$ (m)	s	$\overline{h}_{max}$ (m)	$h_{0.5}$ (m)	s	$\overline{h}_{max}$ (m)
The Baltic Sea, *T*=35 (years), $h_{0.5}$ =0.66 (m), *s*=1.81												
5%	0.63	1.45	2.2	0.51	1.67	1.7	0.48	1.94	1.3	0.56	1.52	2.0
25%	0.68	1.56	2.7	0.55	1.86	1.9	0.52	2.11	1.5	0.66	1.68	2.4
50%	0.76	1.72	3.2	0.60	2.04	2.3	0.56	2.31	1.7	0.75	1.79	2.7
75%	0.84	1.87	3.6	0.64	2.21	2.8	0.57	2.48	1.9	0.80	1.93	3.3
95%	0.98	2.02	4.0	0.68	2.39	3.2	0.60	2.83	2.4	0.91	2.14	4.0
M[•]	0.77	1.74	3.19	0.60	2.04	2.38	0.55	2.35	1.74	0.75	1.81	2.9
σ[•]	0.11	0.21	0.55	0.06	0.22	0.51	0.04	0.29	0.29	0.11	0.18	0.69
The Black Sea, *T*=35 (years), $h_{0.5}$ =0.73 (m), *s*=2.45												
5%	0.74	1.72	2.6	0.66	2.19	1.8	0.49	2.95	0.9	0.66	2.31	1.5
25%	0.87	2.04	2.9	0.69	2.62	1.9	0.58	3.50	1.1	0.69	2.56	1.9
50%	0.93	2.17	3.4	0.72	2.94	2.4	0.61	3.88	1.2	0.71	2.80	2.2
75%	1.00	2.24	4.1	0.76	3.28	2.7	0.63	4.07	1.4	0.74	3.01	2.8
95%	1.07	2.37	4.8	0.79	3.60	4.0	0.64	4.50	2.1	0.77	3.44	3.3
M[•]	0.92	2.13	3.59	0.73	2.94	2.58	0.60	3.81	1.29	0.72	2.83	2.38
σ [•]	0.10	0.20	0.85	0.05	0.44	0.73	0.04	0.45	0.34	0.04	0.35	0.60
Mediterranean Sea, *T*=15 (years), $h_{0.5}$ =0.60 (m), *s*=2.61												
5%	0.63	1.82	1.9	0.59	2.25	1.5	0.45	3.79	0.8	0.50	2.60	1.40
25%	0.69	2.07	2.7	0.63	2.67	1.8	0.49	3.97	0.9	0.52	3.02	1.50
50%	0.73	2.21	3.0	0.64	2.83	2.1	0.51	4.18	1.0	0.54	3.27	1.90
75%	0.77	2.28	3.2	0.66	2.92	2.2	0.52	4.59	1.1	0.56	3.44	1.90
95%	0.89	2.74	3.8	0.70	3.13	2.8	0.55	4.98	1.3	0.57	3.61	2.40
M[•]	0.75	2.27	3.03	0.65	2.80	2.12	0.51	4.36	1.03	0.54	3.29	1.89
σ [•]	0.09	0.30	0.53	0.03	0.23	0.42	0.03	0.46	0.15	0.02	0.40	0.42
Caspian Sea, *T*=39 (years), $h_{0.5}$=0.65 (m), *s*=2.46												
5%	0.62	1.92	1.5	0.59	2.19	1.4	0.52	2.60	1.0	0.60	2.03	1.4
25%	0.67	2.08	2.0	0.63	2.44	1.7	0.55	2.76	1.0	0.62	2.34	1.7
50%	0.72	2.27	2.2	0.66	2.65	1.9	0.56	2.92	1.2	0.64	2.56	1.9
75%	0.77	2.49	2.6	0.71	2.90	2.2	0.58	3.08	1.3	0.69	2.83	2.0
95%	0.84	2.82	3.1	0.74	3.16	2.7	0.63	3.32	1.5	0.79	3.08	2.8
M[•]	0.73	2.34	2.33	0.67	2.67	1.96	0.57	2.93	1.19	0.66	1.94	1.94
σ[•]	0.07	0.30	0.47	0.05	0.31	0.39	0.03	0.22	0.20	0.06	0.42	0.42

Probability bounds for the seasonal maximum h_{max} can be considered as the seasonal maximum wave heights that can occur once in T years. Therefore, the 90% probability margin can be taken as an estimate of 10 – year wave height for a particular season, while the 99% probability margin corresponds to the hundred-year wave height. There are several ways to estimate these, including using formulae (2.5) and (8.4) for first elements of the ranked sample of 360 elements. At the same time, the quantile corresponding to exceedance rate q in distribution (8.5) can be considered as a deterministic function of random arguments $h_{0.5}$, σ

$$h_q = h_{0.5}\, exp\left[\sigma U_q\right] \qquad (8.7)$$

where U_q is the quantile that corresponds to exceedance rate q for the normal distribution.

Using a statistical linearization method one can obtain from (8.7) the following estimates for mathematical expectation and variance:

$$m_h = \bar{h}_{0.5} \, exp\left[\bar{\sigma} \, U_q\right],$$ (8.8)

$$D_h = exp^2\left[\bar{\sigma} \, U_q\right]\left[D_h + \left(U_q \bar{h}_{0.5}\right)^2 D_s + 2\rho\sqrt{D_h D_s} \, U_q \bar{h}_{0.5}\right]$$

where ρ is the correlation between values $h_{0.5}$ and δ. These estimates make it possible to employ data from Table 8.5 and derive parametric estimates for the probabilistic interval h_{max}.

Adequate utilization of estimates (8.3) or (8.8) requires taking into account correlation between elements in the sample. As a first approximation this can be done via transformation towards number (2.15) of "conditionally independent" measurements $\hat{n}$. Thus, if one takes $\hat{n}$ =1 for the Baltic Sea (i.e. uses all 6-hour interval data), then relation (8.8) predicts m_h=3.7 m for winter season. If $\hat{n}$ =2 (corresponding to 12-hour intervals), then m_h=3.3 m. The sample data correspond to m_h*=3.2 m.

Table 8.6 gives estimates of mathematical expectation M[h] and bounds for the 90%

probability intervals of seasonal extreme values $h_{5\%}$, $h_{95\%}$ of wave height at synoptic times, which were constructed using the following methods:

- Method "A". Non-parametric range estimate that interprets h_{max} as the limiting element of the log-normal sample (I.4), (8.2), (8.3);
- Method "B". Parametric range estimate where h_{max} is understood as a random value with asymptotic distribution (2.5) and parameters (2.10);
- Method "C". Parametric range estimate, in which h_{max} is considered as a deterministic function of random argument (8.7);
- Method «D». An ensemble of elements that satisfies (8.5) is simulated by stochastic model (6.9).

The direct computation of probabilistic ranges for distribution (8.5) requires considerable effort. Also, additional approximations of functions under the integral are needed. As a result, it is better to simulate them using a stochastic model. The simulations represent the impulse-like behavior of random maximum wave heights h^+ in storms at the synoptic range (see distribution $F(h,y,z)$ in (8.6)) with parameters y,z of distribution $f_{h_{0.5}}(y,z)$.

Table 8.6.

Point-wise estimates of seasonal maxima of mean wave heights at synoptic times and their 90% probability intervals ($h_{5\%}$ - $h_{95\%}$) computed by methods «A», «B», «C», «D». The Baltic Sea

Method	Winter			Spring			Summer			Autumn		
	$h_{5\%}$	M[h]	$h_{95\%}$	$h_{5\%}$	M[h]	$h_{95\%}$	$h_{5\%}$	M[h]	$h_{95\%}$	$h_{5\%}$	M[h]	$h_{95\%}$
«A»	2.3	3.3	4.5	1.6	2.1	2.6	1.3	1.6	1.9	1.1	2.5	3.9
«B»	2.5	3.5	4.9	1.6	2.1	2.9	1.4	1.7	2.3	2.0	2.7	3.6
«C»	2.3	3.3	4.4	1.5	2.1	2.7	1.2	1.6	2.0	1.5	2.5	3.5
«D»	2.1	3.0	4.2	1.4	2.1	3.3	1.1	1.5	2.1	2.0	2.8	3.8
Data from table 8.5	2.2	3.2	4.0	1.7	2.4	3.2	1.3	1.7	2.4	2.0	2.9	4.0

Table 8.7

Seasonal maxima of wave heights simulated using IDM with $\hat{n}$ =4 (one record in a day). The Baltic Sea

T (years)	Seasonal extreme values (m)				Annual extreme values (m)
	Winter	Spring	Summer	Autumn	
50	5.7	3.3	2.5	5.2	5.6
100	6.4	3.7	2.7	5.7	6.1

A comparison of data with results in Table 8.5 suggests that methods «A»-«D» may lead to significant differences in the estimates. However, in general, they all provide reasonable values of h_{max}.

Values of $h_{95\%}$ in Table 8.6 can be understood as the seasonal maximum wave height at 20 year return period. Table 8.7 shows estimates of waves at longer return periods (namely, 50 and 100 year). These were obtained with the Initial Distribution

Method with mean values of parameters $h_{0.5}$ and s as given in Table 8.5. It is obvious from the table that annual maxima corresponding to 50 and 100 years return periods take place mostly in winter. The fact that the "winter" estimates are slightly larger than the annual maxima illustrates the sensitivity of the IDM results to variations of parameter s. When it comes to actual applications, estimates of seasonal and annual extreme wave heights must correspond to each other precisely.

---oooOooooo---

CHAPTER 9

Comparisons of extreme wave height estimates

As shown in chapters 1-8, several methods for estimation of extreme wave height h_{max} are available. Irrespective of the length of the original data series, the final estimate of h^*_{max} should be treated as a random value. Each of the considered methods is based on specific assumptions, and therefore the estimates obtained with the help of these methods should by definition be somewhat different. It is thus very relevant to compare the basic features of the estimates. Let us make the comparison and summarise the main differences in all the methods.

Table 9.1 demonstrates corresponding $\overline{h}_{max}$ estimates. These were obtained using a wave height data series, which was the same for all the methods. The wave heights in the Baltic Sea were simulated with a hydrodynamic model driven by the observed wind.

The time interval between wave height readings is six hours. Table 9.1 shows only the summary data for mean wave heights. We also analysed wave heights of other probabilities of exceedance, and our conclusions remained largely unchanged.

Table 9.1

Extreme values $\overline{h}_{max}$ of mean wave heights at return periods of 50 and 100 years obtained with the use of different methods. The Baltic Sea

Method	$h^{(50)}$, (m)	$h^{(100)}$, (m)
IDM, $\widehat{n}=1$, $h_{0.5}=0.66$ (m), s=1.8	6.7	7.3
IDM, $\widehat{n}=4$, $h_{0.5}=0.66$ (m), s=1.8	5.7	6.2
IDM, (2.15), $\widehat{n}=10$ (=0.2), $h_{0.5}=0.66$ (m), s=1.8	4.8	5.5
AMS (2.10), $\widehat{n}=1$, a=1.73, b=3.96	6.4	6.8
AMS (2.10), $\widehat{n}=4$, a=1.97, b=3.14	5.3	5.6
AMS (2.10), $\widehat{n}=10$ (ρ=0.2 in (2.15)), a=2.14, b=2.65	4.6	5.0
AMS, sample estimated a=2.50, b=3.25 95% confidence interval (m):	5.0 4.5–5.4	5.2 4.6–5.6
POT, Z=2.5 (m), λ=6.0, (213 storms) 95% interval for return period T (year)	4.7 47–53	4.9 95–106
POT, Z=3.0 (m), λ=2.4, (85 storms) 95% interval for return period T (year)	4.4 44–58	4.6 88–116
POT, Z=3.4 (m), λ=1.0, (35 storms) 95% interval for return period T (year)	4.3 37–63	4.4 73–125
POT, Z=3.6 (m), λ=0.4, (15 storms) 95% interval for return period T (year)	4.2 36–84	4.3 71–167
MENU	6.2	6.9
BOLIVAR, 1st maximum	5.0	5.2
BOLIVAR, 2nd maximum	4.0	4.3
BOLIVAR, 3rd maximum	3.8	4.0

Note: $\widehat{n}$ =1 corresponds to wave height data recorded at every observation time, i.e. with 6 hour intervals; $\widehat{n}$ =4 corresponds to data extracted once in four observation times, i.e. once every 24 hours; and $\widehat{n}$ =10 refers to data taken once every ten observation times, which, in accordance with relation (2.15), is equivalent to using non-correlated (or independent) observations.

The true value of h_{max} is, *a priori*, unknown. It must be located in some range with bounds (h_1, h_2), the width of which depends on the initial assumptions of the methods in use. Therefore, a single value (i.e one point) estimate of h_{max} does not say much about the advantages and shortcomings of the methods. Wave heights also exhibit inter-annual, seasonal and synoptic variability as described by equation (8.5). Therefore, for all of the above methods, the estimated confidence interval of parametric or non-parametric quantiles h^*_p does

not correspond to true variability of h_{max}. If the time series length is increased infinitely, all the methods predict a zero confidence limit range, while in real conditions, mostly due to existence of natural variability of different kinds and scales, there is a lower finite limit of this range. These considerations are relevant for the analysis of data in Table 9.1. To compare the results we need to have an estimate of the true value of h_{max}. Because the AMS method has the strongest theoretical foundation and reflects the existence of the inter-annual variability, let us assume that the estimate obtained with the help of the AMS method (2.17) is the most truthful. Thus in Table 9.1 we provide various range estimates obtained with the help of the AMS method and compare them with single value estimates that are obtained using the other methods.

The AMS method

This method is based on processing of the last elements of the data series. The theoretical foundation of this method is the most elaborated, and from the outset the method was designed for prediction of extreme values. Parameters *a* and *b* in relation (2.5) are evaluated either using original data (more specifically, annual maxima) or relations (2.10) corrected with respect to the correlation range (because the number *n* of readings in the sample enters formula (2.10)).

Processing of observations for the Baltic Sea yields a hundred year wave height h_{max} of 5.2 m. If internal correlation is not taken into account, relation (2.10) yields a hundred year wave height $\overline{h}_{max}$ of 6.8 m. If four consecutive observations are considered correlated (i.e. correlation range is equal to a day), h_{max} =5.6 m. For the correlation range of two and a half days ($\hat{n}$ =10) $\overline{h}_{max}$ =5.0 m. This means that taking into account the correlation between neighbouring observations leads to smaller estimates of $\overline{h}_{max}$. In normal practice the AMS estimates are made with parameter values determined using the annual maxima from the sample.

The IDM method

The initial distribution contains the whole range of wave heights at all observation times. Therefore, it experiences all possible wave generating conditions. Situations with extreme waves constitute only a small part of this variety. All IDM extreme wave height estimates should therefore be interpreted in terms of synoptic observations, as follows, "Once at a single synoptic observation time during *n* years the wave height *h* can be observed". The probability of such extreme wave height depends on the total number of synoptic observation times. This means that the IDM method does not produce a distribution of extreme wave heights but determines the quantile, to which the maximum wave corresponds. Another problem is connected to the need for making extrapolations. Usually, an extrapolation is justified up to the probability level of 0.1 %. However, if the original data series is one hundred years long, it can be made up to 0.01%.

For all IDM results in Table 9.1 the parameters $h_{0.5}$ and s of the log-normal distribution are unchanged. Correspondingly, the differences in the estimates for a 50-year and 100-year return wave height resemble the differences in the corresponding probabilities. Using an equivalent independent number of wave records (i.e. $\hat{n}=10$) instead of correlated wave records (i.e. for $\hat{n}=1,4$) leads to smaller estimates of extreme wave heights, which are closer to the estimates obtained with the help of the AMS method.

Thus, the IDM method, which, in fact, is one of the earliest methods in wave statistics, and which was not intended for use in estimation of extreme wave heights, can, nevertheless, lead to reasonable estimates. In order to successfully use this method it is very important to specify the correct probability of extreme wave heights. It should, however, be remembered that the distribution of extreme wave heights is dependent on the initial distribution. For example, if the initial distribution is of exponential type, then the distribution of extreme (rare) values asymptotically tends to the first limiting distribution (2.5). There are many studies, in which log-normal or Weibull distributions represent the general distribution of wave heights. Both log-normal and Weibull distributions are exponential. In recent years more and more investigators have preferred the log-normal distribution, feeling that it better represents observed and simulated data for mid-latitudes and subtropics where mixed waves dominate.

The POT method

This method is the most popular at present. Extreme waves are observed during storms which alternate with weather windows (See Fig. I.1). In the POT method the sequence of storms is practically treated as a pulse-like random process. The method selects only the highest wave in a storm. This means that it is aimed at estimation of the extreme values.

At the same time, the lack of asymptotic relations in the POT method does not allow a theoretical derivation of quantile h_p. It is dependent on the approximations assumed in (5.1). Furthermore, the method supposes independence of consecutive storms and uses the Poisson distribution for the storm number. This leads to some uncertainty in estimated return period (see Fig. 5.3).

Attempts to consider the consecutive storms correlated and, on the basis of this, to introduce corresponding corrections in the Poisson distribution, do not change the results significantly. The most "influential" parameter in the POT method is the threshold value of wave height, which discriminates between normal variations of the random process and a storm of interest. For example (see Table 9.1), if the selected threshold changes from 2.5 to 3.6 m, the estimated height of a hundred year wave decreases by 60 cm. Equation (5.10) and fig. 5.2 are instrumental in choosing the optimal threshold value of wave height separating storms that should be selected for further analysis. If the POT method is applied to observed series of wave heights, then any change of the threshold value results in recalculation of the combined distribution parameters using the original time series. Thus, in this case, the choice of the threshold affects the final results less strongly than it does when equation (5.10) is used.

It is noteworthy that studies conducted in other regions of the World Oceans also exhibit strong changes of the POT method output wave height in response to the threshold variations. Bjerke et al. (1990) used a nine-year time series of observations conducted every three hours in the coastal waters of Norway and obtained the following estimates of a hundred year wave height: 16 m for threshold of 3 m and to 14.5 m for threshold of 9 m. Estimates of a hundred year significant wave height along the Atlantic coast of Spain by Rossouw et al. (1995) changed from 13.4 m to 11.7 m due to the threshold variations.

The dependence of the POT method results on the choice of the threshold wave height has been studied in many papers and is well known. Several criteria are proposed for the storm selection [Szabo et al., 1989]. The general rule is the higher the threshold, the smaller the estimated extreme wave height hmax. When the threshold values exceed a certain limit, which is sufficiently high, the POT method extreme wave heights tend to a certain stable value. When the threshold decreases, the POT method estimates approach the IDM method estimates.

A serious shortcoming of the POT method is connected to the uncertainty in the estimates of the return period. This is clearly seen in Table 9.1, and is illustrated in Fig. 5.3. For higher values of the threshold the number of selected storms in the sample may become rather small, therefore the estimates of λ become less accurate, resulting in a broader confidence range for the return period. For example, for the threshold of 2.5 m, 213 storms were selected, and the confidence ranges for 50-year and 100-year wave heights are as small as 6 and 11 years, respectively.

When the threshold progressively increases from 2.5 m to 3.6 m, the number of selected storms decreases from 213 to 15, and the uncertainty in the return period of 50-year and 100-year wave height estimates increases to 48 and 96 years, respectively.

Summarizing, the POT method results in somewhat smaller estimates of extreme wave height in comparison with the AMS method. The higher the threshold, the smaller the final estimate.

The MENU method

This method represents the wave series as a random process. A return period of the extreme wave height h is considered as the expected time of the first up-crossing of this level. As a result, MENU extreme wave height estimates do not differ greatly from the corresponding estimates obtained from the IDM method.

The BOLIVAR method

The method does not assume that consecutive storms are not correlated. It takes into account not only all storms in which wave heights exceeded a certain threshold, but includes data for the strongest storm in each year in the time series.

This means that at least one record for any year is included in the analysis. This procedure makes it possible to utilize asymptotic distributions for maximum wave heights.

The use of the multi-dimensional distribution function (7.3) also makes it possible to extend the analysis from the first to other consecutive maxima that can be recorded at different return periods. It is possible that the second maximum of wave height at return period of 100 years is larger than the estimated 50-year wave height. The ability to produce such estimates is an advantage of the BOLIVAR method.

---oooOooo---

CHAPTER 10

Kinematic characteristics of the highest waves

Estimates of significant or mean wave height, irrespective of the method of their generation, refer to a quasi-stationary interval. The highest wave in a quasi-stationary interval depends on its duration. Other quantiles of wave height distribution can be obtained in deep water using the Rayleigh (I.1) or Forristall (I.2) distributions. In practical applications, it is common to associate the maximum wave height with the estimate of 0.1 % probability. Then, for the Rayleigh distribution $h_{0.1\%}=2.96\,\overline{h}$. An apparently more efficient approach, however, is comprised of the three following steps. The first step is the estimation of the extreme storm duration for the location of interest. The second step is the calculation of the corresponding probability of the maximum wave (see [Boukhanovsky et al., 1998].) Then, finally, its height can be evaluated.

In shallow water, Glukhovsky's distribution [Glukhovsky, 1966] is used most often in Russia:

$$F(h)=1-exp\left\{-\frac{\pi}{4\left(1+\frac{h^*}{\sqrt{2\pi}}\right)}\left(\frac{h}{\overline{h}}\right)^{\frac{2}{1-h^*}}\right\} \quad (10.1)$$

where $h^*=\overline{h}/H$ is relative average wave height, and H denotes water depth.

The Rayleigh and Forristall distributions are theoretically unlimited and may predict unrealistically large wave heights. Thus, a limiting height is introduced associated with wave breaking. The extreme height (i.e. the height at which wave breaking occurs) is determined by an equation from the finite amplitude wave theory [Easson, 1997; Sarpkaya, Isaacson, 1981]:

$$h_b/g\tau^2=C_1th(C_2H/g\tau^2) \quad (10.2)$$

where h_b is the breaking wave height, g is the acceleration of gravity, H is local water depth, τ is the wave period.

The constants in equation (10.2) are: C_1=0.02711 and C_2=28.77. Constant C_1 determines the maximum possible steepness of a finite amplitude wave in deep water, while constant C_2 reflects the influence of shallow water effects.

For $H\rightarrow 0, h_b=0.78H$.

For $H\rightarrow\infty, h_b/\lambda\rightarrow 1/7$, λ being the corresponding wavelength.

A more comprehensive description of extreme waves should include not only wave height, but other kinematic characteristics such as period τ, length λ and crest height c. The conditional distribution of wave periods for a certain height $F(\tau/h)$, which is also called associated, can be approximated by a Weibull distribution with shape parameters depending on the wave height and period accordingly [Wind, 1974]. The Weibull distribution for the conditional distribution can be written as

$$F(\tau/h)=1-exp\left(-A_h\left(\frac{\tau}{m_{\tau|h}}\right)^{k_h}\right)$$

$$A_h=\Gamma^{k_h}\left(1+\frac{1}{k_h}\right) \quad (10.3)$$

where $m_{\tau|h}$ is the regression between τ and h.

The shape parameter k_h for $\tau|h$ varies from 2.62 to 7.47 [Wind, 1974]. In practice, shape parameters do not depend on the degree of wave development and the type of wave system. The regression

$$m_{x|y}=\int xf(x|y)dx$$

is defined as the conditional mean of one random value (the other one is invariant), and the skedastic ratio (conditional variance) is defined as

$$D_{x|y}=\int_{-\infty}^{\infty}(x-m_{x|y})^2 f(x|y)dx$$

The behaviour of the regression and skedastic ratios for calculated conditional distributions $F(\tau|h)$ is presented in Fig 10.1. Similar figures have been published in many papers (see, e.g., [Wind, 1974; Boukhanovsky et al., 1999; Lopatoukhin, 1974]).

The figure shows that conditional average values of wave periods for a given wave height $m_{\tau|h}$ strongly depend on h and τ only for values smaller than the average. For wave height or period exceeding the average, these two parameters become nearly constant. Dependence of conditional variances $D_{\tau|h}$ and $D_{h|\tau}$ on the height and period is seen over the whole range of variability. A parabolic shape of the conditional variance curve indicates that the greatest diversity is pertinent for waves with heights close to the distribution centre. For practical purposes, it may

be assumed that mean wave period associated with large waves (at least larger then the mean wave height) is about 1.15-1.20 $\overline{\tau}$. An analysis

based on a breakdown of various wave generating conditions would result in a wider probability interval for the scedastic ratio.
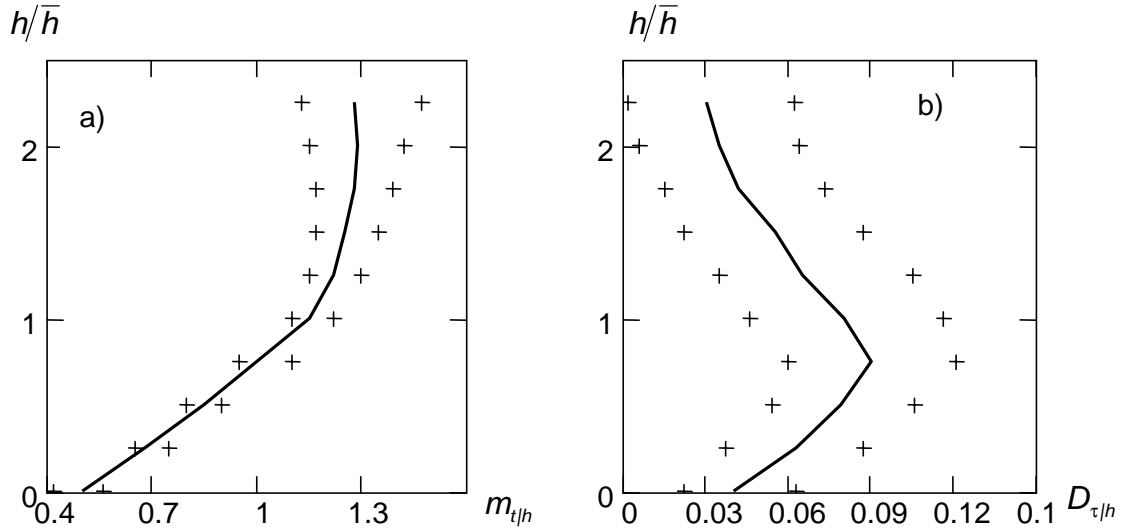

Figure 10.1: Regression (a) and skedastic (b) ratios for the wave periods with prescribed wave height for the Black Sea. Crosses are the borders of 90% confidence interval.

In practical computations of mean period $\overline{\tau}$, which is associated with wave heights h of a certain probability of exceedance, parameterizations of the conditional mean $m_{\tau|h}$ and of its probability range bounds ($\tau|_{lower}$, τ_{upper}) are used:

$$\tau(h) = Ah^B \qquad (10.4)$$

Davidan et al. (1978) used an extensive array of field observations and suggested the following approximations for the parameters in relation (10.4): A=4.8, B=0.5.

The lower bound $\overline{\tau}_{lower}$ of mean wave periods depends on wave kinematics and can be determined using an equation for maximal wave steepness. For example, Battjes (1972) proposed the following relation:

$$\overline{\tau}_{lower} = (32\pi h_s / g)^{1/2} \qquad (10.5)$$

where h_s stands for significant wave height.

[Teng et al., 1993] used observations from buoys moored off the Atlantic and Pacific coasts of the U.S. and proposed the two following modifications of equation (10.4):

$$\overline{\tau}_{lower} = 3.23 h_s^{0.47} \quad or \quad \overline{\tau}_{lower} = 3.28 h_s^{0.43} \qquad (10.6)$$

Other studies (see [Chung-Chu-Teng et al., 1993]) showed that the approximation by Battjes tended to overestimate $\overline{\tau}_{lower}$ while the second formula (10.6) by Teng and co-authors (1993) underestimated it.

The limit on the upper bound $\overline{\tau}_{upper}$ can be defined as a certain quantile of the conditional distribution of wave periods ($\tau|h$) for a given wave height; the 5% probability quantile is a reasonable choice.

Another useful kinematic characteristic of the spectrum is the period τ_p corresponding to its energy peak. Buckley (1988; 1993) and Chun-Chu Teng et al. (1993) used an equation for its lower limit corresponding to a given significant wave height h_s. It is equivalent to the following formula:

$$\left(\tau_p\right)_{lower} = 3.62\left(h_s\right)^{0.5} \qquad (10.7)$$

For the upper limit $(\tau_p)_{upper}$ Buckley (1988) found the following expression fitting the upper envelope of an empirical data set:

$$\left(\tau_p\right)_{upper} = 7.16\left(h_s\right)^{0.5} \qquad (10.8)$$

The ratio of period of the spectral peak τ_p to mean period $\overline{\tau}$ is known to vary from 1.1 to 1.4 [Goda, 1979].

Classical hydrodynamics makes it possible to derive all basic kinematic parameters of the wave of interest if parameters (h, τ) are known. For example, the linear theory of small amplitude waves, which is applicable to sufficiently deep waters, yields:

$$\lambda = \frac{g}{2\pi}\tau^2 = 1.56\tau^2, \quad c = h/2 \qquad (10.9)$$

For shallow water areas with depth H, the theory provides a transcendental equation with parameters τ, H

$$\lambda = \tau \sqrt{\frac{g\lambda}{2\pi} tanh\left[\frac{2\pi H}{\lambda}\right]} \qquad (10.10)$$

which can be solved with respect to wavelength λ.

In locations where the water depth is comparable to wave height, it is necessary to use approximations of the potential theory for waves of finite amplitude, e.g. a third-order Stokes expansion for the velocity potential function $\varphi(x,y)$ (see [Aleshkov, 1996; Sretensky, 1977; Lambrakos et al., 1974)]:

$$\varphi(x, y) = \varepsilon\varphi_1(x, y) + \varepsilon^2\varphi_2(x, y) + \varepsilon^3\varphi_{3(x,y)} + O(\varepsilon)^4 \qquad (10.11)$$

Here ε is the dimensionless small parameter defined by the kinematic characteristics of the wave, φ_1 is the first expansion term corresponding to a linear approximation of the potential theory of small-amplitude progressive waves, and φ_2 and φ_3

are the non-linear addends corresponding to the second and third approximations.

The free-surface ordinate ζ corresponding to equation (10.11) with accuracy to the third expansion term is written as [Aleshkov, 1996]:

$$\zeta = \left(a + a^3 b_2\right) cos\ \chi + a^2 b_1\ cos\ 2\chi + a^3 b_3\ cos\ 3\chi \qquad (10.12)$$

where a is the wave amplitude, χ is the wave phase,

$$b_1 = \frac{k}{4} cthkH\ \frac{2ch^2kH + 1}{sh^2kH}, \quad b_2 = \frac{k^2}{16\,sh^2kH}\left(2ch^6kH + 8ch^4kH - 19ch^2kH + 9\right),$$

$$b_3 = \frac{k^3}{64\,sh^6kH}\left(1 + 8ch^6kH\right)$$

and k is the wave number.

The phase velocity of a third-order Stokes wave is defined as:

$$C = \frac{\omega}{k} = \sqrt{\frac{g}{k} thkH\left(1 + \frac{a^2k^2}{16\,sh^4kH}\left(8ch^4kH - 8ch^2kH + 9\right)\right)} \qquad (10.13)$$

The height of a Stokes wave is equal to:

$$h = 2a\left(1 + a^2k^2b\right) \qquad (10.14)$$

where $b = \frac{1}{64\,sh^6kH}\left(32ch^6kH + 32ch^4kH - 76ch^2kH + 39\right)$.

The crest height c and the trough depth are determined, respectively, for $\chi=0$ and $\chi=\pi$.

The length of a Stokes wave is $\lambda=2\pi/k$, and its amplitude a is determined based on the established period $\tau = 2\pi/\omega$ and height h by numerical solution of the set of transcendental equations (10.13) and (10.14).

In practice the individual wave crest (c) distribution is provided, for example in [Haring, Heideman, 1980]) as

$$P(c) = 1 - exp\left[-\frac{c^2}{2m_0}\left(1 - B_1\frac{c}{H}\left(B_2 - \frac{c}{H}\right)\right)\right],$$

$$B_1 = 4.37,\ B_2 = 0.57 \qquad (10.15)$$

where m_0 is the zeroth moment of wave spectrum. The crest height of p% probability is estimated as a solution to this equation with initial value $c_{init}=0.5h_p$, in accordance with the analytical solution (10.9) for waves of infinitely small amplitude.

However, to estimate the crest height of waves at n-year return period (n=1, 5, 10, 25, 50, and 100 years) for a shallow water area, it is recommended that the crest of a higher-order theory of wave profile is used.

Lambrakos and Brannon (1974) estimated wave crest heights using the higher order Extended Velocity Potential (EXVP) wave theory. The theory considers a Stokes-type wave, which has front-to-back symmetry of its crest and propagates without deformation. The EXVP wave theory is instrumental in determining the geometry and

kinematics of individual waves. In the theory the velocity potential has the form

$$\varphi(x,z,t) = \sum cosh(k_n z)[B_n \, sin(k_n x - \omega_n t)]$$

(10.16)

In this expression, z is positive upwards from the seafloor, x is positive in the direction of wave propagation, the summation is made over n = 1,2,...,N frequencies, $k_n = 2\pi/\lambda_n$ is wave number for frequency n, $\omega_n = 2\pi/\tau_n$ is angular wave frequency for frequency n, λ_n is wave length for frequency n, and τ_n is wave period for frequency n. The input data for EXVP are the water depth H, the wave height h, and the zero-crossing period τ of the wave.

The tables and plots for the estimation of wave crest are published [Sarpkaya, Isaacson 1981]. A part of those tables is reproduced in Table 10.1.

Let us consider an example. Suppose $H=17.1$ m, $h=10.7$ m, and $\tau=12.5$ s.

Then from (10.2) we get $h_b= 12.8$ m, $h/h_b=0.83$, and $H/g\tau^2=0.01094$. Interpolating data in the Table we obtain: $c/h=0.766$, i.e. $c=8.2$ m.

In real situations the ratio c/h varies in the range from 0.50 to 0.80.

Table 10.1

Crest/wave height (c/h) ratio as a function of h/h_b and $H/g\tau^2$

h/h_b	$H/g\tau^2$												
	0,0090	0,0140	0,0190	0,0240	0,0290	0,0340	0,0390	0,0440	0,0490	0,0540	0,0590	0,0640	0,0690
0,00	0,5000	0,5000	0,5000	0,5000	0,5000	0,5000	0,5000	0,5000	0,5000	0,5000	0,5000	0,5000	0,5000
0,08	0,5369	0,5262	0,5193	0,5165	0,5145	0,5130	0,5117	0,5109	0,5105	0,5102	0,5098	0,5095	0,5092
0,16	0,5724	0,5509	0,5388	0,5333	0,5294	0,5267	0,5244	0,5229	0,5221	0,5213	0,5206	0,5199	0,5193
0,24	0,6064	0,5751	0,5587	0,5505	0,5447	0,5409	0,5377	0,5356	0,5344	0,5333	0,5322	0,5313	0,5304
0,32	0,6382	0,5994	0,5792	0,5681	0,5604	0,5556	0,5514	0,5488	0,5473	0,5459	0,5447	0,5435	0,5424
0,40	0,6665	0,6234	0,5996	0,5859	0,5764	0,5704	0,5653	0,5622	0,5604	0,5588	0,5574	0,5560	0,5548
0,48	0,6926	0,6468	0,6200	0,6038	0,5925	0,5855	0,5795	0,5758	0,5737	0,5717	0,5700	0,5683	0,5669
0,56	0,7187	0,6698	0,6415	0,6227	0,6095	0,6013	0,5942	0,5898	0,5871	0,5846	0,5824	0,5803	0,5784
0,64	0,7422	0,6934	0,6643	0,6433	0,6283	0,6186	0,6103	0,6049	0,6016	0,5985	0,5957	0,5932	0,5908
0,72	0,7630	0,7178	0,6878	0,6657	0,6493	0,6381	0,6283	0,6221	0,6182	0,6147	0,6114	0,6085	0,6058
0,80	0,7811	0,7407	0,7112	0,6889	0,6718	0,6590	0,6479	0,6410	0,6369	0,6332	0,6298	0,6267	0,6238
0,88	0,7933	0,7564	0,7299	0,7090	0,6924	0,6791	0,6676	0,6604	0,6561	0,6522	0,6486	0,6454	0,6423
0,96	0,7970	0,7614	0,7371	0,7179	0,7031	0,6918	0,6821	0,6756	0,6712	0,6673	0,6636	0,6603	0,6573

---oooOooo---

CHAPTER 11

Ship design and offshore engineering require not only estimates of wave height h_{max} but also information on wave frequency spectrum $S(\omega)$ that corresponds to extreme wave conditions. Recent years have been marked by the availability of new wave observations. Automated buoys started to measure waves regularly in the offshore waters of many countries [Hamsley, 1996].

Wave measurements from satellites now cover a period of almost 15 years. The wave data exists as measured and simulated wave heights and wave spectra, both omni-directional $S(\omega)$ and directional $S(\omega,\beta)$. They are functions of spatial co-ordinates (such as x,y) and time t. Thus, it is possible to draw some parallel between a "wave weather ensemble" and a wave spectra $S(\omega,\beta,x,y,t)$ ensemble, and to make a step from classification of wave heights to a classification of spectra. The term «spectral wave climate» was approved by a major conference on wind waves (1998), in which experts representing open ocean shipping, shelf engineering and construction participated along with specialists in wave modelling and research ["Provision ...", 1998].

Let us consider several examples of wind wave spectrum variations during a storm passage.

Fig. 11.1 shows an example of the variation of the frequency spectrum $S(\omega,t)$ at a point located in the North Atlantic, as measured by RV "Weather Reporter" of the UK, from 15th to 19th December 1959 [Wilson, 1965]. The upper panel of the figure also shows data on wind speed u, wave height variance D_ζ, and mean wave period τ. Wind strengthening up to 30 knots occurred from 6 to 18 h December 16, 1959. The wind wave spectrum during that period of time did not change significantly. From 18 h December 16th to 03 h December 17th the wind veered and strengthened up to 62 knots.

The wave spectrum was growing quickly and reached its peak by 18 h December 17. Then, it weakened a little following a corresponding decrease in the wind speed and again strengthened reaching the maximum at 0 h December 18th. Subsequent variations of the spectrum correspond to the storm wave decay.
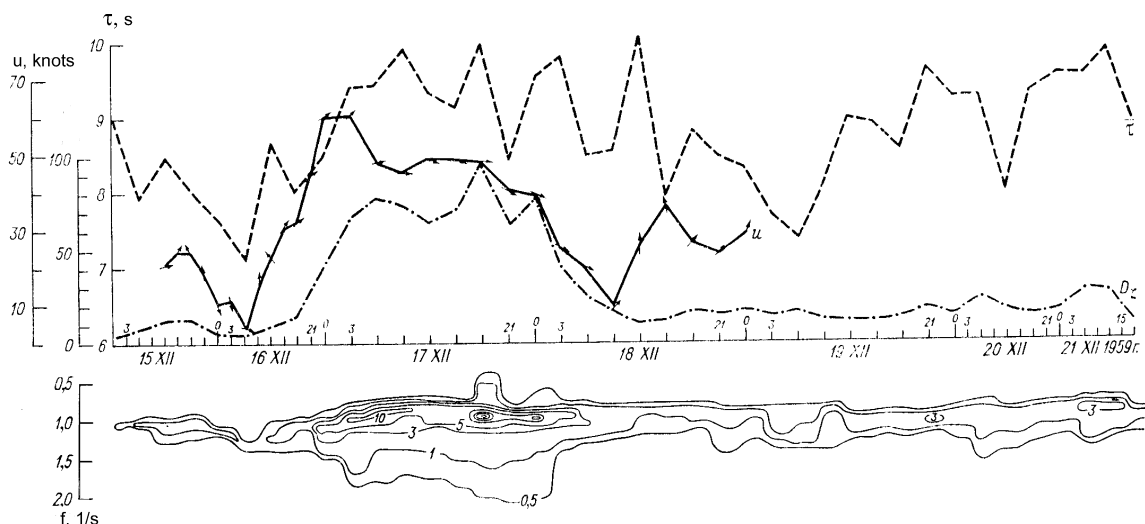

Figure 11.1: Lower panel: An example of variations of frequency spectrum $S_\zeta(\omega,t)$ (m^{2}s). The upper panel: variations of total variance $D_\zeta(t)$ (m^2), mean wave period $\tau(s)$ and wind speed u (knots).

Fig. 11.2 shows sections of function $S(\omega,t)$ from 22nd August to 6th September 1966 measured by research vessels "Iceberg" of Russia and "Weather Adviser" of the UK. Three phases of storm development can be noticed, namely a development of wind sea from an initial complex wave field, then a transformation of the wind wave to swell and, finally, the existence of a new complex wave field.

From August 28 to September 6, 1966, Ocean Weather Station (OWS) "I" experienced the impact of three cyclones and the hurricane "Vera". Features of the wind wave spectrum variations that were observable by naked eye were its growth under the action of a strengthening wind and associated changes of the total spectrum variance. Then, following a change of wind direction, the wave field became mixed, and the spectrum

developed a second peak. The storm decay was accompanied by a decrease of the total wave spectrum variance. Later on, swell started to dominate the whole pattern. These processes are seen in Fig. 1.3.

According to [Goldman, 1977], it is possible to reconstruct conditions of a hypothetical (artificial) storm that would lead to the highest practically possible waves at a location of interest. The idea is to look at a situation that did not happen as yet but can, in principle, happen in future.
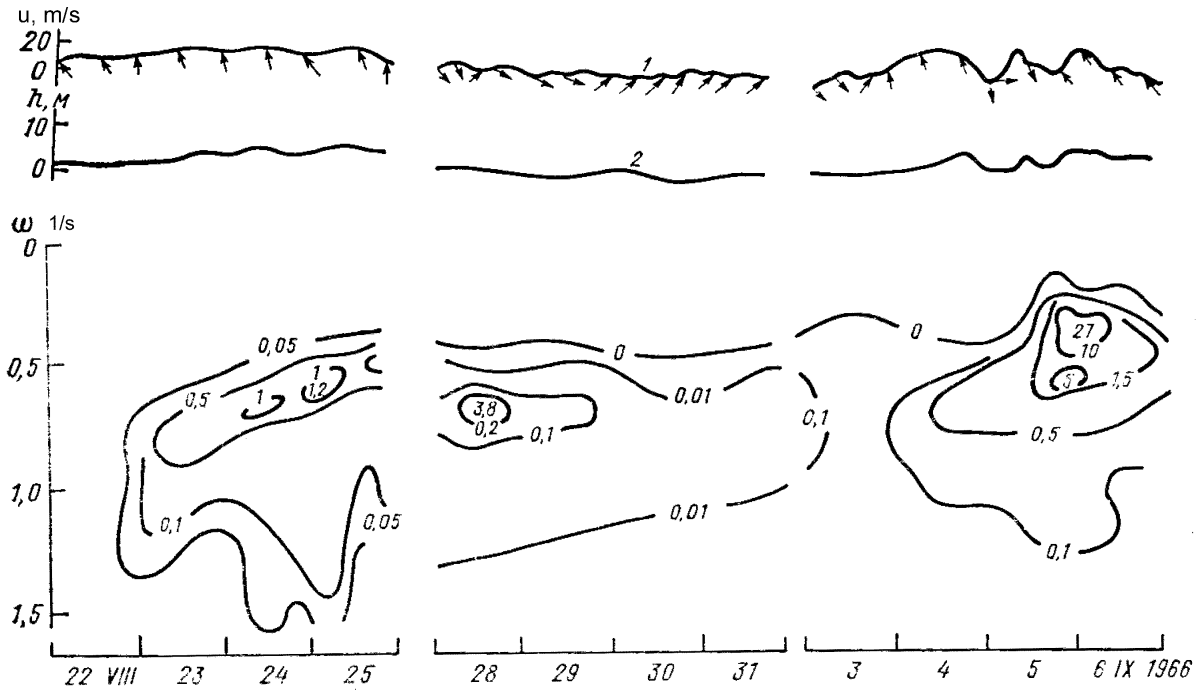
Figure 11.2: Spectral density $S(\omega,t)$ (m^{2}s) of wind waves in the North Atlantic from August 22 to September 6, 1966. 1: wind speed (m/s), with arrows indicating the direction. 2: significant wave height (m).
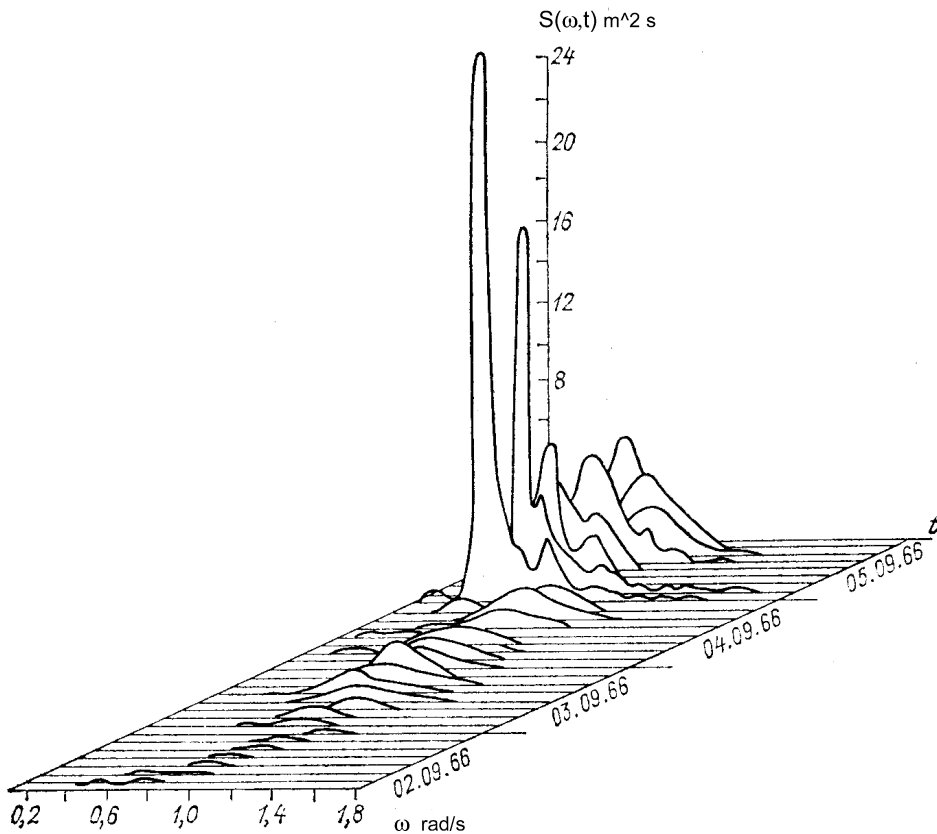
Figure11.3: Changes of wave frequency spectrum at OWS "I" during the hurricane "Vera".

For example, for the Gulf of Alaska, and for area around Iceland, a combined wave height of 35 m could be anticipated. The combined wave was composed of a wind wave (sea) of 33 m with period of 27 s, and a swell wave of 12 m with period of 31 s. It was generated in conditions of strong atmospheric pressure gradients along a cold front. Persistent strong winds blew over fetches of several hundreds of kilometers superimposed on considerable horizontal gradients of sea surface temperature. Apparently, the geographical and meteorological conditions of both areas do not preclude such a combination of factors from happening. However, the possibility that such storm could happen requires additional study.

Participants at the 18th Assembly of the International Maritime Organization (1993) agreed upon the following definition. The extreme wave spectrum is to be understood as the spectrum corresponding to the maximal possible value of significant wave height (h_s) derived using wave measurements at different locations during time period not shorter than 10 years. The climatic wave spectrum is defined as the averaged spectrum over an ensemble of spectra that have a certain probability, and correspond to dominant

$$S(\omega)=\frac{1}{4}\sum\frac{\left[\omega_{m_j}^4\left(4\lambda_j+1\right)/4\right]^{\lambda_j}}{\Gamma\left(\lambda_j\right)}\frac{\left(h_s^2\right)_j}{\omega^{4\lambda_j+1}}exp\left[-\frac{4\lambda_j+1}{4}\left(\frac{\omega_{m_j}}{\omega}\right)^4\right]$$ (11.2)

where h_s denoted significant wave height, ω_m was the frequency of the spectral maximum, λ was a parameter defining shape of the spectrum, and $\Gamma(\lambda)$ was the Gamma-function.

Equation (11.2) takes into account that, as a rule, wave spectra contain two peaks, at low and higher frequencies. This makes it possible to find a correspondence between a series of spectra $S_i(\omega)$, i=1,..,n, and six parameters $(h_s, \omega_m, \lambda)_j$, j = 1, 2. Then these parameters can be used in developing a classification of wind waves.

[Buckley, 1988] analyzed more than 2 million spectra that were generated over 12 years at 13 buoys located in coastal waters of the USA. All the wave situations that the study included were broken down into twelve types, according to their significant wave height. The highest waves had h_s>9.5 m. The abundance of data series made it possible not only to compute the average spectrum $\bar{S}(\omega)$ for all the classes, but even to derive a distribution function $F_s(x)$ and corresponding quantiles $S_p(\omega)$ of this distribution. Fig. 11.4 gives three statistical characteristics of spectra corresponding to two classes of h_s.

It is relevant to note that the quantile spectrum $S_p(\omega)$ for given probability p, e.g. for $p = 0.05$,

wave generation conditions over the area. Some progress in studying the climatic wave spectra can be reported.

The first averaged wave spectra were computed using 204 wave records at OWS "I" in the North Atlantic. Wind speeds there ranged between 2 and 25 m/s and mean wave heights varied from 0.5 to 4.5 m [Skott, 1968].

The following approximation was obtained for the average spectrum $\bar{S}(\omega)$:

$$\bar{S}(\omega,h_s,\bar{\tau})=\left(\frac{h_s}{3.98}\right)^2\bar{\omega}^{-4}\omega^{-5}exp\left[-0.318\left(\frac{\bar{\omega}}{\omega}\right)^4\right]$$ (11.1)

Relation (11.1) makes it possible to compute $\bar{S}(\omega)$ for some areas of the World Oceans and for different seasons, provided two-dimensional (height and period) distributions are known (e.g., from a reference book).

[Ochi, 1978] analyzed 800 spectra of wind waves at nine Ocean Weather Stations in the North Atlantic, and showed that the most general representation for such spectra would be

coincides for every frequency ω_k with different spectra $S_i(\omega_k)$. Thus, $S_{max}(\omega_k)$ is the upper envelope for the family of spectra $S_i(\omega_k)$ composed of maximum elements in samples $(S_1...S_n)$ composed of values $S_i(\omega_k)$ for i=1,..,n (where n is number of spectra in the sample). Only tuning of the parameters can force the spectrum $\bar{S}(\omega)$ to coincide with any known single-peaked or double-peaked approximation, such as (11.1), (11.2) or JONSWAP. Computations of climatic wave spectra for the Barents and Black Seas were carried out in [Lopatoukhin, Boukhanovsky, 1997; Boukhanovsky, Lopatoukhin, Rozhkov, 1998a, Lopatoukhin, et al., 1999].

Several researchers, e.g. [Vincent et al., 1977], represent ensemble $S_i(\omega_k)$ using the expansion with respect to orthogonal eigen-components:

$$S_i(\omega_k)=\sum_v a_{iv}\varphi_v(\omega_k)$$ (11.3)

where $\varphi_v(\omega_k)$ denote basis functions and a_{iv} are coefficients.

The fastest convergence of series (11.3) takes place when $\varphi_v(\omega_k)$ are equal to eigenfunctions of the correlation matrix $K_{S^*}(\omega_i, \omega_j)$ of spectral estimate $S^*_i(\omega_k)$.
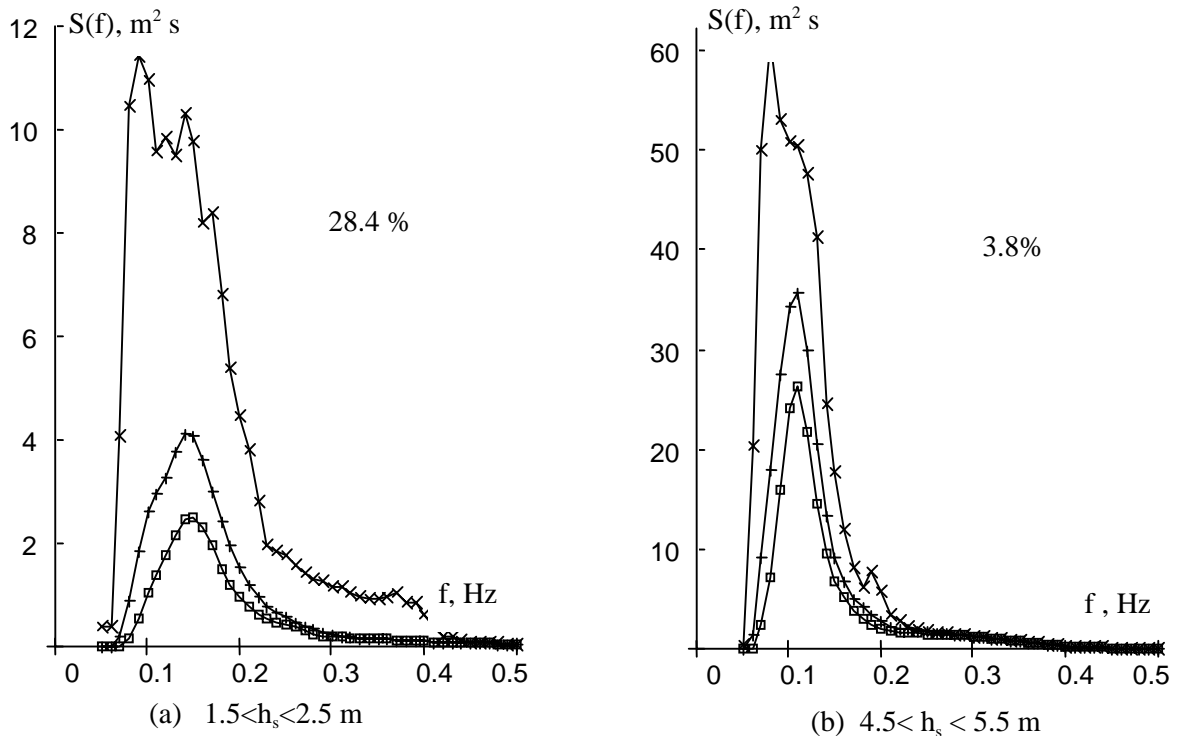
Figure11.4: Climatic wave spectra for buoy No. 44004 (Atlantic coast of the USA) [Buckley, 1988], (a): sample of 8771 spectra, (b): sample of 1156 spectra. Notations: – – denotes mean spectrum, –+– stands for the mean spectrum plus standard deviation, and –x– denotes the maximal spectrum. Values of 28.4% and 3.8% are the probability of spectra in this location
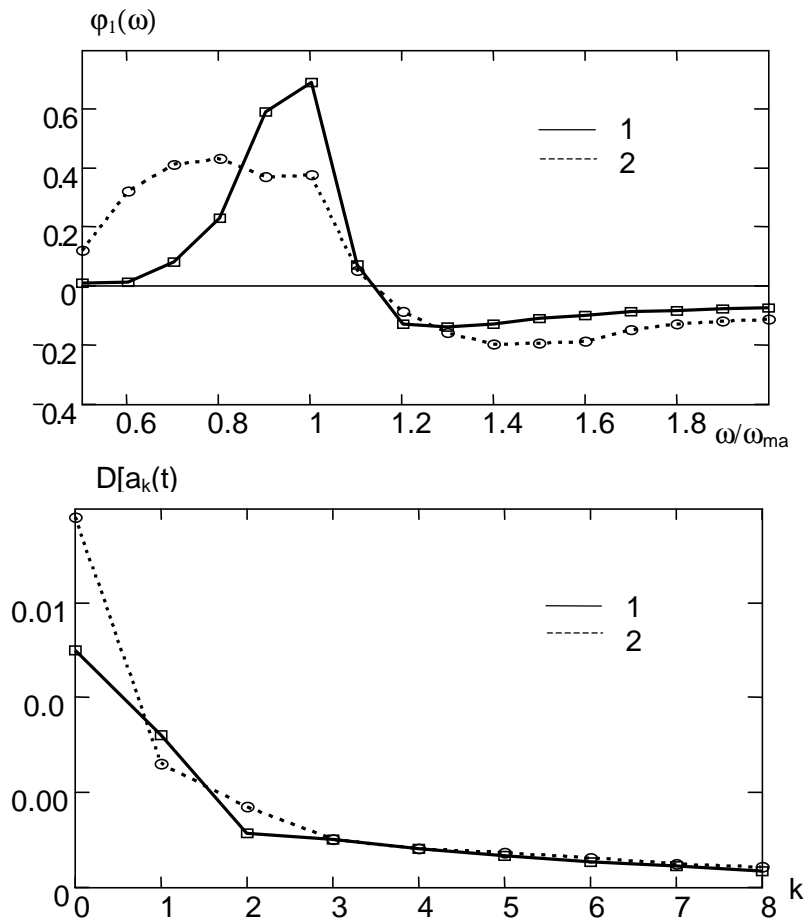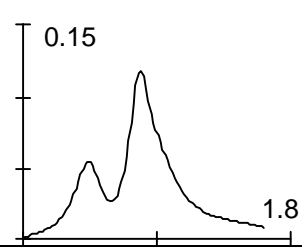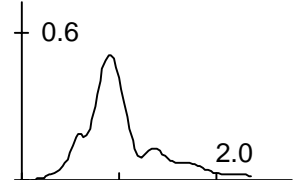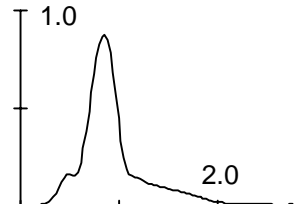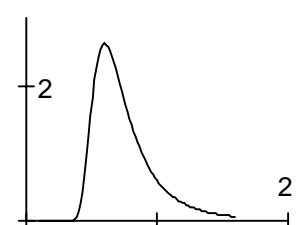

Figure 11.5: First eigenfunctions $\phi_1(\nu)$ and variances $D(a_k)$ of expansion (11.3) for wind wave spectra. 1: wind sea spectra, 2: double-peaked spectra of combined wave field

Fig. 11.5 gives estimates for $\varphi(\omega)$ and variances D_{a_v} of coefficients a_{iv}, which were computed using two kinds of spectra, namely single-peaked spectra of wind waves and double-peaked spectra for mixed waves. These two kinds of spectra differ considerably, but their first eigenfunctions $\varphi_1(\omega)$ are not that different (eigenfunctions $\varphi_v(\omega)$ of higher order being less similar). Variances D_{a_v} decrease rapidly as number v increases.

A classification of spectra $S_i(\omega, h_s)$ based on a single parameter, h_s or dispersion D_ξ, would lead to difficulties in interpretation of probabilistic characteristics. A more fruitful approach, which also leads to a better interpretation of results, is based on classification with respect to "persistent conditions". For example, [Lopatoukhin et al., 1990] proposed four types of wave generating conditions for the tropical Pacific, leading to development of common features in their spectra (see Table 11.1). Variability of wind wave spectra within each of the four groups can be expressed using quantile diagrams as shown in Fig. 11.6. As can be seen, the main spectral peak $S_{max}(\omega)$ at frequency $\omega_{max} = 0.9$ rad/s can vary from minimal value of 0.4 m^{2}s to a maximum value of 1.2 m^{2}s (with median value of 0.9 m^{2}s). ω_{max} varies from 0.6 to 1.0 rad/s. The secondary maximum at $\omega = 0.5$ rad/s, which corresponds to swell, can be as large as $S(\omega) = 0.5$ m^{2}s, and its frequency can vary in the range of $\omega \in [0.4; 0.6]$ rad/s.

Table 11.1
Typical frequency spectra for the tropical part of the North Pacific Ocean

Type	%	Wind, m/s	Variance, cm^2	Peak No1, Rad/s	Peak No.2, Rad/s	Spectral shape $S(\omega)$, (m^2 s)
ITCZ	40	<6	650-1300	0.4-0.7	0.8–1.1	
MTW	25	<8	1500-2800	0.4-0.7	0.8–1.1	
STW	25	8-15	2500-4500	0.4-0.7	0.7–1.0	
TC	10	>15	>4500	0.4–0.7	—	

Note: ITCZ is Inter-Tropical Convergence Zone, MTW is moderate Trade Winds, STW is strong Trade Winds, TC is tropical cyclone.

[Lopatoukhin, Boukhanovsky et al., 1999] used long term wave measurements in the Black Sea and proposed a classification of wave spectra according to their genesis, i.e. for wind sea, swell and combined waves (see Table 11.2). They also determined probabilities of their occurrence and of consequential transformations between the different types.

Table 11.2
Probability of wave types

Wave	Subtype	Type	N	Winter	Transient seasons	Summer	Year
Swell	Steep	I-1	366	5%	2%	10%	6%
	Middle	I–2	1037	22%	8%	19%	17%
	Slope	I–3	1220	–	32%	30%	20%
Wind waves		II	1952	47%	27%	22%	32%
Combination without separation	Swell	III–1	793	16%	15%	8%	13%
	Wind waves	III–2	184	4%	4%	2%	3%
Combination with separation	Swell	IV–1	427	5%	10%	7%	7%
	Wind waves	IV–2	123	1%	2%	2%	2%
Total			6102	100%	100%	100%	100%
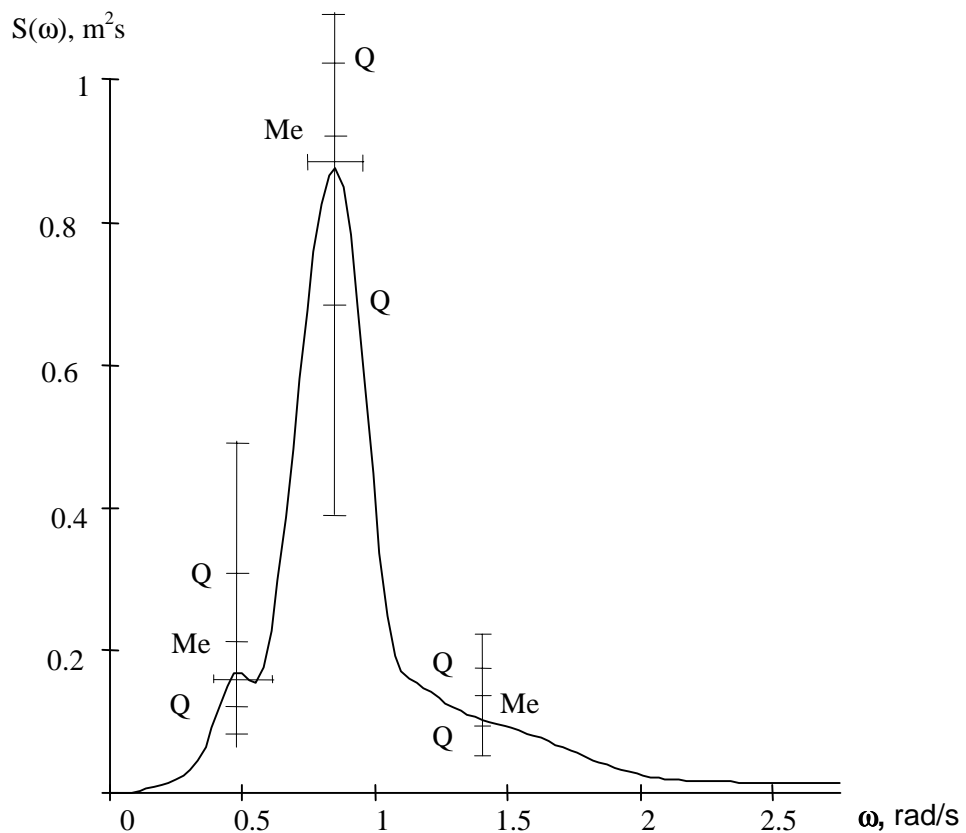
Figure 11.6: A typical wave spectrum generated under the action of strong trade winds in tropical part of the North Pacific Ocean.

Functional representation of such classes of spectral densities $S(\omega)$ can be made using the following well known approximation:

$$S(\omega) = A\omega^{-k} exp[-B\omega^{-n}] \qquad (11.4)$$

where *A, B, k, n* are parameters reflecting wave generating conditions.

Mean wave height $\overline{h}$ is the only parameter needed for description of the wind sea. Mean wave period can be estimated by various relations [Wind, 1974], (e.g. as in the chapter 10). A single-peaked spectral approximation (10.4) for swell depends on two parameters, namely $\overline{h}$ and $\overline{\tau}$.

The combination $\delta=g\tau 2/h$ reflects the non-dimensional steepness. A complex wave can be expressed, in the first approximation, as the sum of spectra:

$$S_{Complex}(\omega) = S_{WindSea}(\omega) + S_{Swell}(\omega) \qquad (11.5)$$

The proposed approximation uses spectral moments and some other related variables. It makes it possible to represent any spectral density function S(ω) as S(ω,Ξ), where Ξ denotes a set of parameters. All operations with such functions S(ω) inside their class are ones with deterministic functions (11.1), (11.2) or (11.4) of random arguments Ξ. For example it is possible to define the mean spectrum

$$\overline{S}(\omega) = S(\omega, \overline{\Xi}), \qquad (11.6)$$

quantile spectrum

$$S_p(\omega) = S(\omega, \Xi_p), \qquad (11.7)$$

and variance of spectra:

$$D_S(\omega) \cong \sum_{i=1}^{n} \left(\frac{\partial S(\omega)}{\partial \xi_i} \right)^2_{\xi=\overline{\xi}} D_{\xi_i} + 2\sum_{i>j} \left(\frac{\partial S(\omega)}{\partial \xi_i} \right)_{\xi=\overline{\xi}} \left(\frac{\partial S(\omega)}{\partial \xi_j} \right)_{\xi=\overline{\xi}} cov(\xi_i,\xi_j) \qquad (11.8)$$

In the above expressions $\overline{\Xi}$, Ξp stand for sets of mean values of parameters and their quantiles, $D_{\xi_i}, cov(\xi_i,\xi_j)$ are the variance and covariance of the parameters, respectively.

The above examples dealt with wave frequency spectra only. As mentioned at the beginning of this chapter, a considerable volume of measured and simulated data is available at present not only for omni-directional spectra S(ω), but for the directional spectra S(ω,) as well. This information is very important in actual applications. [Krogstad et al., 1997; Krogstad, 1998] studied existing approximations for angular wave energy distribution and proposed their generalization.

The 3-D pattern of a wave spectrum is particularly complicated for moderate wave heights. In the case of a strong storm or "dead" swell the spectrum is characterized by relatively narrow directional distribution.

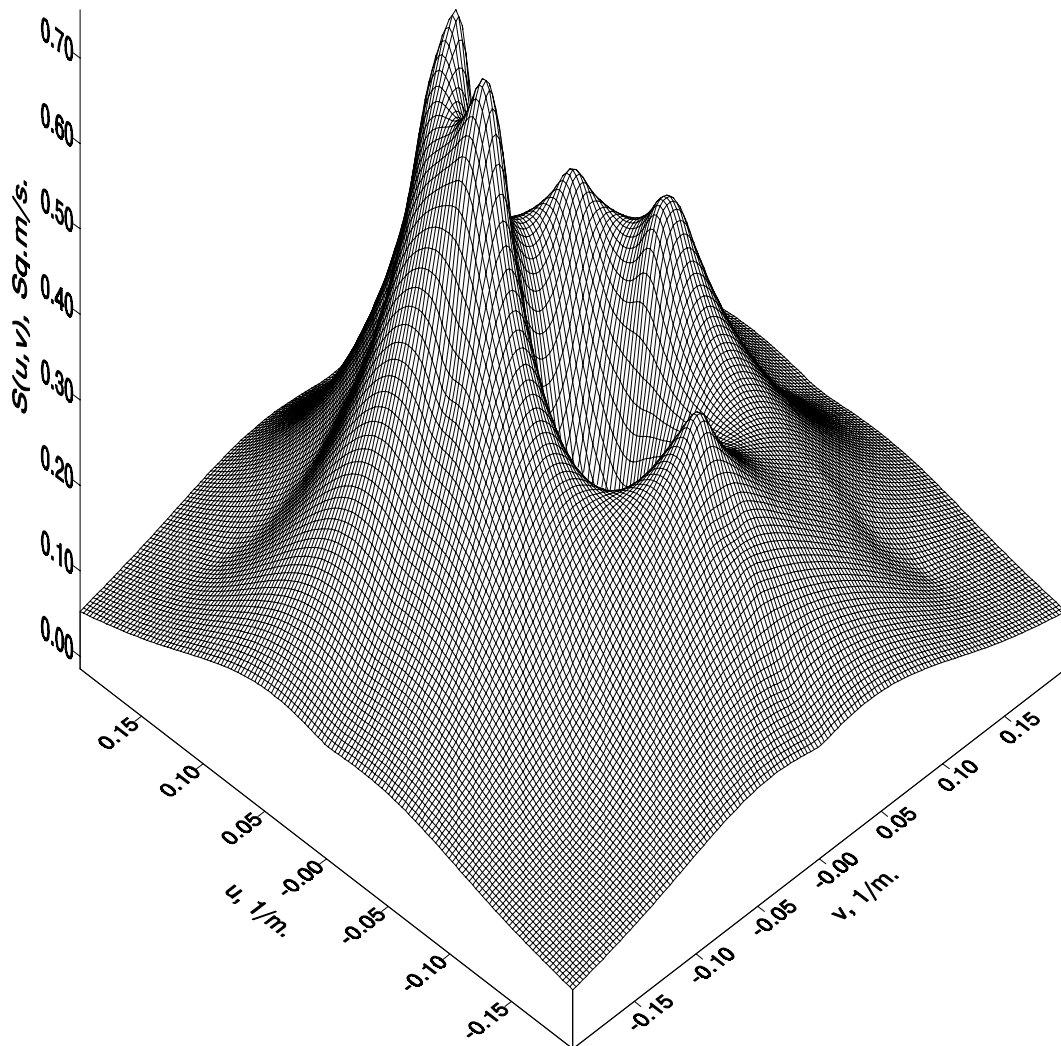**Figure 11.7**: Climatic directional spectrum of wave energy for storm conditions in the Barents Sea. It corresponds to 90%- distribution probability of directional spectra

Fig. 11.7 shows a climatic spectrum for storm waves in the Barents Sea. It corresponds to 90% decile of directional wave energy spectra. Further studies of directional spectra of different intensities are needed.

---oooOooo---

CHAPTER 12

Climatic trends and scenarios

In the preceding chapters we have described in detail several methods of performing extremal analysis for wave heights, which can be applied to any time series of wave data, whether in situ measurements, satellite estimates or produced from numerical models. However, by virtue of the very long temporal extent of the time series required to produce these long return period estimates, e.g. 50- or 100-year (or longer) wave heights, the requirement of stationarity in the data set may not be met due to changes in the wave regime caused by climate variability and/or trend. It is therefore relevant to consider possible implications of intensification or weakening of waves on decadal or century time scales for estimating long return period wave heights.

The first indication that such changes were taking place in the North Atlantic was given by [Carter, Draper, 1988] using wave measurements at the Ocean Weather Stations. Subsequent analysis of similar data by [Hogben, 1988] showed that such trends were characteristic for mean wave heights, but they were not present in maximum wave heights. [Hogben, 1988] suggested that the mean wave height trend is explained by some intensification of background swell, which is associated with oscillations of the North Atlantic current.

Subsequently, Bouws et al. (1996) at the Netherlands Meteorological Institute, using operational ship routing wave analyses, found trends in a box west of Ireland (50-55N, 10-20W) over the period 1961-1987 on the order of 0.3% per year for both the annual maximum and the 99th percentile wave height. The trend in the 90th percentile values was larger, 0.7 % per year. These trends were considered (WASA, 1998) to suffer from some inhomogeneity, leading to an artificial increase in wave heights, and thus to be an upper bound on real trends.

A significant advance on the issue of wave height variability and trend was made by the project WASA (Waves and Storms in the North Atlantic [WASA group, 1998]). Within the WASA project Gunther et al. (1998) attempted to reconstruct the time-space wave fields statistics using a proven wave model driven by a 40-year time series (1955 to 1994) of 6-hourly wind fields for the Northeast Atlantic ocean. While the wind fields used in the analysis (Fleet Numerical Meteorological and Oceanographic Center operational winds, and Norwegian Meteorological Institute operational

analyses) contained some inconsistencies and inhomogeneities over the 40-year period of the hindcast, comparison of the resultant wave fields with in situ measurements showed reliable results.

Analysis of the resulting wave fields in the northeast Atlantic showed the existence of areas of wave growth and decrease. The 90% percentile value of significant wave height was shown to increase at 2 cm/year rate in the area to NW of Scotland, and 1 cm/yr over a wide area extending from the North Sea through the Norwegian Sea. The same percentile decreased at rate of 1 cm/year in the open ocean west of Ireland and the Bay of Biscay. Comparison of the 99th percentile and maximum wave heights at OWS Mike, and the Brent and Ekofisk platforms showed the largest increases in wave height (and wind speed) to be associated with the maxima, the lowest for the 90th percentiles; this results in a widening of the distribution. Off the coast of Ireland the increases are much smaller (1 cm/yr) than those derived by Bouws et al. (1996) (2.7 cm/yr). This analysis is also notable in that, when the full 40-year hindcast period is considered in contrast to the shorter ship routing analysis, that the trend west of Ireland is actually decreasing.

WASA (1998) extended the time series of the hindcast through statistical reconstruction based on redundancy analysis (RDA; von Storch and Zwiers, 1998). This technique predicts the intramonthly wave height patterns based on monthly mean air pressure patterns. Using this approach the statistically derived wave heights for Brent and Ekofisk were generated for the period 1899 to 1994. The reconstruction confirmed the increase in the 40 years of the numerical hindcast. What is noteworthy is that the trends were not apparent when the longer period was considered, i.e. the reconstructed wave heights from the early part of the century were similar to those in the last decades of the hindcast.

Gunther et al. (1998) explicitly looked at trends in the tails of the distributions, representing the most extreme events. Extremal analysis was carried out for each point in the northeast Atlantic for the four ten-year time slices in the hindcast. A peak-over-threshold technique (average 5 peaks per year), using least squares fitting with a Fisher-Tippet III distribution (at most points) was applied in the analysis.

The results of this analysis showed clear spatial patterns. In the area between Scotland and Iceland the trend in 100-year wave height was increasing

(exceeding 2m/decade), while this statistic decreased southwest of Ireland (< 1m/decade).

The trends in storminess were also found in geostrophic wind analyses by Alexandersson et al. (1998) for the British Isles, North Sea and Norwegian Sea. The trends increased significantly from 1960 onward, but when extended back to the beginning of the record in 1881 no trends were apparent.

The WASA project also attempted to predict the effects on extreme waves of a double CO_2 scenario. A time-slice experiment was performed on two 5-year intervals (Rider et al. 1996). Gunther et al. (1998) calculated the 20-year return period wave height on both the control and 2X CO_2 runs. The results were very similar to the patterns found in the 40-year hindcast, increases south of Iceland, and decreases southwest of Ireland.

A significant advance in numerical wave hindcasts resulted from the NCEP/NCAR meteorological re-analysis project (see, e.g. [Kalnay et al., 1996]), which produced global data series of great interest to wave modelling. NCEP reanalysis data were used in [Swail and Cox, 2000; Cox and Swail, 2000] for both a global reconstruction of past wave fields, and a detailed wave reconstruction of the North Atlantic Ocean. The use of the reanalysis products to drive the wave model removed many of the inhomogeneities present in earlier data sets; the further analysis efforts described by Swail and Cox (2000) for the North Atlantic Ocean removed still more inhomogeneities, and equally importantly produced a much finer grid scale analysis which resolved to a much greater degree both tropical and extratropical storms. This additional analysis is critical in the modelling of the most extreme waves, as selected in the computation of long return period estimates.

Wang and Swail (2000) analyzed the global model hindcast results for the Northern Hemisphere. As in the WASA study, the analysis showed areas of increasing wave height and corresponding areas of decrease. In both the North Atlantic and North Pacific, significant linear trends in the seasonal extremes (90th, 99th percentiles) were identified. In the North Atlantic, significant increases in the northeast Atlantic over the last four decades (similar to WASA) are matched by significant decreases in the subtropical Atlantic.

Increases in the 99th percentile wave height in the area between Scotland and Iceland are typically 0.4 to 0.5 %/yr. In the North Pacific, significant changes are found in the winter and spring wave heights, with increases over much of the north Pacific, and some decrease in the subtropics. Increases in winter 99th percentile waves of 0.25 to 0.50 %/yr are common across the area.

As in WASA, Wang and Swail (2000) also extended the time series of the hindcast through statistical reconstruction based on redundancy analysis. Statistically derived wave heights were generated for the period 1899 to 1997. The reconstruction confirmed the increase in the 40 years of the numerical hindcast for both the North Atlantic and North Pacific. For both oceans, no significant trends of seasonal wave extremes are found for the last century, though significant changes do exist in the past four decades. There is, however, significant long-term variability, especially in the North Pacific.

Analysis of the detailed North Atlantic hindcast, described by Swail et al. (2000), was carried out by Swail and Wang (2001). The seasonal patterns were very similar to those from the global hindcast, but with generally greater rates of change. In the North Atlantic hindcast a larger area of significant decreases of SWH was observed in the western subtropical Atlantic in winter. Significant increases are identified off the coast of Canada in summer, and for the central North Atlantic in fall. These differences result from the enhanced wind fields for tropical storms and kinematic reanalysis of wind fields.

In the North Atlantic study, monthly statistics were also described. There were large variations from month to month. Rates of change were generally larger than for the seasonal analysis.

Extremal analysis was also carried out, as in WASA. A Gumbel (and Weibull) analysis was applied for each grid point in the North Atlantic using a peak-over-threshold-approach. Since the hindcast covered the entire North Atlantic, and not just the northeast portion as in WASA, separate analyses were run on tropical and extratropical system peaks. Ten- and twenty-year time slices were analyzed; results of the four 10-year slices for extratropical storms are shown in Figure 12.1.

Details of the extremal analysis are given in Swail et al. (2000). Examination of Figure 12.1 shows that, while there is some consistency among the four time slices, there is considerable variability in the magnitude of the return period wave heights, and in the spatial patterns of the extremes, as storm tracks migrate from one position to another.

The decadal time slice extremal analyses done in both WASA and Swail et al. (2000) are one way to try and gauge the change and variability of the most extreme wave conditions. However, the sample for the trend analysis is necessarily reduced to four, in a 40-year hindcast. Another approach which is often taken is to compute time slices is based on a running sample. As an example, the 100-year wave based on years 1-10 is computed and assigned to year 10; the 100-year wave is recomputed for years 2-11 and assigned

to year 11, and so on. The number of points then available for the trend and variability analysis is then $(N-(m-1))$, where N is the length of the database (e.g. 40 years) and m is the length of the slice (e.g. 10 years).
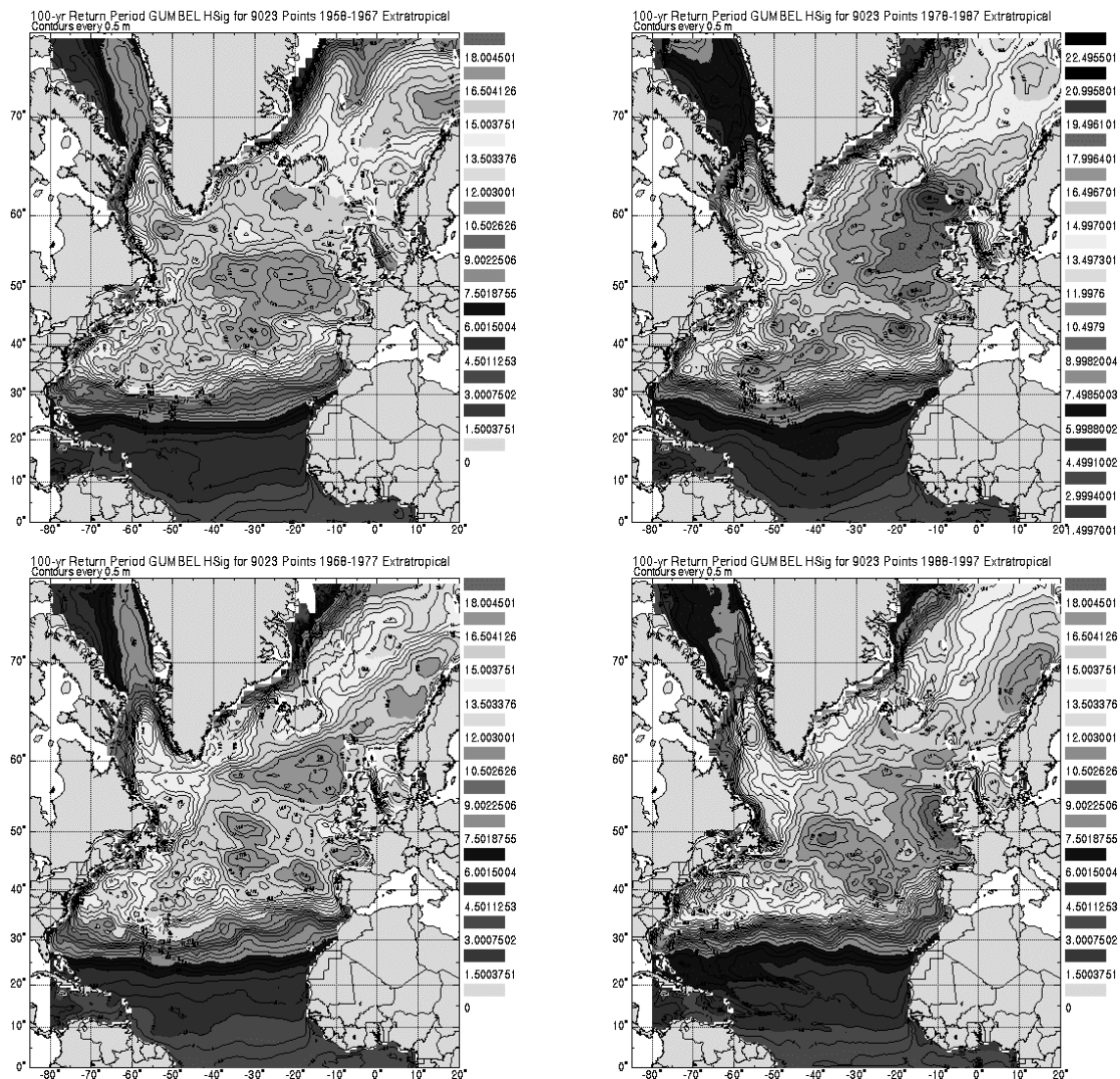

Figure 12.1: Decadal time slice extremal analysis (Gumbel) of extratropical storms

This method is easiest to visualize with the Annual Maximum method, but can also be used with other approaches, e.g. peak-over-threshold. An example of the year-to-year variability and trend in the 100-year return period wave height at Hibernia is shown in Fig. 12.2. Two things are immediately evident from this figure: (1) the 100-year wave height varies considerably depending on which 10-year slice it is based on and, (2) the 100-year wave height has a slight increasing, but statistically insignificant trend over the sampled time interval.

Another area of important research is the analysis of different scenarios of climate change and their implications for wind waves and storm surges. This is the subject of the project STOWASUS-2100 (STOrm WAves and SUrges Scenarios for the 21st century, [http://gate.dmi.dk/pub/project/STOWASUS-2100/])

The project envisages modelling of storm conditions in the 21st century according to several different scenarios on the atmospheric CO_2 increase. Two 30-year time slice simulations with the ECHAM4 climate model are performed. Investigations regarding systematic anomalies in frequency, intensity or location of extreme events, and the physical mechanisms responsible for them are carried out. Preliminary analysis has shown (STOWASUS-2100, 2nd Progress Report) that significant wave heights are slightly increased in the Northeast Atlantic and North Sea region, with increases in the 99th percentile values at some locations of almost 10%. Differences in the mean wave heights between the control run and the 2X CO_2 model run are small, mostly less than 0.15m.

The preceding paragraphs present a bewildering array of information on trend and variability of extreme wave conditions. Trends may be either

increasing or decreasing; similarly, the variability may be increasing or decreasing. The uncertainties in the estimates of variability can be large. This presents something of a dilemma in how to account for such changes. Are these changes the result of anthropogenic climate change, which can be expected to continue? Or are they merely part of the natural variability of the atmosphere-ocean system, which can be accounted for if the sampling period is sufficiently long?
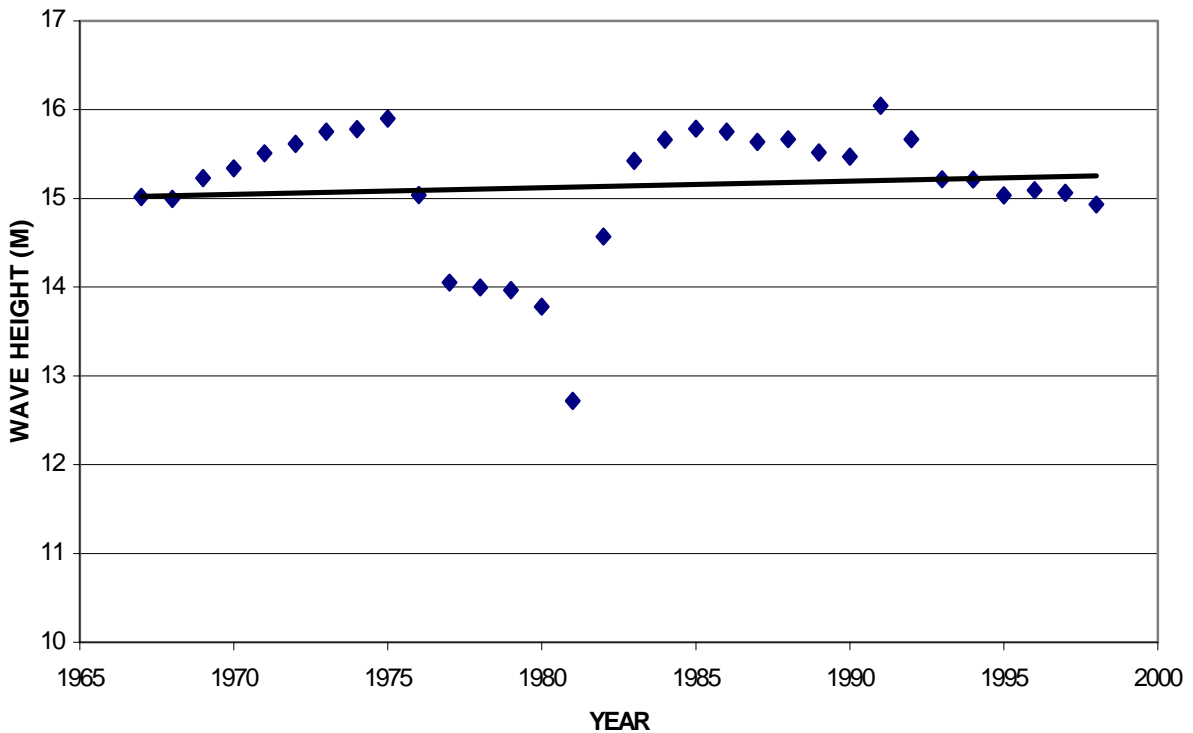

Figure 12.2: 100-year return period wave height variations. Hibernia

The basic issue for the analysis of long-term data series or simulation output is the significance of trend estimates. Various statistical models can be used to estimate the trends. The simplest model is parametric linear regression

$$\zeta(t) = b_0 + b_1 t + \varepsilon \qquad (12.1)$$

where b_0, b_1 are parameters and ε denotes white noise.

If the white noise ε, which in fact is the deviation of annual averages from the trend, is Gaussian, then it is possible to use the following relations to estimate parameters in (12.1):

$$b_1 = \frac{\sum_i (t_i - \bar{t})(\zeta_i - \bar{\zeta})}{\sum_i (t_i - \bar{t})^2}; \quad b_0 = \bar{\zeta} - b_1 \bar{t} \qquad (12.2)$$

For data series of finite length the estimates (β_0, β_1) for parameters (b_0, b_1) represent a system of random values. Let us introduce a new notation:

$$\gamma = \begin{bmatrix} \gamma_0 \\ \gamma_1 \end{bmatrix} = \begin{bmatrix} \beta_0 - b_0 \\ \beta_1 - b_1 \end{bmatrix} \qquad (12.3)$$

Using it we can represent a two-dimensional confidence range $(1-\alpha)$% for values (β_0, β_1) as the internal part of the ellipse

$$n\gamma_0^2 + 2\gamma_0\gamma_1 \sum_i t_i + \gamma_1^2 \sum_i t_i^2 = c \qquad (12.4)$$

and express the solution in variables (γ_0, γ_1). The roots of the equation are

$$\begin{bmatrix} \gamma_{11} \\ \gamma_{12} \end{bmatrix} = \left\{ \left(-\gamma_0 \sum_i t_i \right) \mp \sqrt{\left(\gamma_0 \sum_i t_i \right)^2 - \left(\sum_i t_i^2 \right)(n-c)} \right\} \Bigg/ \sum_i t_i^2 \qquad (12.5)$$

where $c = pS^2 F(p,v,1-\alpha)$, $p=2$, $v=n-p$ and α is the confidence level. They determine the orientation of the ellipse main axes.

If the point (β_0,0) is covered by the $(1-\alpha)$% confidence limit ellipse, we can say that the significant criterion for the trend is satisfied. Then we can assume that the original data series is

stationary. If the criterion is not satisfied, the series is not stationary.

More detailed quantitative analysis of trends in the parameters of probability distributions requires processing of mixture of various distributions, which goes beyond the scope of this review.

Importantly, possible existence of trends in the data series does not alter basic conclusions of this review.

---oooOooo---

REEFERENCES

Aleshkov, Yu. Z. 1996. Oceanic Currents and Waves. Leningrad, LSU.

Алешков Ю.З. Течения и волны в океане. Ленинград, ЛГУ, 1996.

Bukhanovsky, A.V., Lopatoukhin, L.I., Rozhkov, V.A. 1997. Approaches to , experiences of , software for , and examples of wave climate computation. Proceedings of the Third International Conference on Russia Arctic Off-shore "RAO-97", St. Petersburg.

Бухановский А.В., Лопатухин, Л.И., Рожков В.А. Подходы, опыт, программное обеспечение и примеры расчета волнового климата. Труды третьей международной конференции: «Освоение шельфа арктических морей России». С.Пб. 1997, с. 583-598.

Bukhanovsky, A.V., Lopatoukhin, L.I., Rozhkov, V.A. 1998. Highest wave estimates using probabilistic models. Proceedings of the Second International Conference on Ship Design "ICS'98, St. Petersburg.

Бухановский А.В., Лопатухин Л.И., Рожков В.А. Оценки высот наибольших волн по вероятностным моделям. Труды второй Международной конференции по судостроению. - ICS'98. Секция С, Санкт-Петербург, 1998, с.270-277.

Bukhanovsky, A.V., Lopatoukhin, L.I., Rozhkov, V.A. 1998. Climatic wind wave spectra. Proceedings of the Second International Conference on Ship Design "ICS'98, St. Petersburg.

Бухановский А.В., Лопатухин Л.И., Рожков В.А., Дегтярев А.Б., Климатические спектры ветрового волнения, Труды второй международной конференции по судостроению ICS'98, секция В, СПб, 1998, с.375-382

Bukhanovsky, A.V., Lopatoukhin, L.I., Rozhkov, V.A., Divinsky, B.V., Kos'yan R.D. 2000. A classification of wind waves in the Black Sea using instrumental data. "Oceanologia", No. 2.

Бухановский А.В., Лопатухин Л.И., Рожков В.А., Дивинский Б.В., Косьян Р.Д., Типизация ветрового волнения Черного моря по инструментальным данным. "Океанология", 2000, N 2

Wind and waves in the oceans and seas. A reference book. Register of shipping USSR. Eds. Davidan I.N., Lopatoukhin, L.I., Rozhkov, V.A., Leningrad, "Transport" Publisher, 1974.

Ветер и волны в океанах и морях. Справочные данные. Регистр СССР/Ред. И.Н. Давидан, Л.И.

Лопатухин. В.А. Рожков. 1974, Л. «Транспорт», 359с.

Davidan I.N., Lopatoukhin, L.I., Rozhkov, V.A. 1978, Wind waves as random hydrodynamic process. Leningrad, "Gidrometeoizdat" Publisher, 287p.

Давидан И.Н., Лопатухин Л.И. Рожков В.А. Ветровое волнение как вероятностный гидродинамический процесс. Л. «Гидрометеоиздат», 1978, 287с.

Gloukhovsky B.H. 1966. Investigations of wind waves. L. "Gidrometeoizdat" Publisher, 284p.

Гдуховский Б.Х. Исследования морского ветрового волнения. Л. Гидрометеоиздат, 1966, 284с.

Davidan I.N., Lopatoukhin, L.I., Rozhkov, V.A. 1985.Wind waves in the World Oceans. Leningrad, "Gidrometeoizdat" Publisher.

Давидан И.Н., Лопатухин Л.И., Рожков В.А., Ветровое волнение в Мировом океане, Гидрометеоиздат, Л., 1985, 256 с.

Dragan Ya.G., Rozhkov, V.A., Yavorsky I.N. 1987. Methods of probabilistic analysis of the oceanographic process rhythmic. Leningrad, "Gidrometeoizdat" Publisher.

Драган Я.Г., Рожков В.Н., Яворский И.Н. Методы вероятностного анализа ритмики океанологических процессов. Л. Гидрометеоиздат. 1987, 319с.

Lavrenov, I.V. 1998. Mathematical modelling of wind waves in a spatially-non-uniform ocean. St. Petersburg, "Gidrometeoizdat" Publisher.

Лавренов И.В. Математическое моделирование ветрового волнения в пространственно-неоднородном океане. С. Петербург. Гидрометеоиздат. 1998, 499с.

Lopatoukhin L. J. 1974. Distribution of wave elements. VNIIGMI MCD Proceedings, 1, 116-142.

Лопатухин Л.И. Анализ распределений элементов волн. Труды ВНИИГМИ, 1974, вып.1, с116-142.

Lopatoukhin, L.I., Rozhkov, V.A., Trapeznikov Yu. 1990. A. Spectral structure of waves. In book "Results of oceanographic studies in the eastern part of the Pacific Ocean tropical zone", St. Petersburg, "Gidrometeoizdat" Publisher.

Лопатухин Л.И., Рожков В.А., Трапезников Ю.А. Спектральная структура волнения. В кн.: «Результаты океанологических исследований в

- 66 -

восточной части тропической зоны Тихого океана», Л., Гидрометеоиздат., 1990, с.128-135.

Lopatoukhin, L.I., Mikulinskaya, S.M., Rozhkov, V.A. 1991. Maximal wave heights and reliability of their estimates. "Shipbuilding", No. 9.

Лопатухин Л.И., Микулинская С.М., Рожков В.А. Максимальные высоты волн и их достоверность. Судостроение, 1991, №9, с.3-9.

Rozhkov, V.A. 1979. Methods of probabilistic analysis for oceanographic processes. Leningrad, "Gidrometeoizdat" Publisher.

Рожков В.А., Методы вероятностного анализа океанологических процессов, Л. Гидрометеоиздат, 1979, 280с.

Rozhkov, V.A., Trapeznikov Yu. A. 1990. Probabilistic methods for oceanographic processes. Leningrad, "Gidrometeoizdat" Publisher.

Рожков В.А., Трапезников Ю.А. Вероятностные методы океанологических процессов. Л. Гидрометеоиздат. 1990, 272с.

Handbook on marine hydrological forecasting. St. Petersburg, "Gidrometeoizdat" Publisher.1994.

Руководство по морским гидрологическим прогнозам. С.-Петербург. Гидрометеоиздат. 1994 525с.

Smirnov, N.V., Dunin-Barkovsky, I.V. 1969. A course of the theory of probability and mathematical statistics. Moscow, "Science".

Смирнов Н.В., Дунин-Барковский И.В. Курс теории вероятностей и математической статистики. М «Наука», 1969, 511с.

Sretensky, L. N. 1977. Theory of Wave Motion in Fluid. Moscow, Nauka.

Сретенский Л.Н. Теория волновых движений жидкости. М., Наука, 1977, 816 с.

Tikhonov, V.I., Khimenko, V.I., Outbreaks of random process trajectories. Moscow, "Science".

Тихонов В.И., Хименко В.И., Выбросы траекторий случайных процессов. М. «Наука», 1987, 304с.

Alexandersson, H., T. Schmith, K. Iden and H. Tuomenvirta, 1998: Long-term trend variations of the storm climate over NW Europe. Global Atmosphere - Ocean System 6, 97-120 .

Angelides D.C., Veneziano D., Shyam Sunder. 1981. Random sea and reliability of offshore foundations. -J. Eng. Mech. Div., v.107, N 1, pp. 131-148.

Athanassoulis G.A., Soukissian T.H., Stephanakos Ch.N. 1995a Long-term variability and its impact on extreme-value prediction from time series of significant wave height. 4th Intern. Workshop on Wave Hindcasting and Forecasting, Alberta, Canada, October 16-20, 1995

Athanossoulis G.A., Yranas P.B., Soukissian T.H., 1992. A new model for long-term stochastic analysis and prediction. Journ. Ship Res., v 36, N1, pp. 1-16.

Athanossoulis G.A., Stephankos Ch.N., 1995. A nonstationary stochastic model for lon g-term time series of significant wave height, Journ. Geoph. Res., v 100 (C8), pp. 16149-16162.

Bacon S., Carter D.J.T. 1989. Waves recorded at Seven Stones light vessel 1962–86. Institute of oceanographic sciences, DEACON laboratory, Rep. N268, 94 p.

Battjes J.A. 1972. Long-term Wave Height Distribution at Seven Stations around the British Isles. Deutsche Hydrographische Zeitschrift, J.25,H.4,179-189.

Bjerke P.L., Mathienseen M., Tortsethaugen K. 1990. Haltenbanken area metocean study. Main Report./ Norwegian Hydrotechnical Laboratory, Trondheim.

Boukhanovsky A.V., Davidan I.N., Degtyarev A.B., Lopatoukhin L.J., Rozhkov V.A. 1996. The experience of extreme wind and wave estimation in the Barents and Kara seas. /Proc. Int. Conf. Development and Commercial Utilization of Technologies in Polar Regions. POLARTECH'96, Workshop D, St. Petersburg, pp. 66 - 74.

Boukhanovsky A.V., Divinsky B.V., Kosy'an R.D., Lopatoukhin L.J., Ozhan E., Abdalla S. 1999. Short-term wave statistics by the measurements of the buoy near the Russian coast of the Black sea. Proc. Int. MEDCOAST Conf. «Wind and wave climate of the Mediterranean and the Black sea», Turkey, p.59-70.

Boukhanovsky A.V., Lavrenov I.V., Lopatoukhin L.J., Rozhkov V.A. 1999. Extreme wave heights and types of storms in the seas. /Proc. Int. Conf. «Russian Arctic Offshore» RAO'99, St. Petersburg, pp. 332-329.

Boukhanovsky A.V., Lavrenov I.V., Lopatoukhin L.J., Rozhkov V.A., Divinsky B.V., Kosy'an R.D., Ozhan E., Abdalla S. 1999. Persistence wave statistics for Black and Baltic seas. Proc. Int. MEDCOAST Conf. «Wind and wave climate of the Mediterranean and the Black Sea»,, Antalya, Turkey, pp. 199-210.

Boukhanovsky A.V., Lopatoukhin L.J., Rozhkov V.A 1996. The Experience and Software of Marine Natural Hazards Estimation / Proc. of the International Workshop on MED & Black Sea ICZM. November 2-5, 1996. Sarigerme, Turkey, vol.2, pp. 523-531.

Boukhanovsky A.V., Lopatoukhin L.J., Rozhkov V.A. 1998. Wave climate spectra and wave energy resources in some Russian seas/ World Meteorological Organization/ Marine Meteorology and Related oceanographic Activities. WMO/TD-No 938. «Provision and engineering/operational application of ocean wave data. UNESCO Paris, 21-25 September. 1998. A conference

cosponsored by WMO, MeteoFrance and CNES, pp. 324-333.

Boukhanovsky A.V., Lopatoukhin L.J., Rozhkov V.A. 1998. Approaches and Methods of wave climate calculation. Proc. Fourth Int. Conf. Littoral'98. Barcelona, Spain, 1998, pp. 63-70.

Boukhanovsky A.V., Lopatoukhin L.J., Ryabinin V.E. 1998. Evaluation of the highest wave in a storm WMO/TD - No. 858, 18 p.

Bouws, E., D. Jannick and G.J Komen, 1996. On increasing wave height in the North Atlantic Ocean. Bull. Amer. Meteor. Soc., 77, 2275-2277

Buckley W.N. 1988. Extreme and climatic wave spectra for use in structural design of ships. Naval Engineering Journal Soc. pp. 36-57.

Buckley W.H. 1993. Design Wave Climates for the World Wide Operations of Ships.. Part 1: Establishments of Design Wave Climate. Int. Maritime Organisation (IMO), Selected Publications. October 1993.

Carter D.J.T., Draper L. 1988. Has the northeast Atlantic become rougher? Nature, v.332, p. 494.

Chung-Chu Teng, Timple G., Palao I.M. The development of design wave spectra for use in ocean structure design.

The Society of Naval Architect and Marine Engineers, Annual Meeting, 1994, Nov.17-18. New Orleans, Louisiana, p. (20-1)-(20-20).

Chung-Chu Teng, Timple G., Palao I.M. 1993. Design waves and wave spectra for engineering applications./ In: Proc. Int. Conf. «Ocean wave measurements and analysis' WAVES'93», Nov 17-18. New Orleans, p.993-1007

Cox A.T., Swail V.R. 2000. A global hindcast over the period 1958-1997: validation and climate assessment. Accepted in Journal Geophysical Research (Oceans) 2000.

David H., 1970. Order statistics. New York, J. Wiley

Denby L., Landwehr J.M. 1983. The q-q plot. A graphical method for comparing two samples. UMAP Journal, v.IV, N 4, p. 425-452.

Easson W.J. 1997. Breaking waves and offshore design. Proc. of 7 Int. Offshore and Polar Engineering Conf. Honolulu, USA, , pp. 200-205.

Forristall G.Z. 1978, On the statistical distribution of wave heights in a storm. Journal of Geophysical Research, 83, N C5, 2353-2358.

Goda Y. 1979. A review on statistical interpretation of wave data. Report of the Port Harbour research Institute. v.18, N 1, p.5-32.

Goldman I.L., 1977. An approach to the maximum storm, Proc. 9 Ann. Offshore Conf Houston, v.2, pp. 309-314.

Gumbel E.J. 1958. Statistics of extremes. Columbia University Press, New York, 375pp.

Günther, H., W. Rosenthal, M. Stawarz, Carretero, J.C., M. Gomez, I. Lozano, O. Serano, and M. Reistad, 1998: The wave climate of the Northeast Atlantic over the period 1955-94: the WASA wave hindcast. Global Atmosphere - Ocean System, 6, 121-163.

Guide to Wave Analysis and Forecasting. 1998 (second edition). World Meteorological Organization. WMO – No. 702. Geneva. Switzerland. 159 p.

Hamsley J.M. 1996. Wave gauging networks world-wide - an overview/ Proc. 25 Int Conf. «Coastal Engineering 1996» Sept. 2-6, Orlando, Florida, USA, vol. 1, pp. 616-628.

Haring, R.E. and J. C. Heideman, 1978: Gulf of Mexico rare wave return periods. Offshore Technology Conference Paper #3230.

Haring, R.E. and J. C. Heideman, 1980: Gulf of Mexico rare wave return periods. J. Petrol. Tech., p. 35-37.

Hirtzel C.S. 1984. Analysis of extreme values of natural processes: statistical description of maximum. Applied Mathematics and Computations, v. 15, No. 4, pp. 283–303.

Hogben N. Increase in wave heights measured in the North-Eastern Atlantic: A preliminary reassessment of some recent data. Underwater Technology, 1989, 15, N1, pp. 2-10.

Hosking, J.R.M., J.R. Wallis and E.F. Wood, 1985. Estimation of the generalized extreme value distribution by the method of probability weighted moments. Technometrics, 27(3): 251-261.

Hosking, J.R.M., 1988. Fortran routines for use with the method of L-moments. Research Report RC13844, IBM Research, Yorktown Heights, N.Y.

Hosking, J.R.M., 1989. Some theoretical results concerning L-moments. Research Report RC14492, IBM Research, Yorktown Heights, N.Y.

Hosking, J.R.M., 1990. L-moments: analysis and estimation of distributions using linear combinations of order statistics. J. Royal Statistical Soc., Series B, 52(1): 105-124.

Hoybye J., Laszlo, I. Analysis of extreme hydrological events in monsoon climate catchment: the Hongru river, China. Hydrological Sciences Journal, 42(3), June 1997, pp. 343 – 356.

Kalnay E., Kanamitsu M., Kistler R., Collins W. et al. 1996. The NCEP/NCAR 40-year reanalysis project. Bulletin of the American Meteorological Society., v.77, N3, pp. 437-471.

Komen G.L., Cavaleri L., Donelan M., Hasselmann K., Hasselmann S., Janssen P. 1994. Dynamics and modelling of ocean waves. Cambridge University Press., 532 p.

Krogstad H.E., Bartsaw S.F., Haug O., Peters D.J.H. 1997 Directional distribution in wave spectra/ Proc. WAVES'97 Conference, Virginia, USA, , pp. 1-13.

Krogstad H.E. 1998. Directional characteristics of wave spectra. / World Meteorological Organization/ Marine Meteorology and Related oceanographic Activities. WMO/TD-No 938. «Provision and engineering/operational application of ocean wave data. UNESCO Paris, 21-25 September. A conference cosponsored by WMO, MeteoFrance and CNES, pp. 117-127.

Lambrakos, K. F., and Brannon, H. R., 1974. "Wave Force Calculations for Stokes and Non-Stokes Waves," OTC 2039, Offshore Technology Conference.

Lawless J.F. 1974. Approximation to confidence intervals of parameters of the extreme value and Weibull distributions. Biometrica, 61(1), pp. 123–133.

Leadbetter M., Lindgren G., Rootzen, H. 1986. Extremes and related properties of random sequences and processes. Springer-Verlag, N.Y.

Longuet-Higgins M.S. 1957. The Statistical Analysis of Random Moving Surface. Phil. Trans. Roy. Soc., London, v.249, N 469, pp.126-217.

Lopatoukhin L.J., Boukhanovsky A.V. 1997. Experience, software and some results of wind and waves climate modelling and calculations, related to port problems. Proc. 1st Int. Conf. Port, Coast, Environment PCE'97. Varna, Bulgaria, v.1, pp.191-198.

Lopatoukhin L.J., Boukhanovsky A.V., Rozhkov V.A., Divinsky B.V., 1999. Climatic wave spectra of the Black Sea, Proc. Int. MEDCOAST Conf. «Wind and wave climate of the Mediterranean and the Black sea», Antalya, Turkey, pp. 97-109.

Lopatoukhin L.J., Lavrenov I.V., Rozhkov V.A., Bokov V.N, Dymov V.I. 1999. Wind and wave climate near the Prirazlomnoye oil field. Proc. Int. Conf. «Russian Arctic Offshore» RAO'99. St. Petersburg. pp. 315-322.

Mardia K.V. 1972. Statistics of directional data. Academic Press. London and New-York.

Muir L.R., El-Shaarovi. 1986. On the calculation of extreme wave heights: a review. / Ocean Eng. v.13, N 1, pp. 93-118.

Ochi M.K. 1978. Wave statistics for the design of ships and ocean structures. Trans. Soc. Naval. Architects and Mar. Eng. V.86, pp. 47-76.

Pilon P.J., Harvey, D.K. Consolidated frequency analysis (CFA). Reference manual. Environment Canada. Ottawa, Ontario, K1A 0H3, March 1993.

Plackett R.L. 1965. A class of bivariate distributions. Journ. American Statistical Assoc. 60, pp.53-77.

Proceedings International Conference "Wave and wind directionality (application to design of structures)"/ Trondheim, 1986.

Provision and Engineering/Operational Application of Ocean Wave Spectra. Programme, Abstracts and Proceedings of Int. Conf. WMO/TD No 938, UNESCO Paris 21-25 Sept. 1998.

Rice S.O. 1944. Mathematical analysis of random noise. Bell System Technical Journal, 23 N3, 282-332.

Rider, K.M., G.J. Komen and J. Beersma, 1996. Simulations of the response of the ocean waves in the North Atlantic and North Sea to CO_2 doubling in the atmosphere. KNMI Scientific Report WR 96-05. [Available from KNMI, P.O. Box 201, 3730 AE De Bilt, the Netherlands]

Rossouw J., Medina J.R. 1995. Design wave estimation –a robust approach. Proc 4th Int. Conf. on Coastal and Port Engineering in Developing Countries. COPEDEC IV, Rio de Janeiro, v.3, p. 1811-1825.

Rozhkov V.A., Boukhanovsky A.V., Lopatoukhin L.J., 1999. Method for calculation of extreme metocean events Proc. Int. MEDCOAST Conf. «Wind and wave climate of the Mediterranean and the Black sea», Antalya, Turkey, p. 189-198.

Sarpkaya, T., and Isaacson, M., 1981. Mechanics of Wave Forces on Offshore Structures, Van Nostrand Reinhold, New York

Skott J.R. 1968. Some average sea spectra. Quarterly Transactions Royal Institution if the Naval Architects, v.110, N 2, pp. 233-245.

Stanton B.R. 1984. Return wave heights off South Uist estimated from seven years of data. Institute of oceanographic sciences, DEACON laboratory, Rep. N164, 54 p.

Stephanakos Ch.N. 1999. Nonstationary stochastic modelling of time series with applications to environmental data / Nat. Techn. University of Athens. /Doct. Degree Diss., Athens, 187 p.

Swail, V.R., E.A. Ceccacci and A.T. Cox, 2000. The AES40 North Atlantic wave reanalysis: validation and climate assessment. Proc. 6th International Workshop on Wave Hindcasting and Forecasting, Monterey, CA, 6-10 November 2000, p. 1-15.

Swail, V.R. and A.T. Cox, 2000. On the use of NCEP-NCAR reanalysis surface marine wind fields for a long-term North Atlantic wave hindcast. J. Atmos. Oceanogr. Technol., (17): 532-545.

Swail, V.R. and X.L. Wang, 2001. Trends of Atlantic wave extremes as simulated in a 40-year wave hindcast using kinematically reanalyzed wind fields. Submitted to J. Climate.

Szabo D., Cardone V.J., Callahan B.T. 1989. Severe storm identification for extreme criteria determination by hindcasting. 2nd Intern. Workshop on wave hindcasting and forecasting. Vancouver, p. 89-95.

Teng C.C., Timple G., Brown D.A. 1993. Design Waves and Wave Spectra for Engineering Applications, Proc. WAVES'93, New Orleans, LA. 993-1007.

Vincent C.L, Resio D.T., 1977. An eigenfunction parameterisation of a time sequence of wave spectra. Coast. Eng. N1, pp. 185-205.

Wang, X.L., and V.R. Swail, 2000. Changes of extreme wave heights in northern hemisphere oceans and related atmospheric circulation regimes. J. Climate, in press.

WASA Group. 1998. Changing waves and storms in the Northeast Atlantic. Bulletin of the American Meteorological Society. v.79, N5, p.741-760.

Wilson B.W., 1965. Numerical prediction of ocean waves in the North Atlantic for December 1959. Deutsch. Hydrograph. Zeitschrift, vol. 18, N 3.

---oooOooo---

ACKNOWLEDGEMENTS

---oooOooo---

KEY TO SYMBOLS

a	Scale parameter of the first-limit (Gumbel) distribution	$h_k^{(T)}$	Estimate of kth annual maximum at T-year return period
a_T	Scale parameter of extrapolation of the first-limit (Gumbel) distribution to a T-year return period	H	Water depth
		$K_x(\bullet)$	Correlation function of process x
		$m_x(\bullet)$	Mathematical expectation of the function x
b	Position parameter of the first-limit (Gumbel) distribution	$M[\bullet]$	Operator of mathematical expectation
b_T	Position parameter of extrapolation of the first-limit (Gumbel) distribution to T-year return period.	$Me[\bullet]$	Operator of median
		m_{00}	Zero – order moment of spectrum
C_n^m	Number of combinations from n to m	$\widehat{n}$	Number of conditionally independent observations
$\overline{C}, \overline{S}$	Angular moments	p	Probability
c	Crest height	s	Scale parameter of log-normal distribution of wave heights at synoptic times
c_f	Colligation coefficient		
$D_x(\bullet)$	Variance of function x	$S_x(\bullet)$	Spectral density of process x
erf	The error function	t	Time
f	Nonlinear functional transformation	t_b	Time of storm commencement
$f(\bullet)$	Probability density function	t_m	Time at which maximum wave height h^+ was observed in a storm
$F(\bullet), G(\bullet)$	Distribution function		
$F_m(\bullet)$	Distribution of extreme element in a sample.	t_e	Time of storm end
		$u(\bullet)$	Non-dimensional deterministic impulse
$F^*(\bullet)$	Estimate of distribution function	U_p	Quantile of normal distribution N(0,1) of p% probability
$G(\bullet)$	Quantile function, distribution function		
h	Wave height (individual or recorded at a synoptic observation time)	$w(\bullet)$	Deterministic impulse with random parameters
$\overline{h}$	Mean wave height recorded at a synoptic observation time	$W(\bullet)$	Stationary random process
		Z	Threshold for wave height selection
h_s	Significant wave height recorded at a synoptic observation time	α	Covariance function decay decrement
		β	Direction of waves
h_{max}	Highest wave height (individual or recorded at a synoptic observation time)	δ	Skewness of a storm
		Δt	Time series discretization or time step
h_{ws}	Wind wave height recorded at a synoptic observation time	ε	White noise
		λ	Parameter of Poisson distribution and of storm number distribution
h_{sw}	Swell height recorded at a synoptic observation time		
h^+	Highest wave height in a storm recorded at a synoptic observation time	ρ	Correlation coefficient
		σ	Standard deviation, r.m.s. deviation
h	Lowest wave height in weather window recorded at a synoptic observation time	τ	Wave period
		$\overline{\tau}$	Mean wave period
h_b	Height of breaking wave	τ_p	Wave period at spectral peak
h_p	P% quantile of wave height distribution	$\Im$	Storm duration
$h_{0.5}$	Median of wave height distribution at a synoptic observation time	φ	Latitude.
		ϕ	Auto-regression parameter.
$\overline{\overline{h}}$	Monthly mean wave height	Φ	Normal (Gaussian) N(0,1) distribution function
$\overline{\overline{h}}_{max}$	Seasonal maxima of monthly mean wave height		
		θ	Longitude
		Θ	Duration of weather window
$\widetilde{h}_p$	p% probability quantile of annual maximum distribution	ζ, ξ, η	Centered time series
		Ξ	Storm parameters (h^+,h,$\Im$, Θ).
$h^{(T)}, h_{max}^{(T)}$	Estimated extreme wave heights at T-year return period.	ω	Angular frequency.
		$\overline{\omega}$	Mean angular frequency.

---oooOooo---